Molecular clouds and star formation

Jan Brand
INAF – Istituto di Radioastronomia
Bologna

Lezioni per dottorandi 9 Nov. 2009

Overview of this lecture:

The galactic interstellar medium (ISM):

constituents and their co-existence; large-scale distribution

Molecular clouds

properties; chemistry; mass and temperature

Kinematics

rotation curve, kinematic distances

Star formation

young stellar objects (YSOs); IMF

manifestations (interaction with surroundings)

Star formation: high-mass

intro only. Is main topic of next lecture, by Cesaroni

THE PHASES OF THE INTERSTELLAR MEDIUM

Not just stars…

ISM: 90% H, 9% He, 1% "rest"

Dust mixed with gas

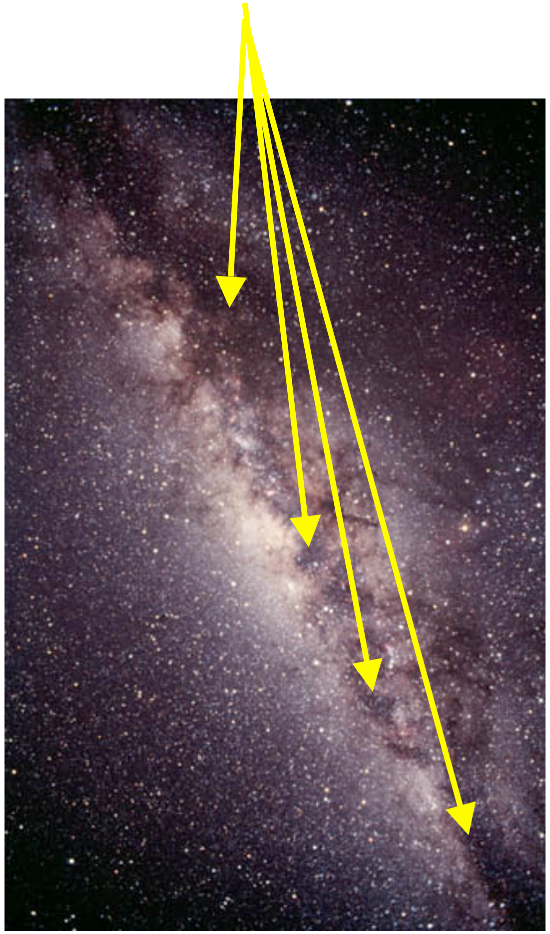

Abundances: for every 10^6 H atoms, there are 250 C, 500 O, 80 N atoms ~solar (≡ cosmic). Other elements: IS abundance <<cosmic: depletion (material locked up in dust grains)

Characterize ISM acc. to condition of H:

HI: M ~ 2 x 10^9 $M_\odot$
H_2: M ~ M(HI)
HII: M ~ 1 x 10^8 $M_\odot$

M(ISM) ~ 4% M(visible matter in Galaxy)
M(dust) ~ 1-2% M(ISM)

Energy in the ISM:
Radiation field, magnetic fields, cosmic rays

High density? Not really… (only in some locations):

High-density molecular cloud core: ≥ 10^6 particles cm^{-3}

Earth's atmosphere at sea level: ~ $3x10^{19}$ particles cm^{-3}

Best terrestrial vacuum: $3x10^{12-13}$ particles cm^{-3} !!

Average density ISM: ~ 1 particle cm^{-3}


H_2 , HII, dust
© Anglo-Australian Obs/Royal Obs. Edinburgh

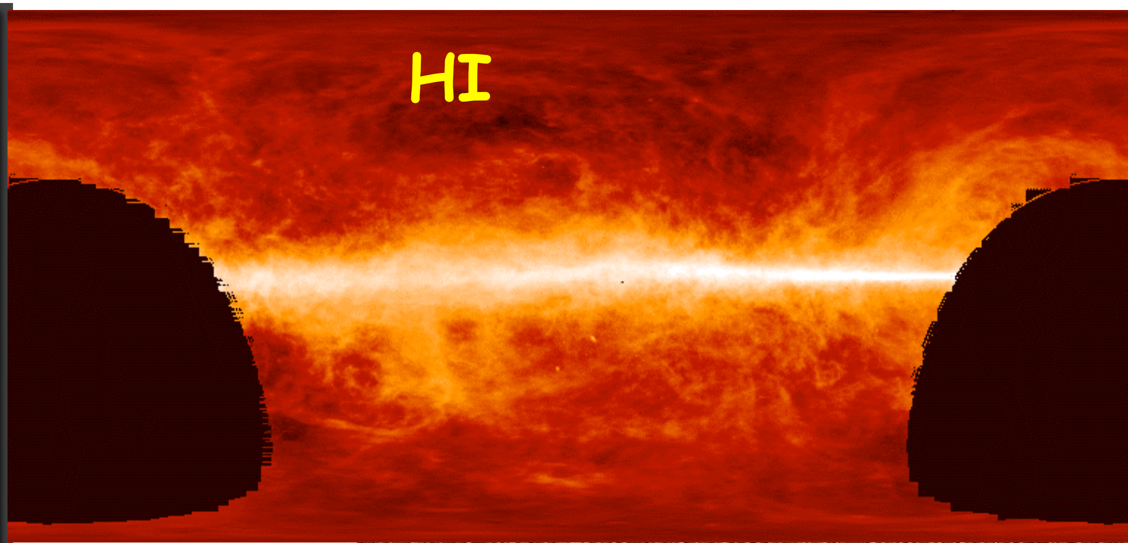
HI

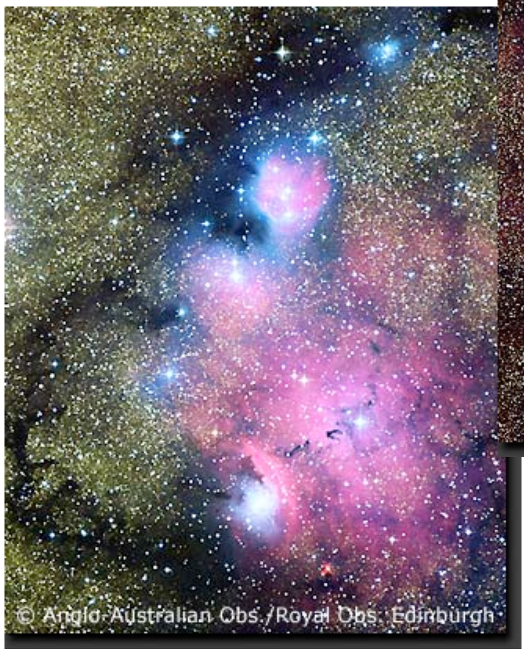
© Anglo-Australian Obs./Royal Obs. Edinburgh


© Anglo-Australian Obs./Royal Obs. Edinburgh


H_2 , dust

What you see depends on frequency

Orion: optical, IR, and mm

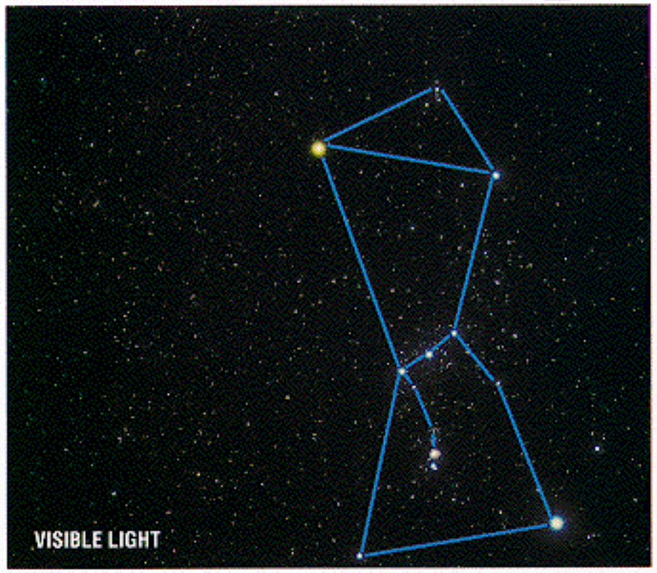

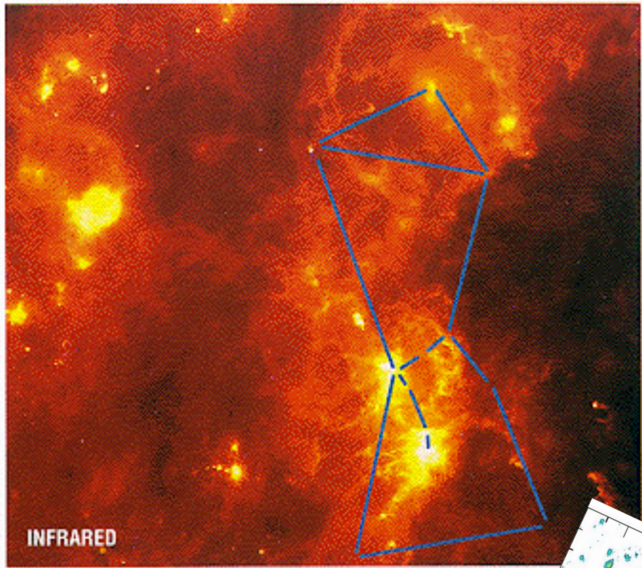

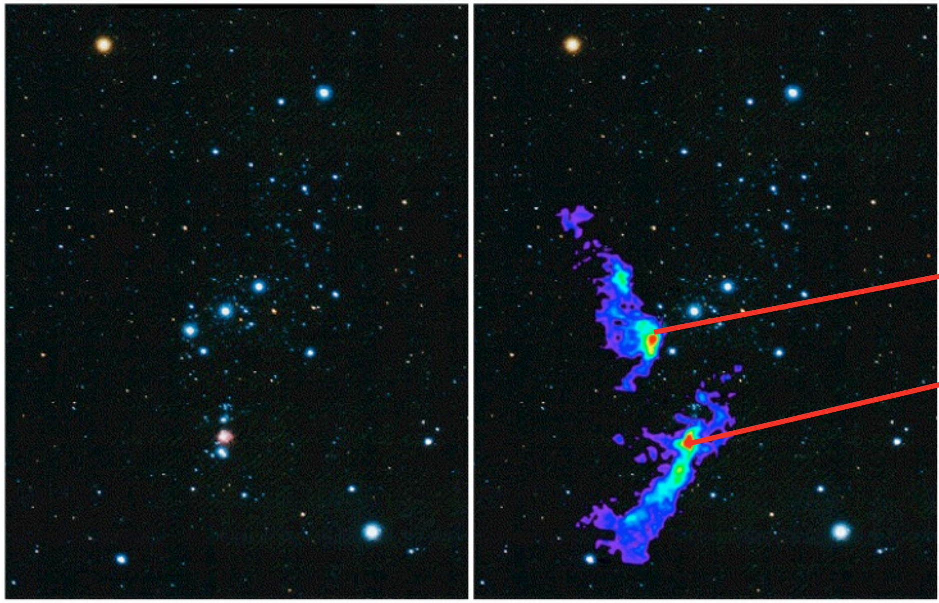

CO

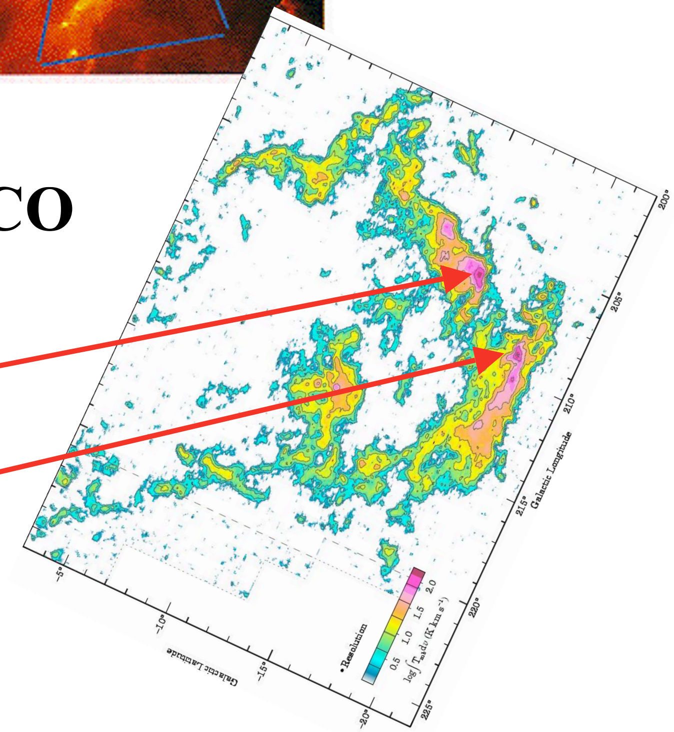

HH46 – Visual → NIR → MIR

The Spitzer-view

Inner, outer, & (far-) outer Galaxy

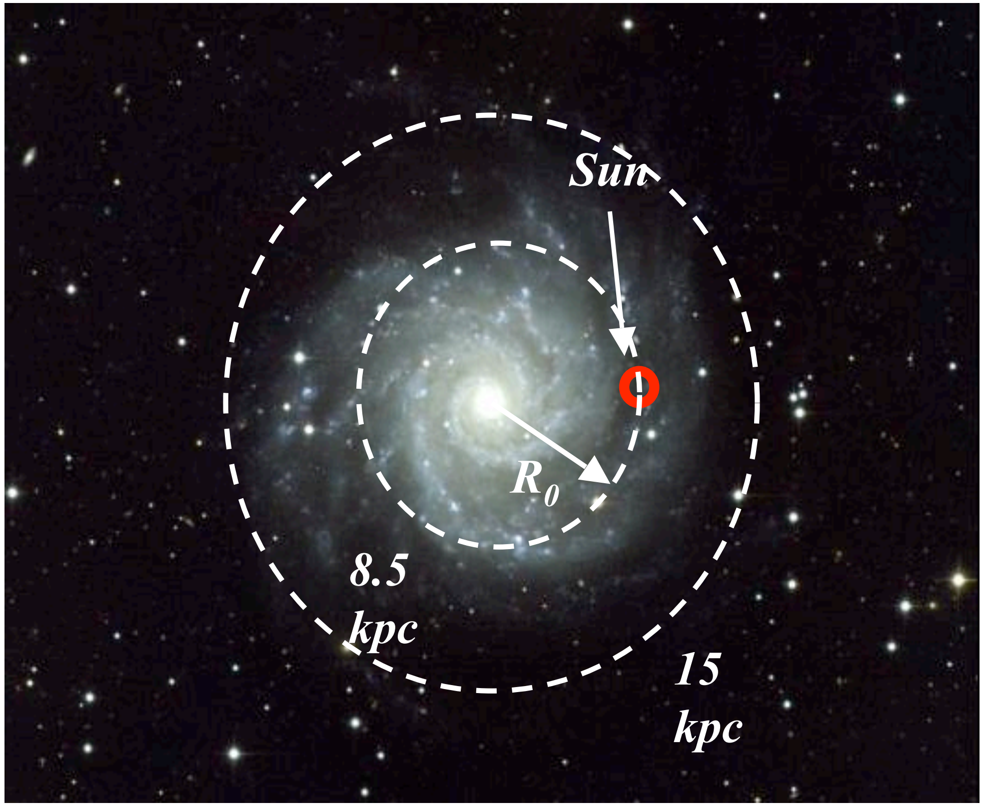

Solar circle: $R = R_0 = 8.5$ kpc

Inner Galaxy: $R < R_0$

Outer Galaxy: $R > R_0$

Far-Outer Galaxy: $R > 15$ kpc

Distribution ISM

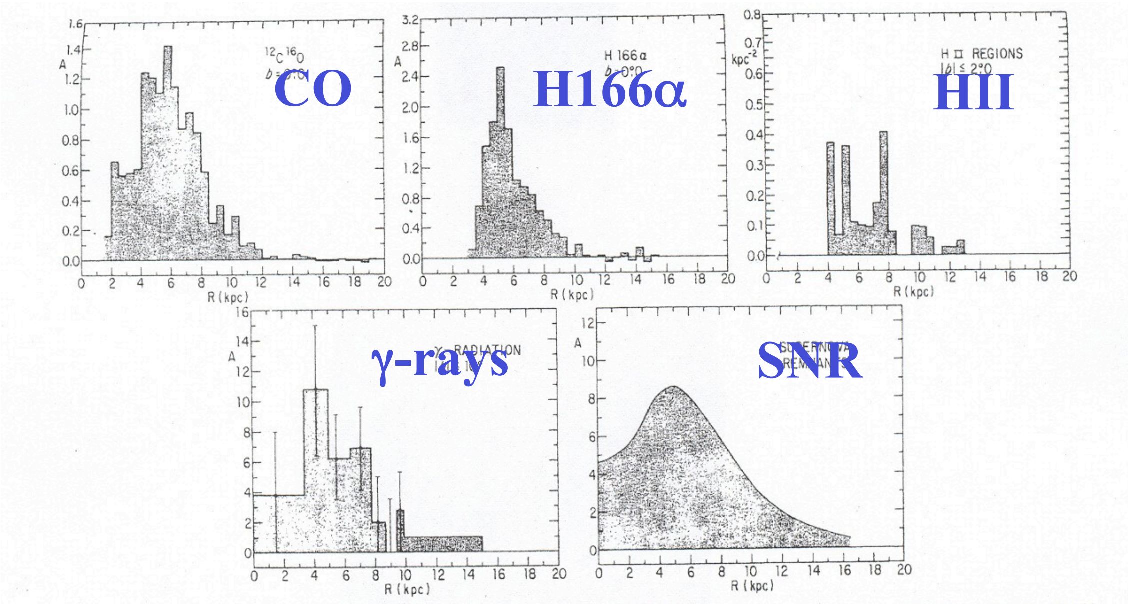

R(kpc): 0 10 20

Galactic ring
4 < R < 6 kpc

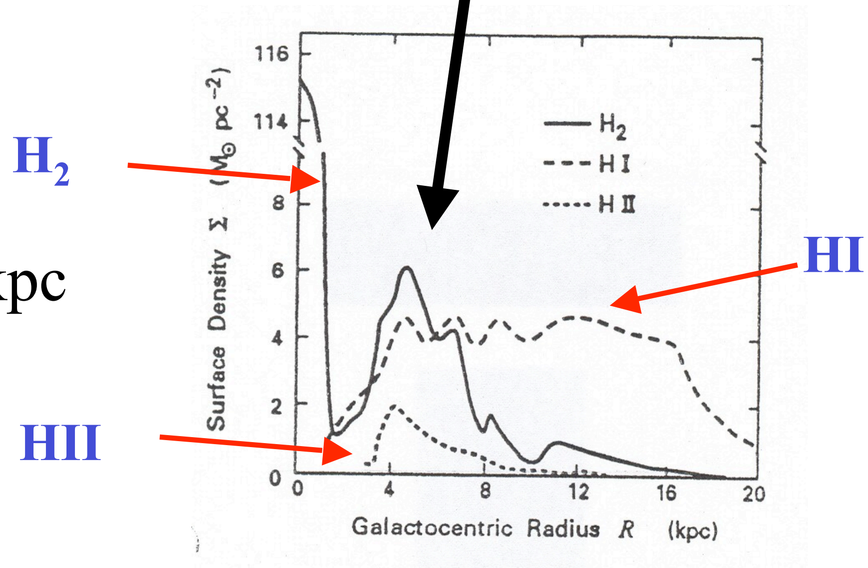

Distributions peak at $R < R_0 = 8.5$kpc
Max. extent ~ 2 R_0

Radiation mechanism of HI

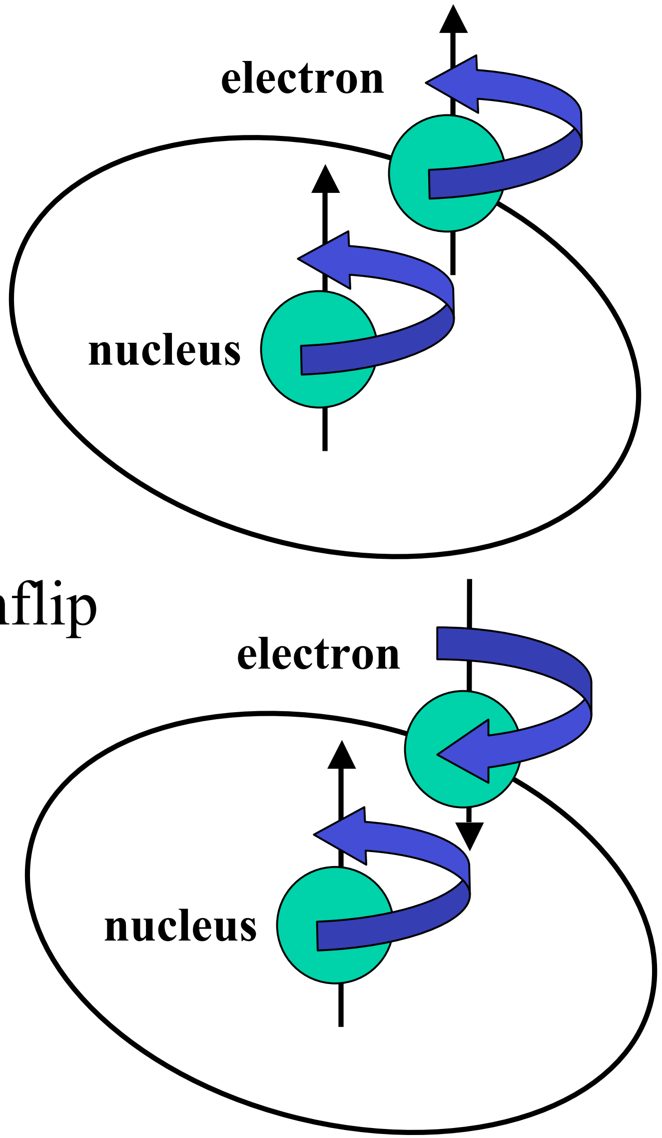

E_2: high

spinflip

$\Delta E = E_2 - E_1 = h\nu$
at 1.4 GHz (21.2 cm)

E_1: low

Spontaneous trans. prob. $A = 2.85\ 10^{-15}\ s^{-1}$,
i.e. once every 12 Myr!
De-excitation governed by collisions.

Galactic distribution HI

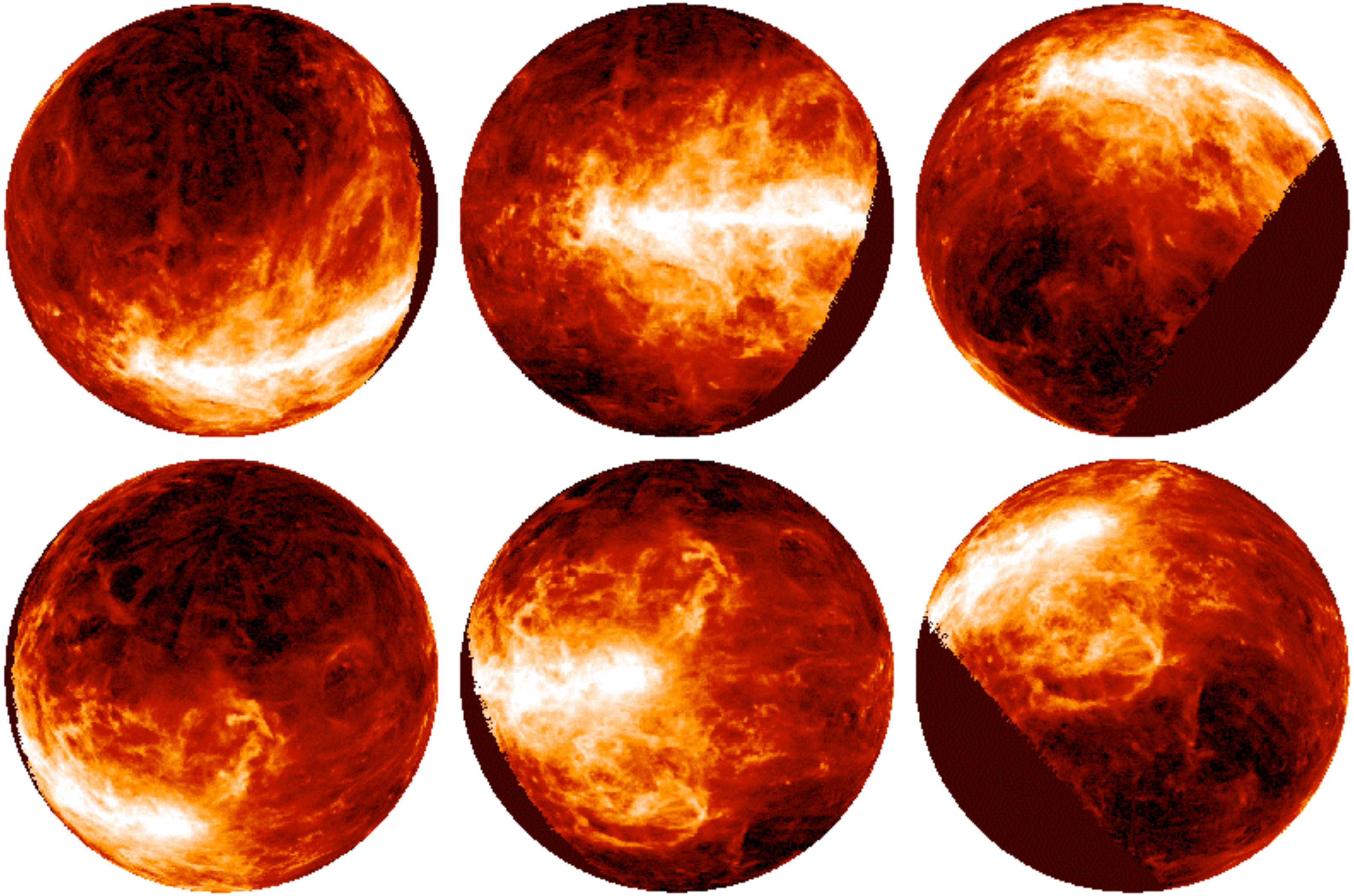

Hartmann & Burton 1994

CO, not H_2

ISM composed essentially of hydrogen:

HI: 21-cm line

H_2: symmetric molecule $\Rightarrow$ no radio emission

- UV absorption lines

- IR emission lines

CO: most abundant after H_2 : $[H_2]/[CO] \sim 1 \times 10^{-4}$.

- excited by collisions with H_2

- easily observed rotational transitions at (sub-)mm wavelengths

- $n(H_2) \geq$ a few $\times\ 10^3\ cm^{-3}$

Galactic distribution CO

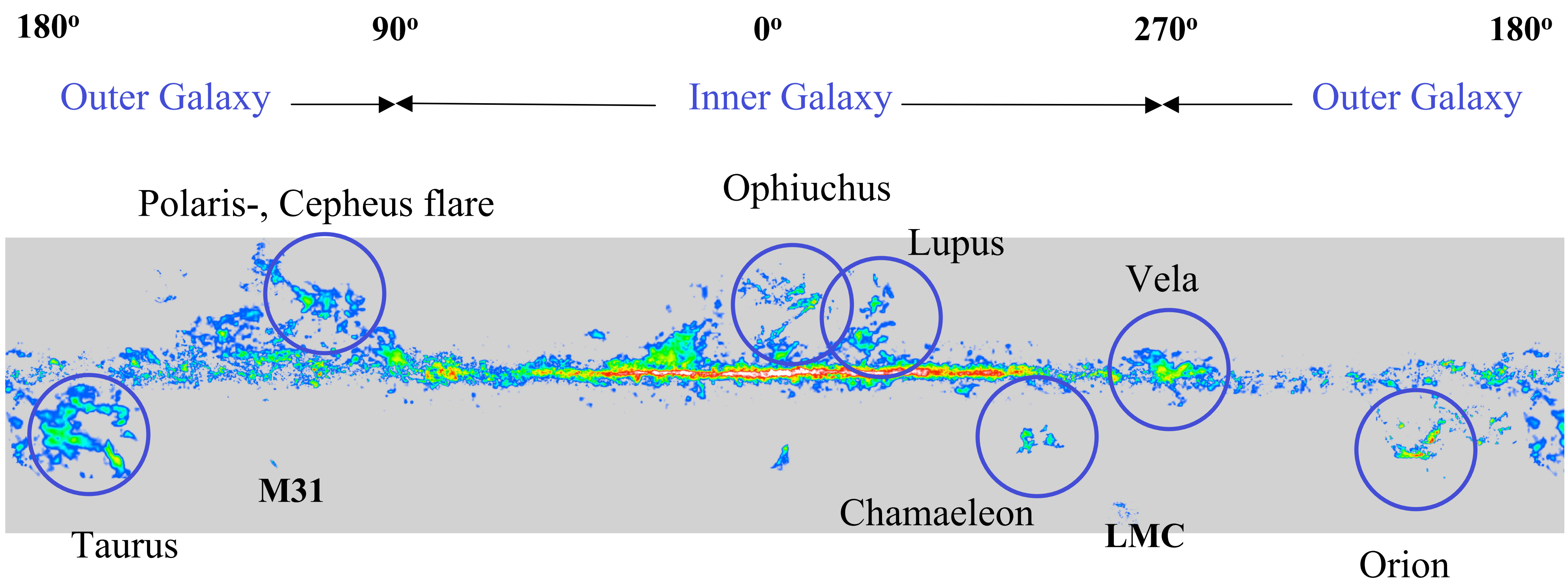

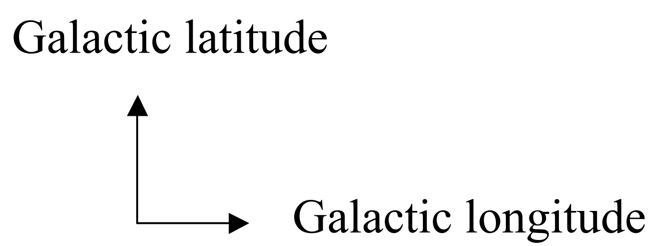

Dame, Hartmann & Thaddeus 2001

HI: tilted disk

HI: warped & flared disk

lopsided

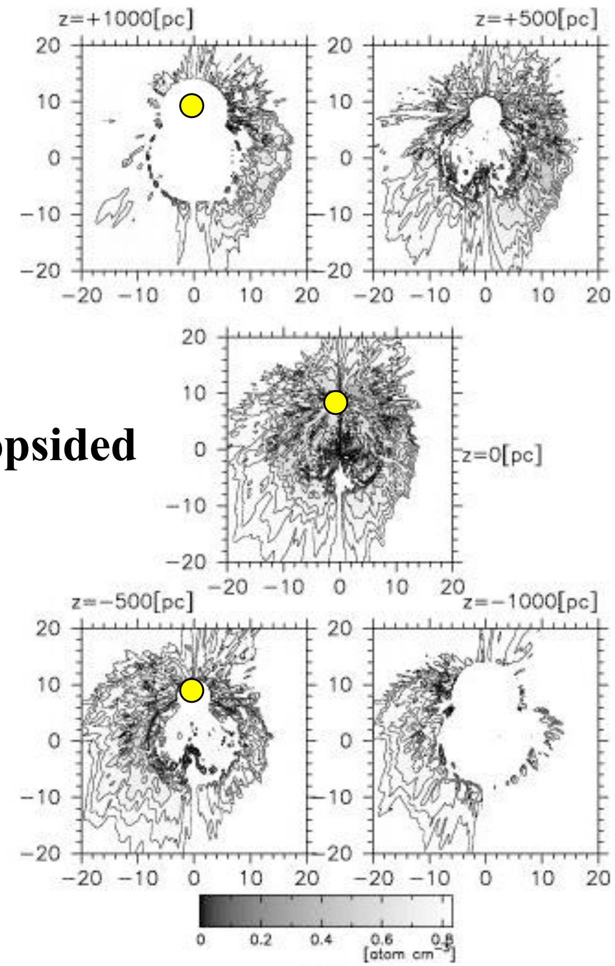

Fig 6

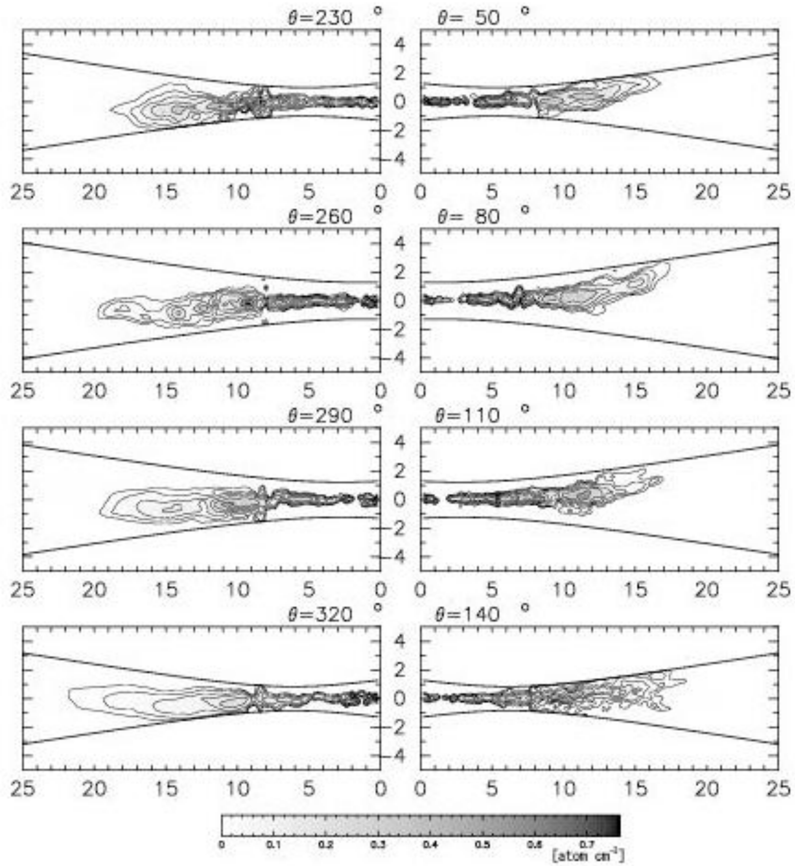

Fig 7

Same seen in H_2/CO

Nakanishi & Sofue 2003 PASJ

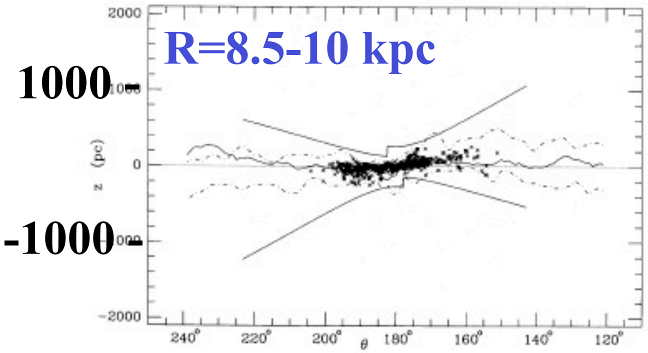

Fig. 8a. Distribution with galactocentric azimuth of the z heights of molecular clouds with kinematic distances in the range $R = 8.5$ to 10.0 kpc

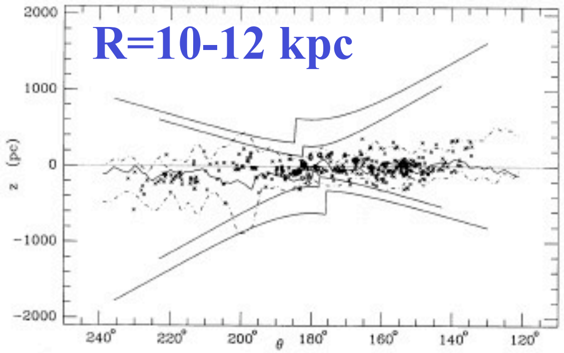

Fig. 8b. Shape of the molecular cloud layer at $10 < R < 12$ kpc

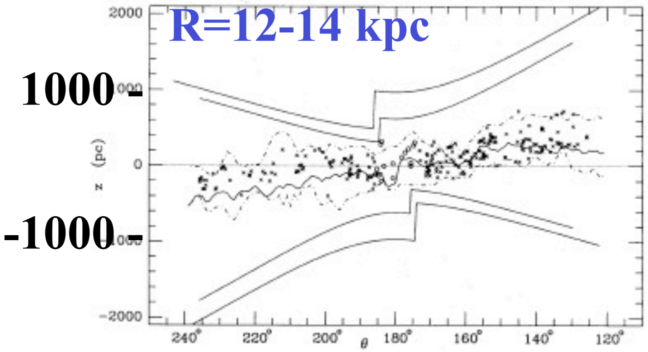

Fig. 8c. Shape of the molecular cloud layer at $12 < R < 14$ kpc

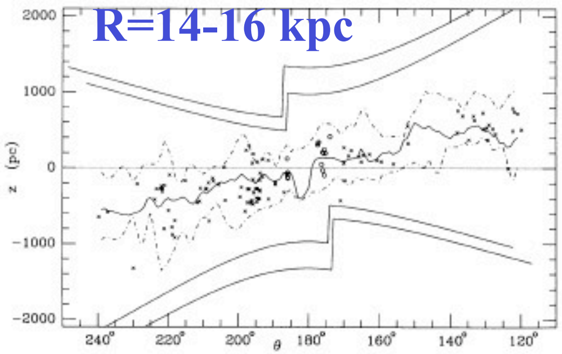

Fig. 8d. Shape of the molecular cloud layer at $14 < R < 16$ kpc

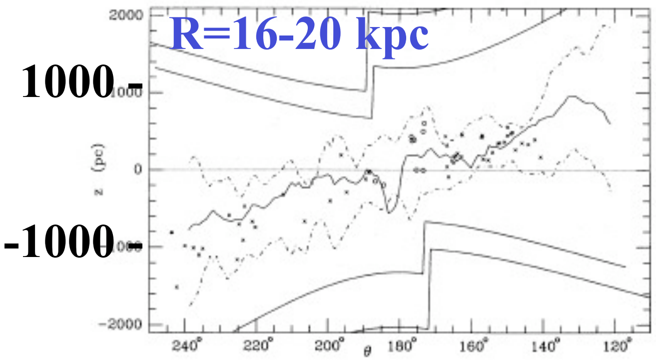

Fig. 8e. Shape of the molecular cloud layer at $16 < R < 20$ kpc

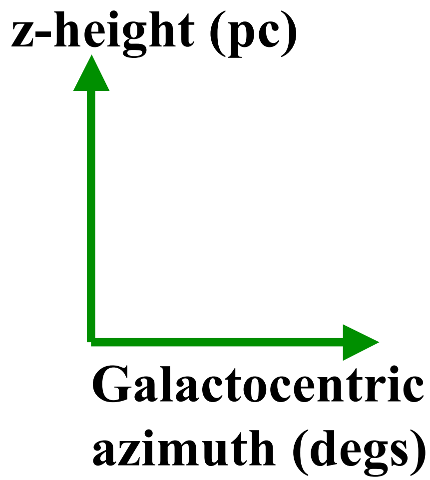

Warping & flaring in CO

Wouterloot, Brand, Burton, & Kwee
1990, A&A 120, 21

Surface density

Scale height

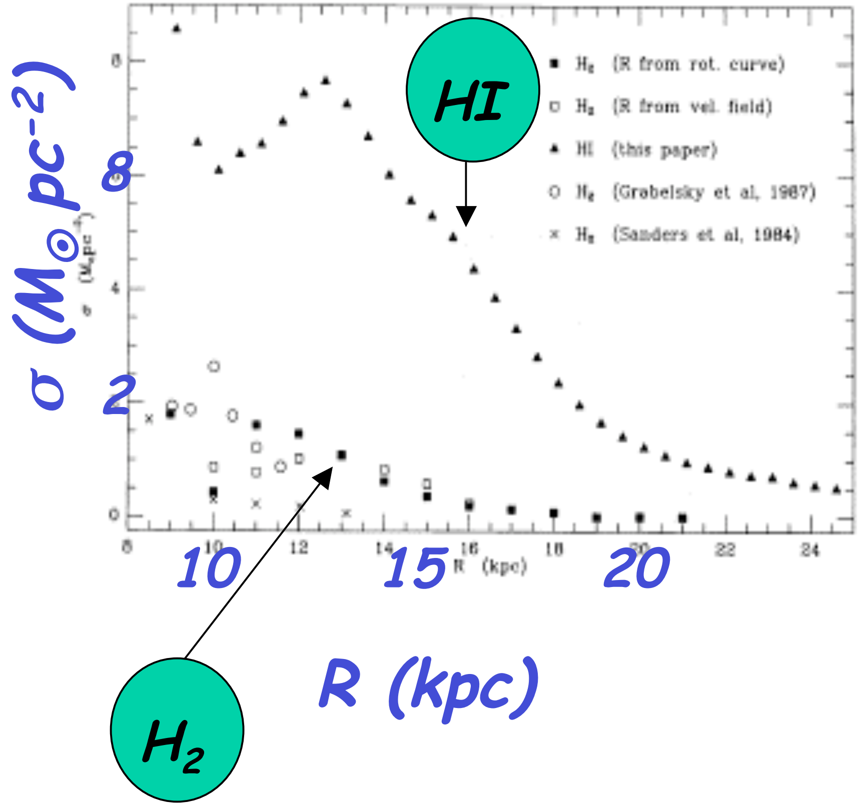

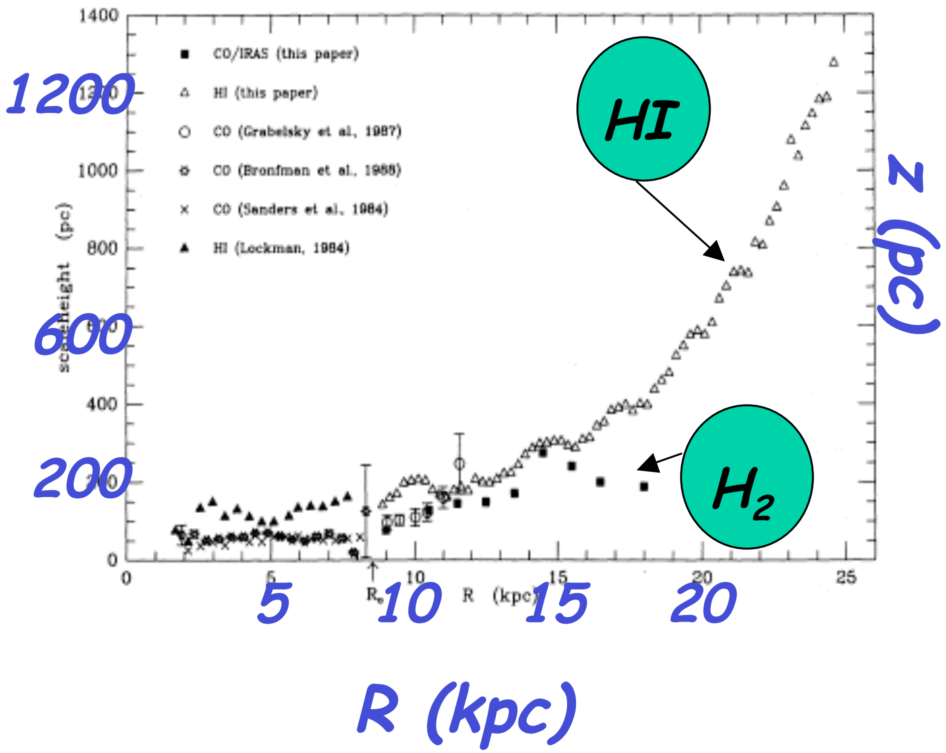

"flared disk" ('a svasato')

In OG: Surface density down, scale height up ⇒ volume density even lower

Wouterloot, Brand, Burton, & Kwee 1990

Displacement of mean plane from b = 0°

Blue, Red = pos

Grey = neg

Darker hues mean higher amplitude

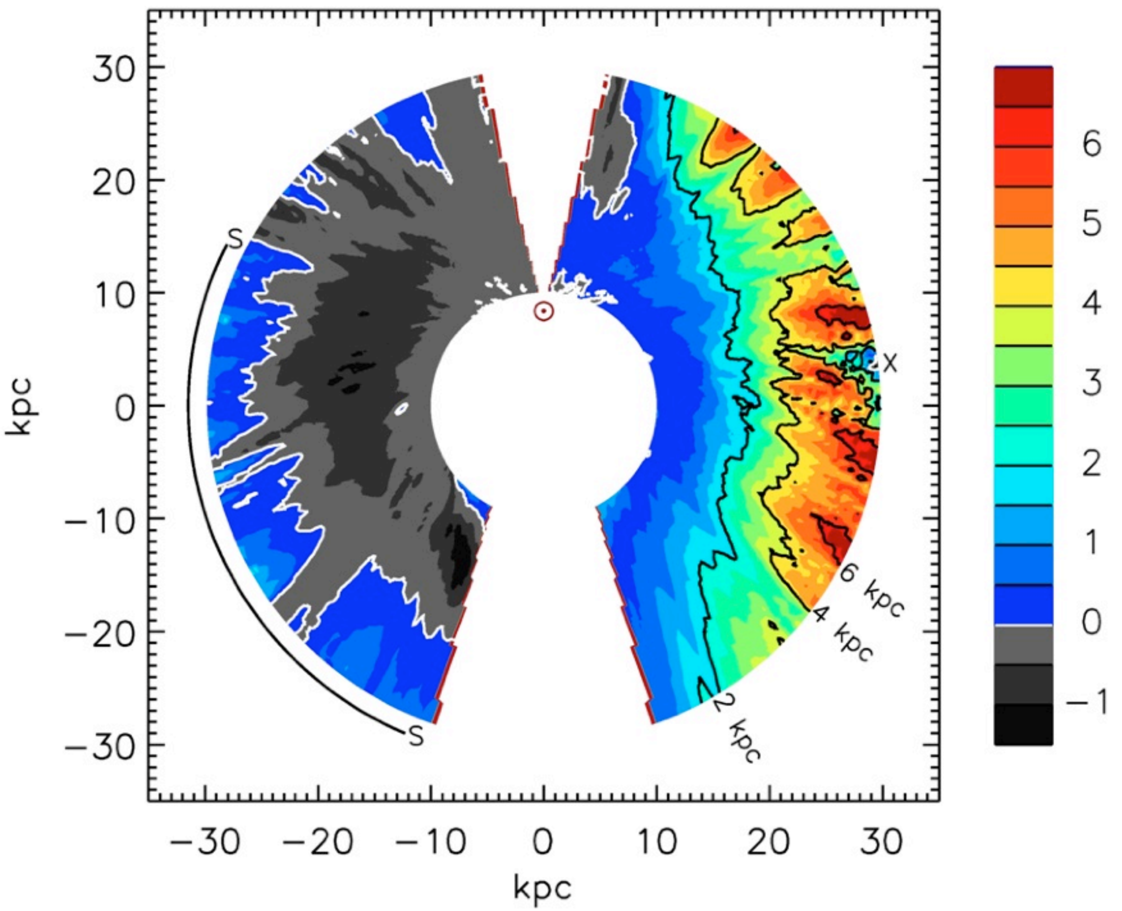

Levine, Blitz, Heiles, Weinberg 2008, 2006

View of warp from l = 30°

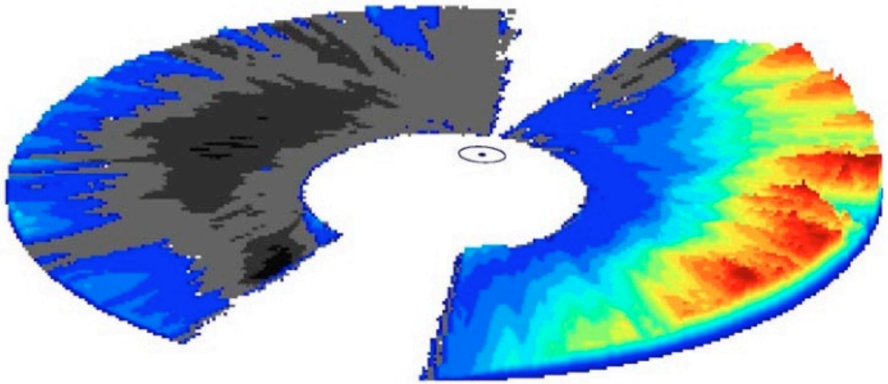

To Scale

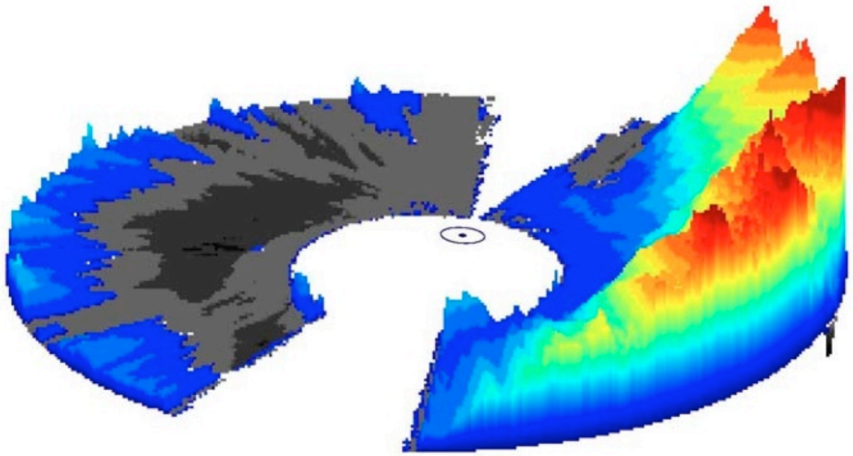

5x exaggeration

Levine, Blitz, Heiles, Weinberg 2008, 2006

Milky Way Galaxy:
"warped and vibrating like a drum"

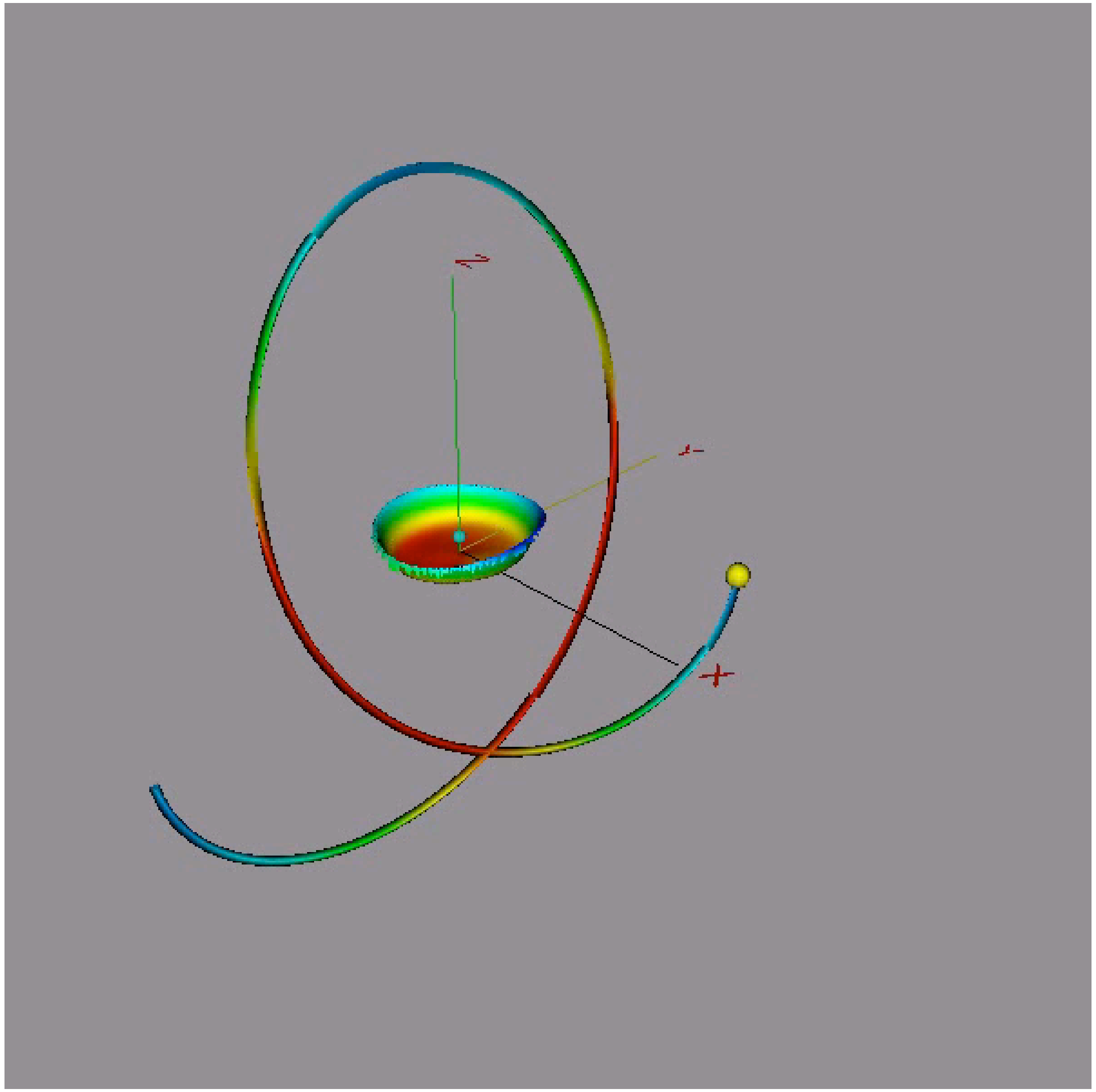

Levine, Blitz, Heiles, Weinberg 2008, 2006

A thick disk in CO

(Dame & Thaddeus 1994)

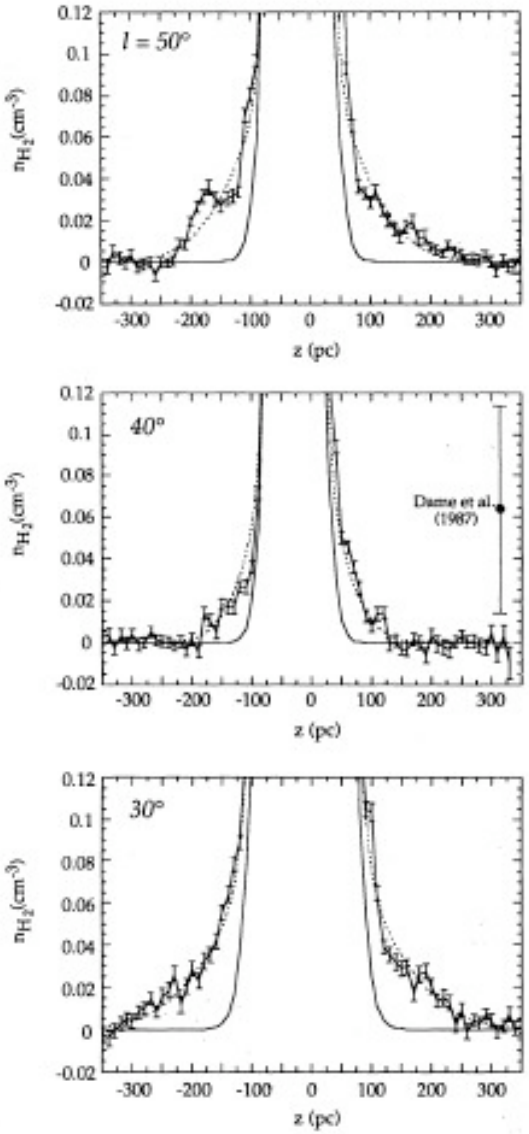

CO (29.5-30.5 degs)

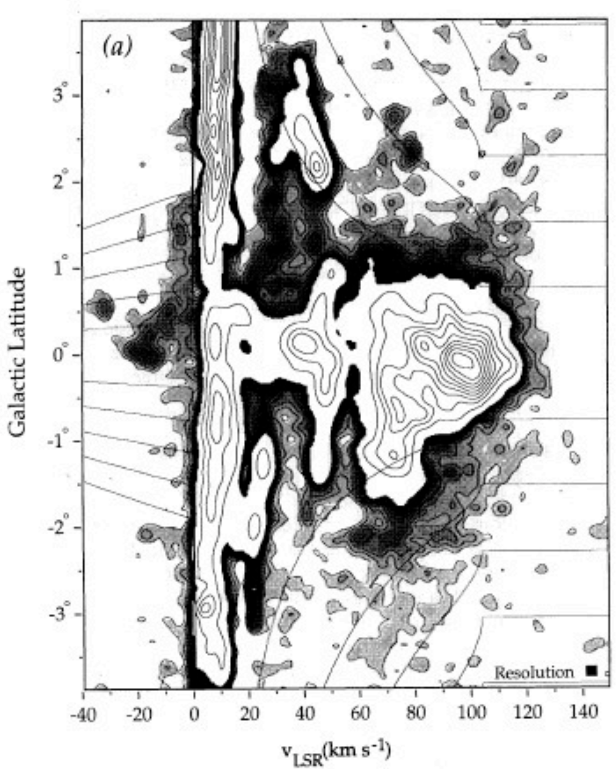

HI

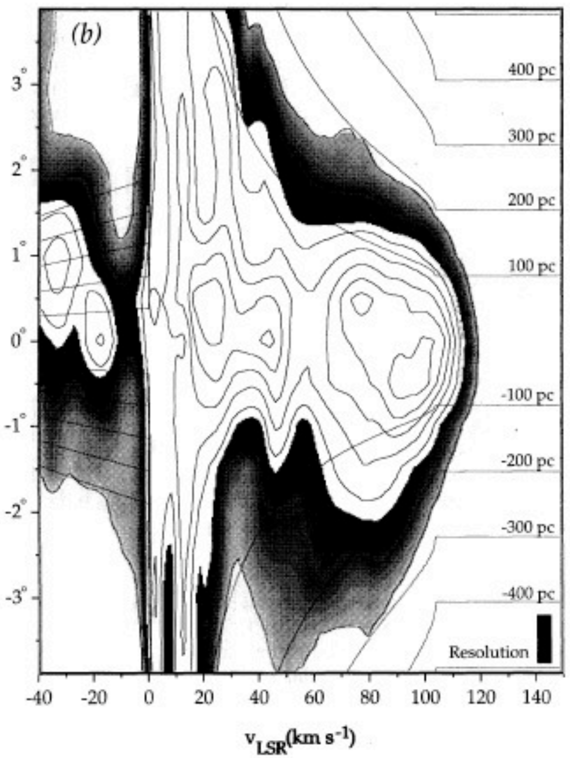

$n(H_2)$ vs. z-height

Is there a spiral arm pattern?

Distribution of
HII regions
(young stars)

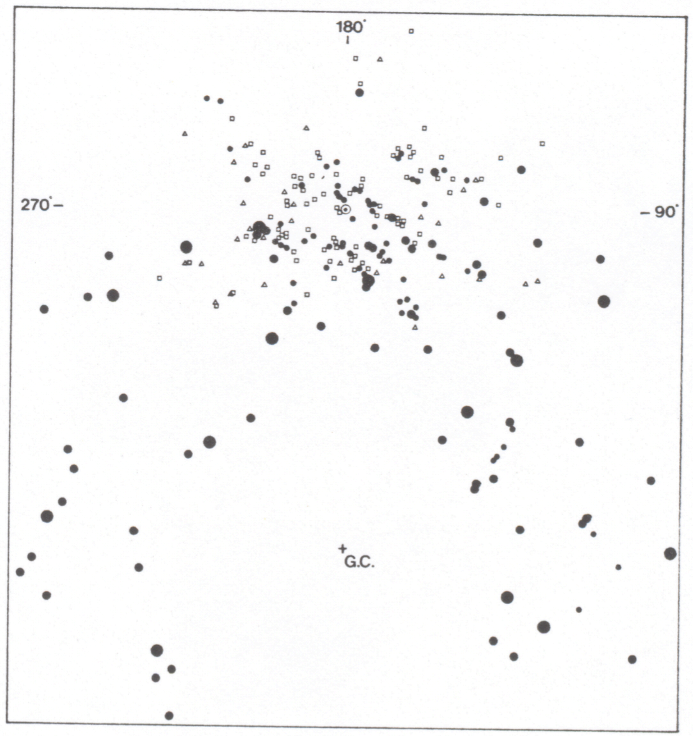

Same, but with
spiral pattern
drawn in

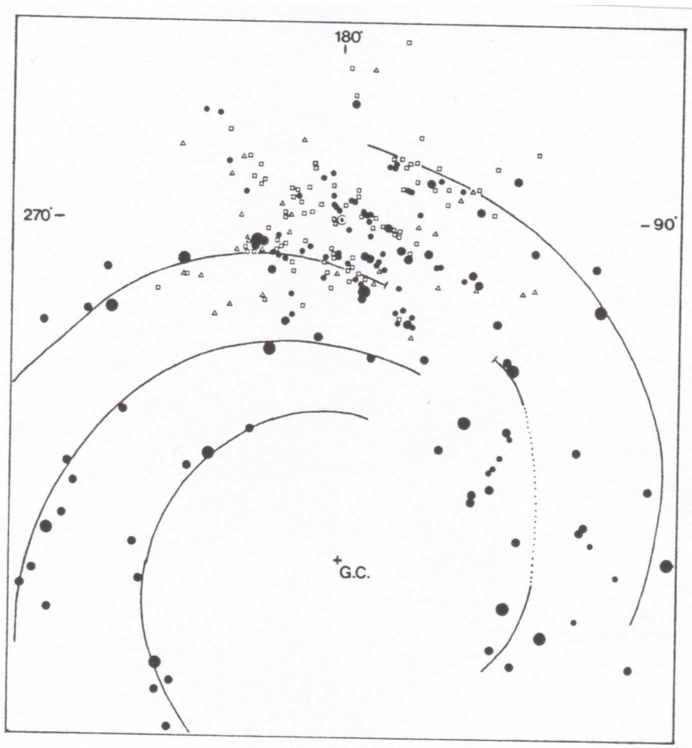

Georgelin 1975

Spiral structure

From Hα (Russeil, A&A 2003)

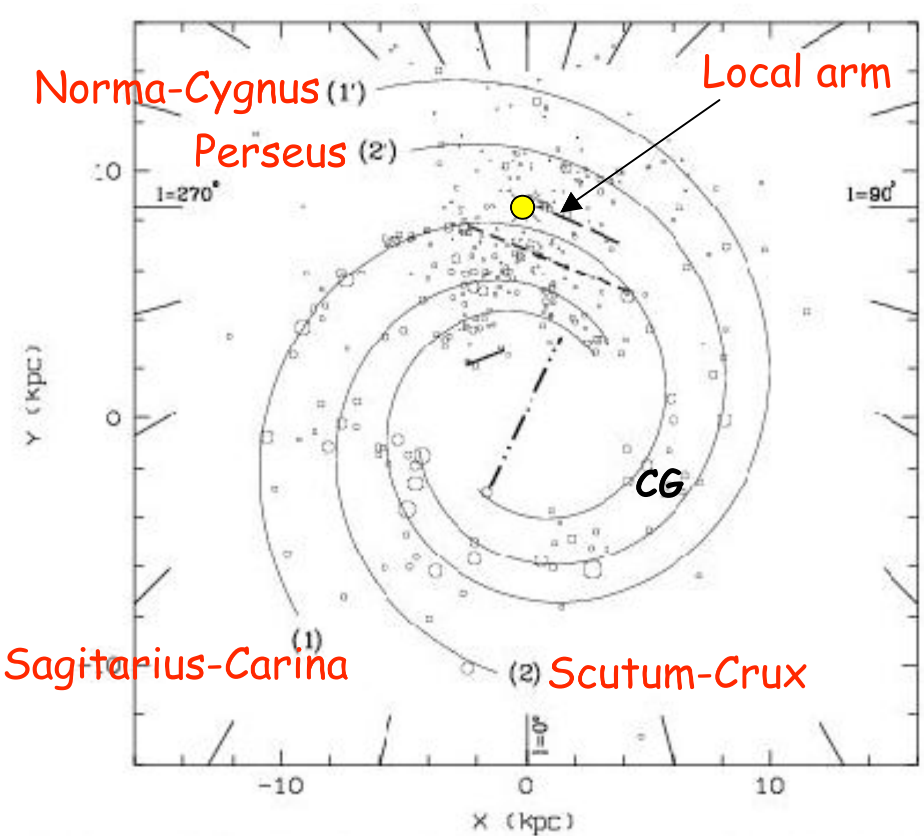

From HI (Nakanishi & Sofue 2003 PASJ)

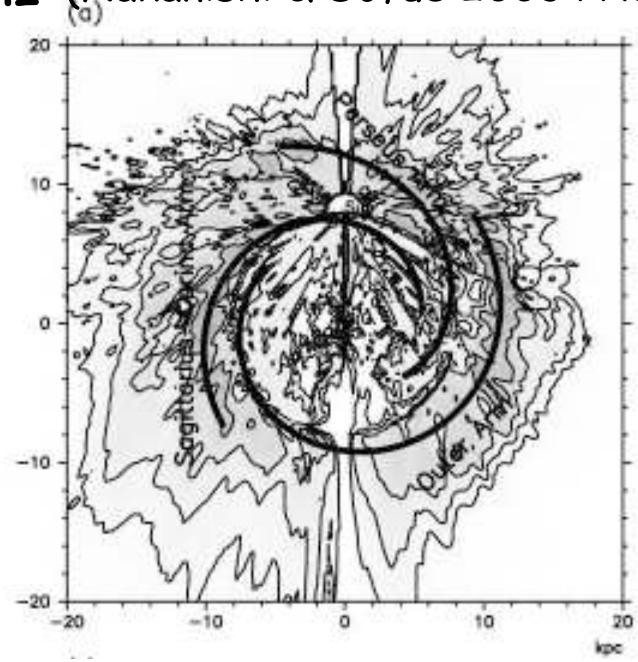

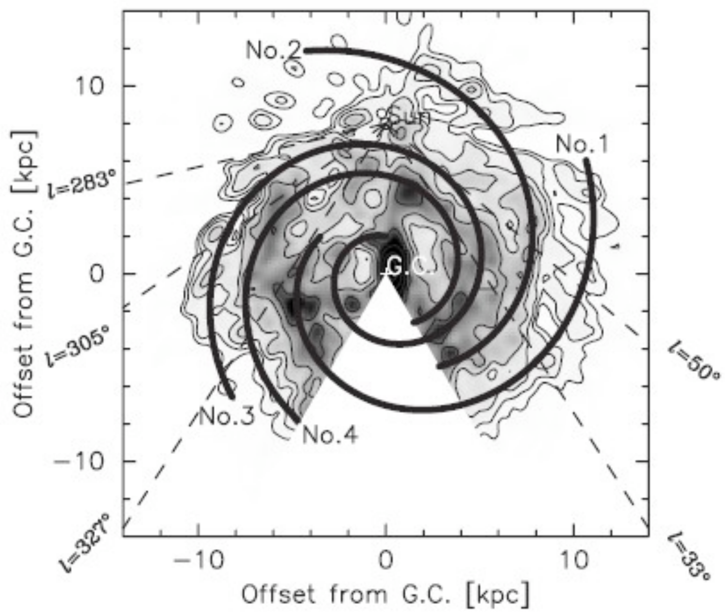

From CO(1-0)

(Nakanishi & Sofue 2006 PASJ)

From HI

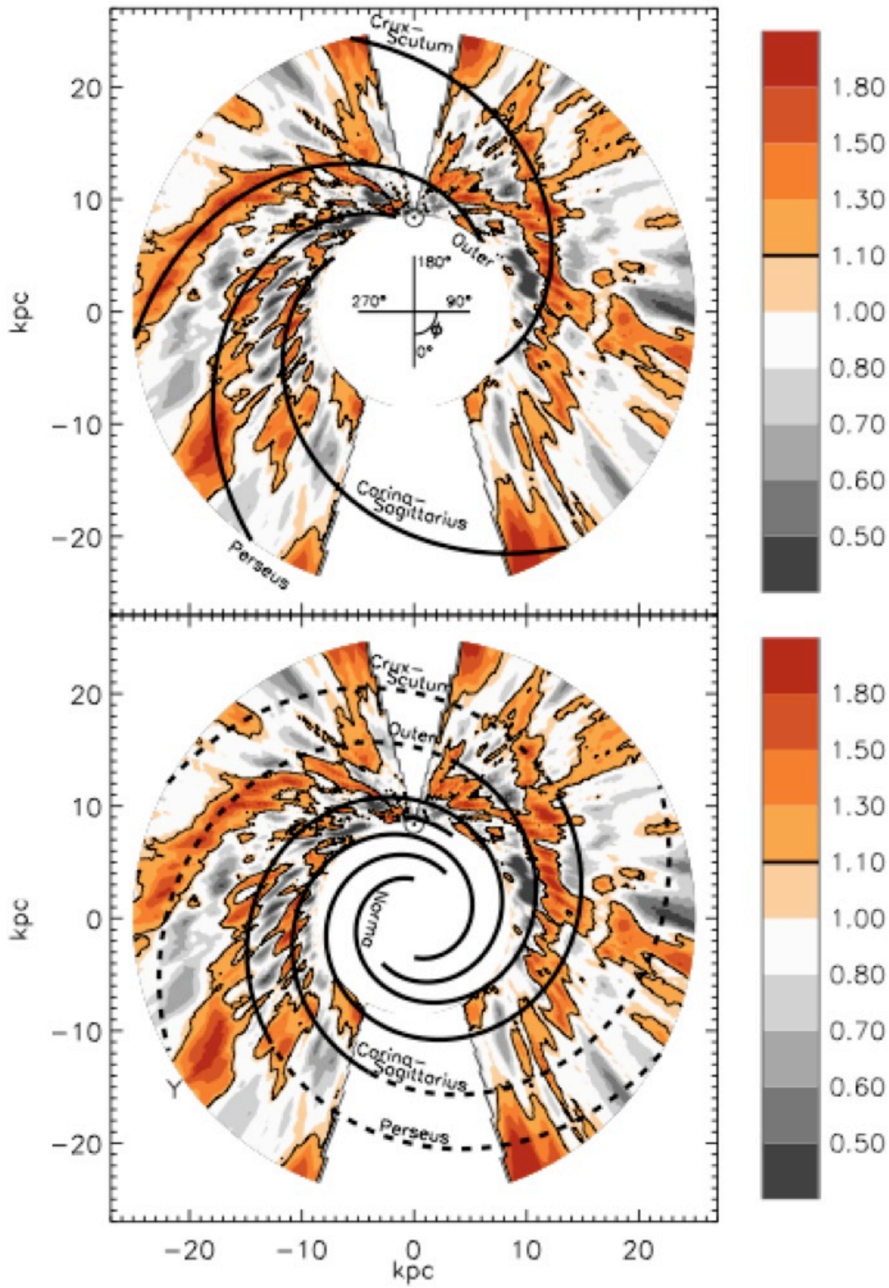

Levine, Blitz, Heiles, Weinberg 2008, 2006

NEW Outer arm in HI

McClure-Griffiths et al. 2004

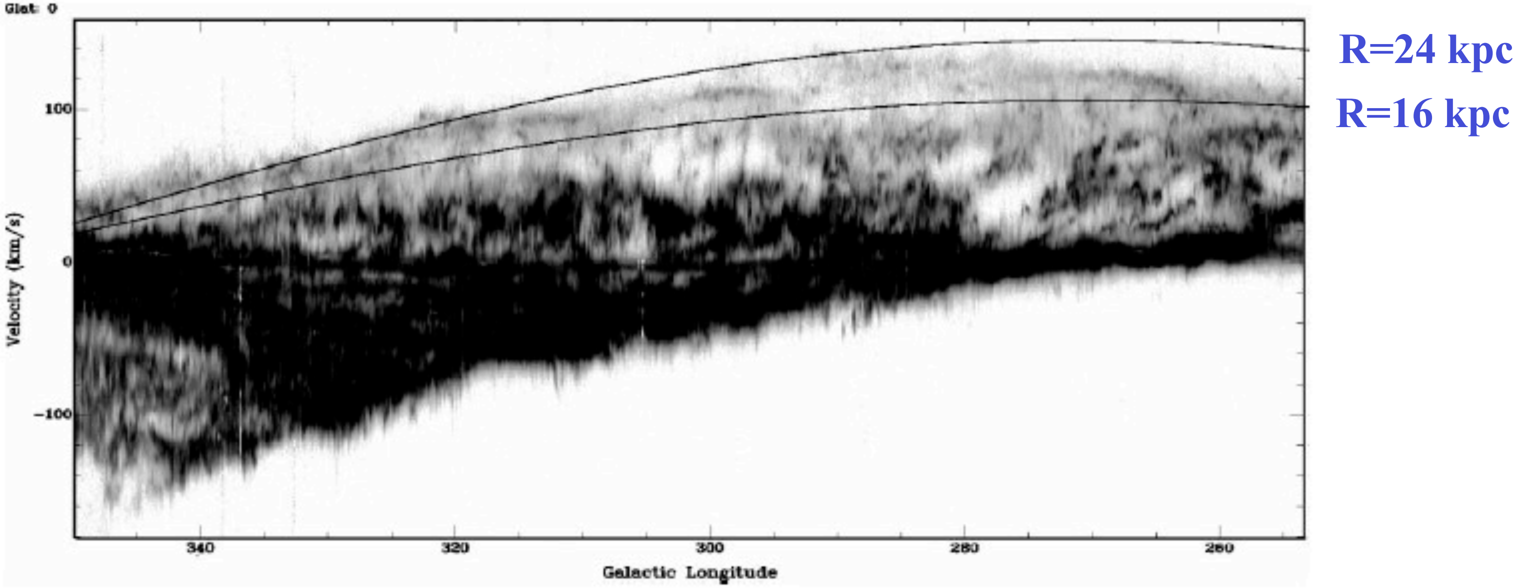

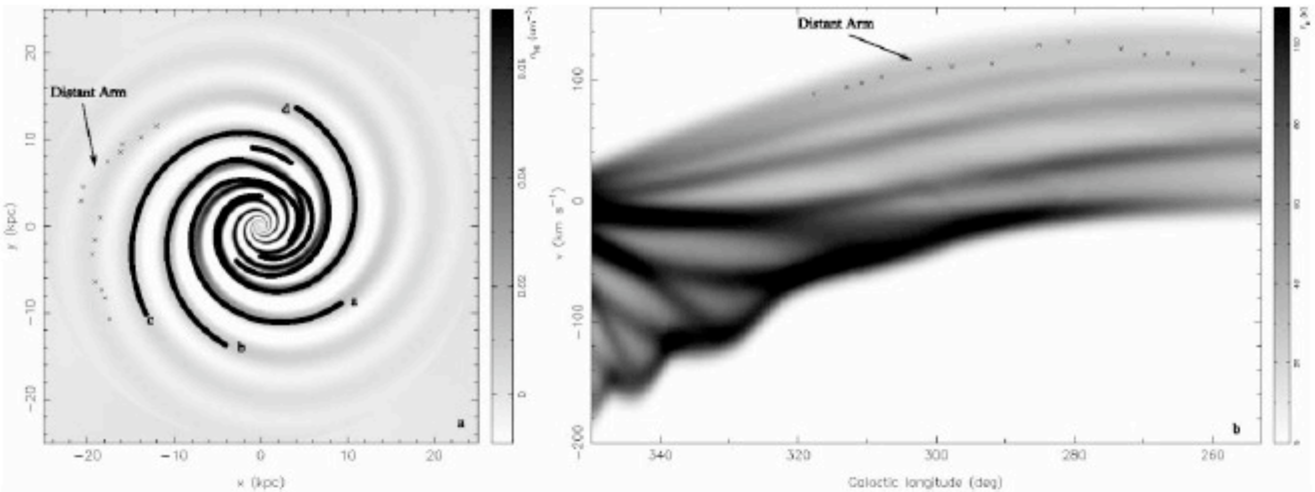

FIG. 1.—(*a*) Differential H I density (spiral perturbation minus the underlying Toomre disk) for the simple four-arm Milky Way spiral model described in § 4.

The multi-phase ISM

		T(K)	$n_H(cm^{-3})$	f_V	f_M	Probes
HII						
traditional		10^4	$0.1\text{-}10^4$	0.001	0.02	Hα, recomb. lines
coronal	HIM	$\geq 3\times10^5$	0.003	0.6?	0.001	[OVI], X-rays
warm	WIM	8000	0.25	0.2	0.1?	HI,Hα, H166α
HI						
clouds	CNM	80	40	0.025	0.4	HI
warm	WNM	8000	0.4	0.1-0.5?		HI
H_2						
diffuse	Transl	30-80	$10^2\text{-}10^3$	≤ 0.01		HI,CO,100μm
dense	Dark	10-100	$10^3\text{-}10^6$	0.005	0.5	mm molec.lines FIR dust

Models of the ISM (2-phase)

Early model: Field, Goldsmith & Habing 1969

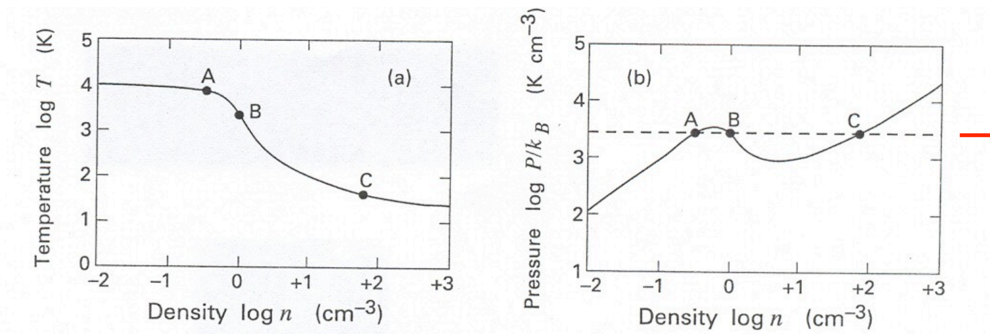

Figure 2.5 (a) Theoretical prediction for the equilibrium temperature of interstellar gas, displayed as a function of the number density n. (b) Equilibrium pressure nT as a function of number density. The horizontal dashed line indicates the empirical nT-value for the interstellar medium.

→ Log(P/k) = 3.5 cm^{-3} K

Assume pressure equilibrium (P/k ∝ nT = constant)

Stable points: A and C, corresponding to:

WNM (n=0.4, T=7000) and CNM (n=60, T=50)

Explained most of the then-known observations.

Models of the ISM (3-phase)

Ostriker & McKee 1977: 3-phase model

Gas distributed among 4(!) forms: HIM, WIM, WNM, CNM
that are in P-equil. at $P/k \approx 3000\ \mathrm{K cm^{-3}}$.

SNe, OB-winds create system of hot tunnels in ISM

Recent assesment: Cox, 2005 Ann. Rev. A&A 43

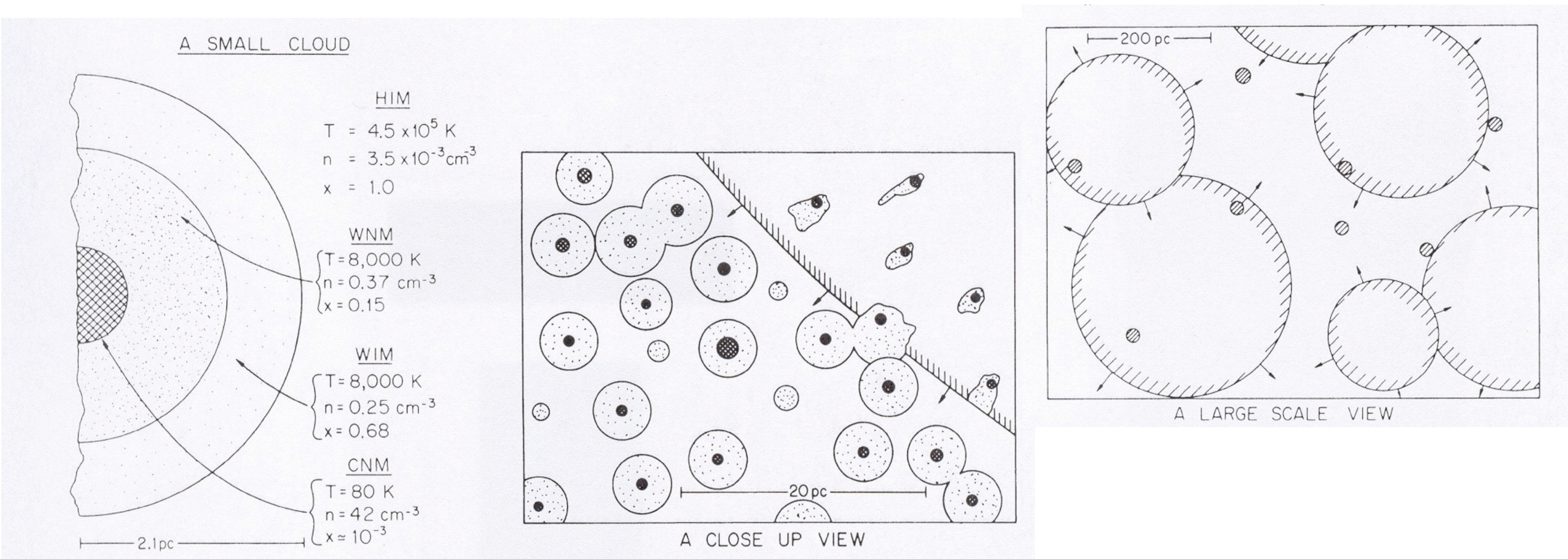

Models of the ISM (Cox upgrade)

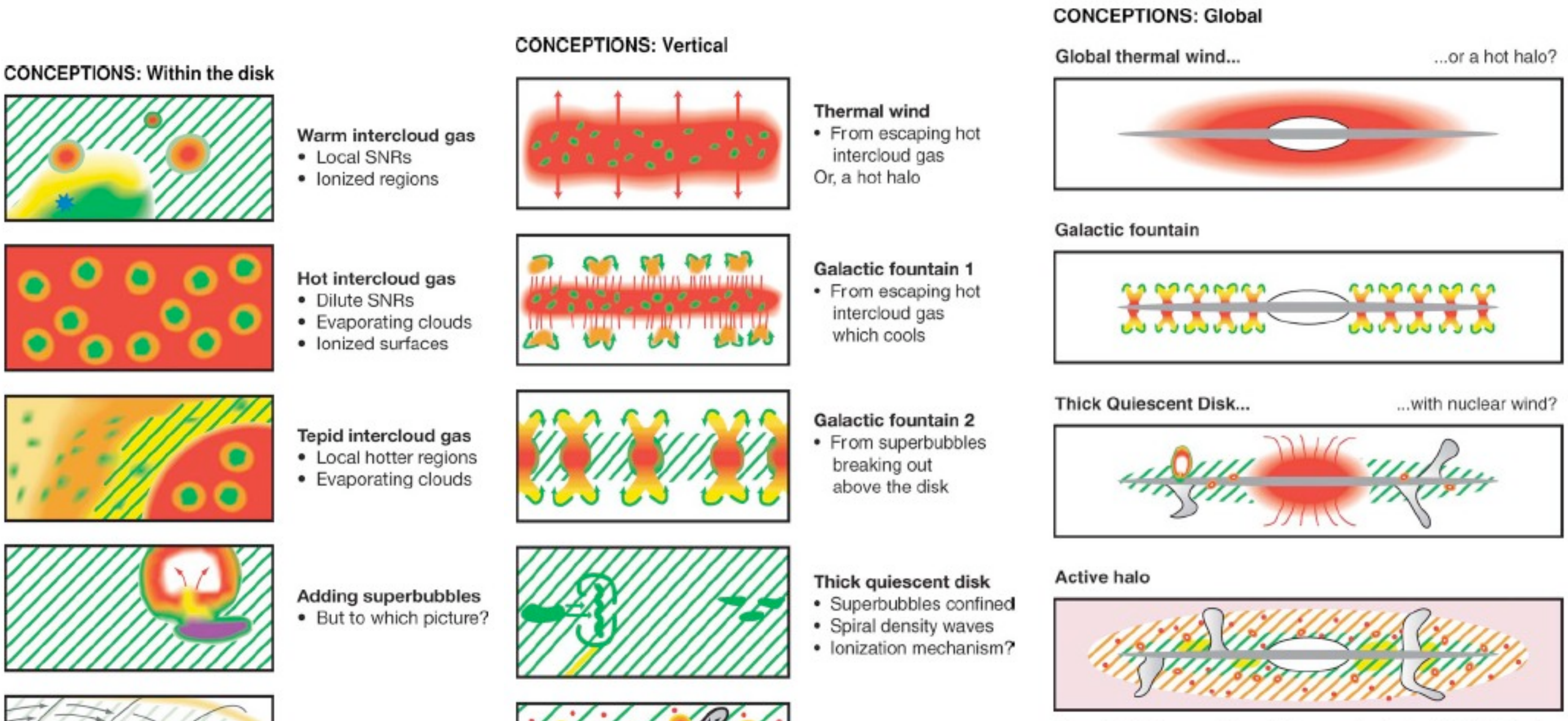

Firure 10 Various conceptions of the larger scale structure of the Galactic atmosphere. In this figure, *hatched green* indicates warm HI; *hatched green on yellow background*—diffuse warm HII; *orange*—hotter gas bearing OVI; *red*—material hot enough to emit X rays; *gray*—plumes of escaping cosmic rays; and *red dots*—microflares. Problems with the *top two panels* are discussed in the text. The *lower two panels* contain some elements of potentially greater realism.

Cox 2005 ARAA 43

Molecular clouds – transition interface

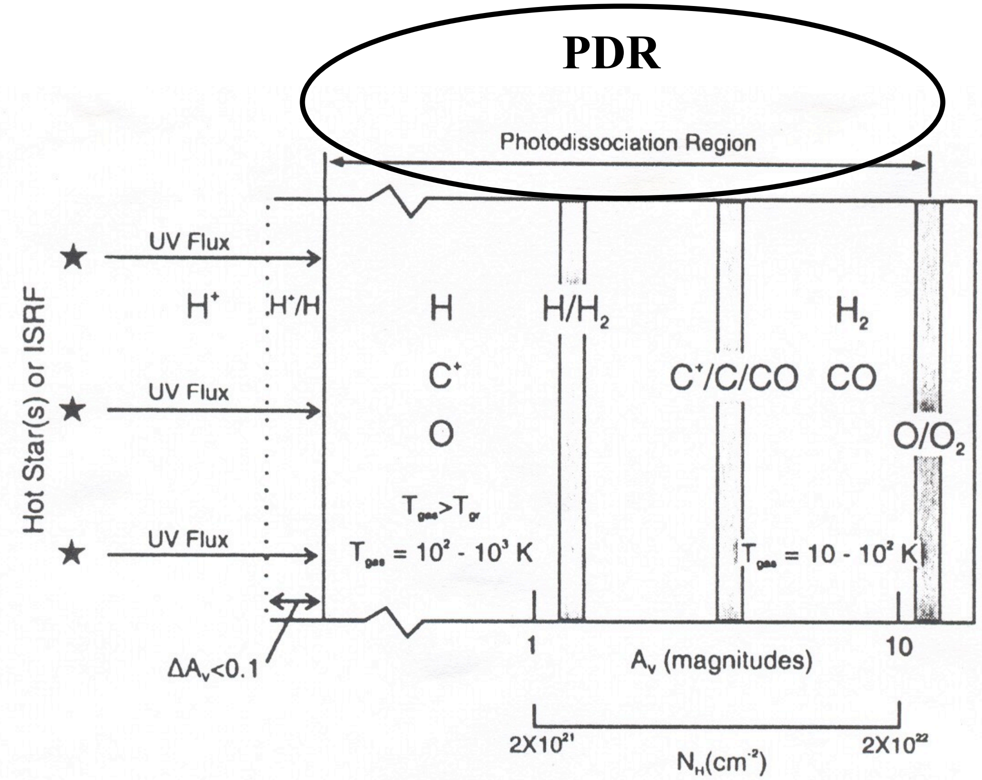

Figure 3 A schematic diagram of a photodissociation region. The PDR is illuminated from the left and extends from the predominantly atomic surface region to the point where O_2 is not appreciably photodissociated ($\simeq$10 visual magnitude). Hence, the PDR includes gas whose hydrogen is mainly H_2 and whose carbon is mostly CO. Large columns of warm O, C, C^+, and CO and vibrationally excited H_2 are produced in the PDR. The gas temperature T_{gas} generally exceeds the dust temperature T_{gr} in the surface layer.

Molecular clouds are self-shielding against UV radiation.

Clouds are surrounded by envelope of HI.

Inside: molecules. Most abundant after H_2 is CO (10^{-4}).

Molecular clouds: atomic envelope

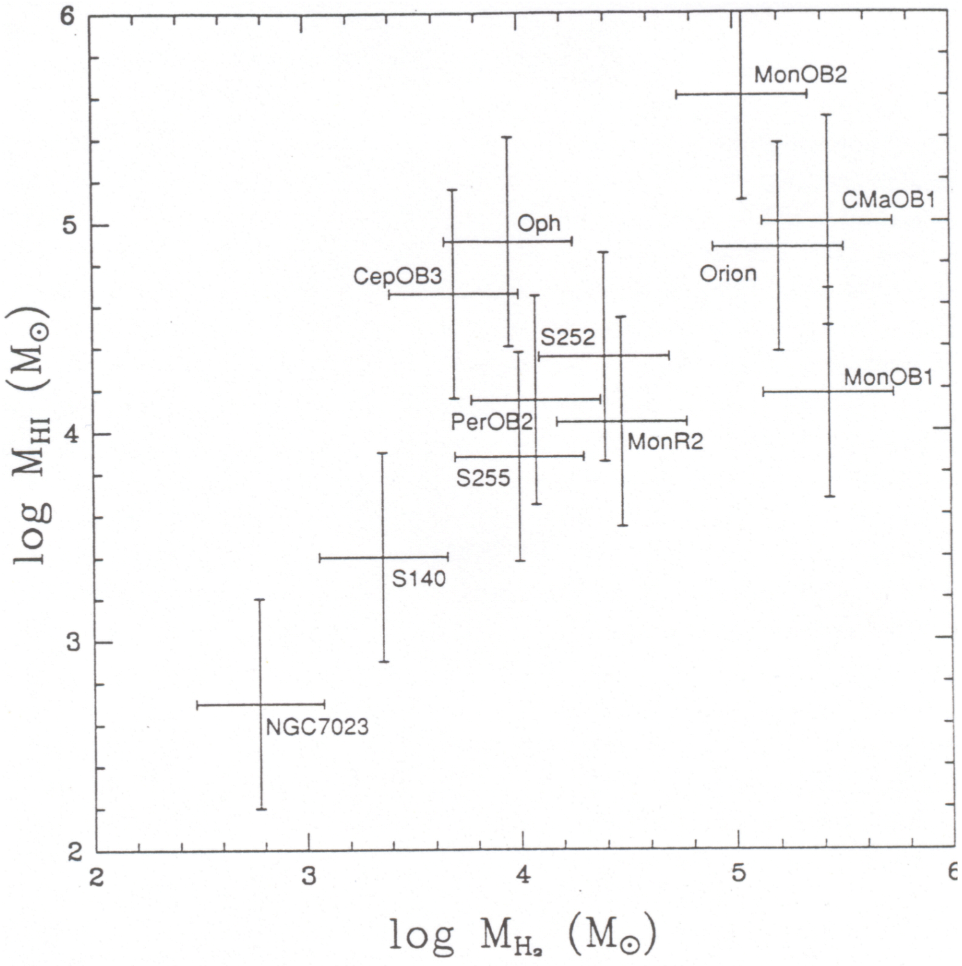

Blitz, 1993 PPIII

Sh 2 - 217 Hα

Deharveng et al. 2003

Sh 2 - 217 Hα Opt. + HI

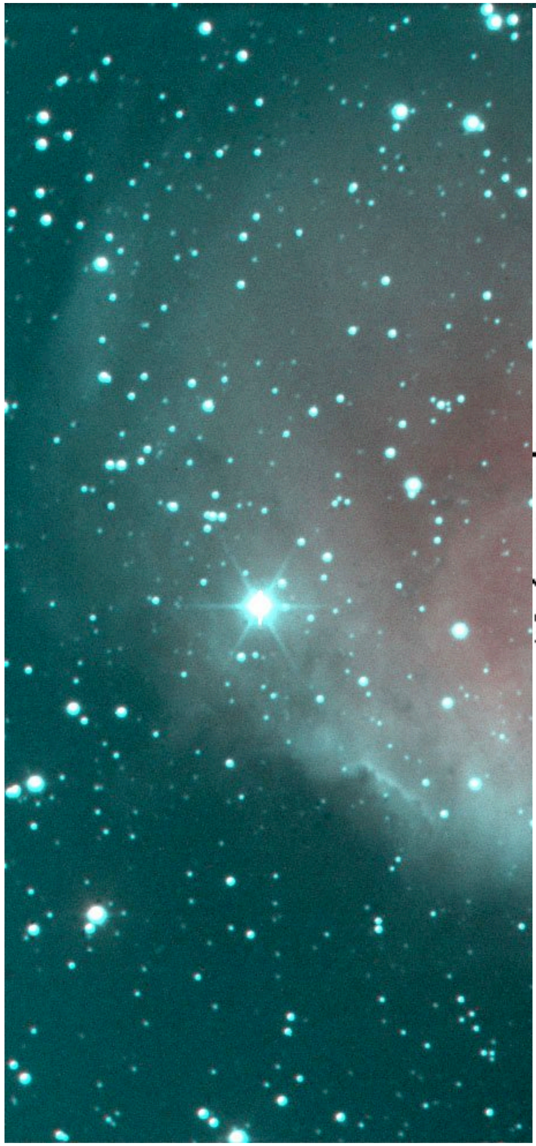

Deharveng et al. 2003

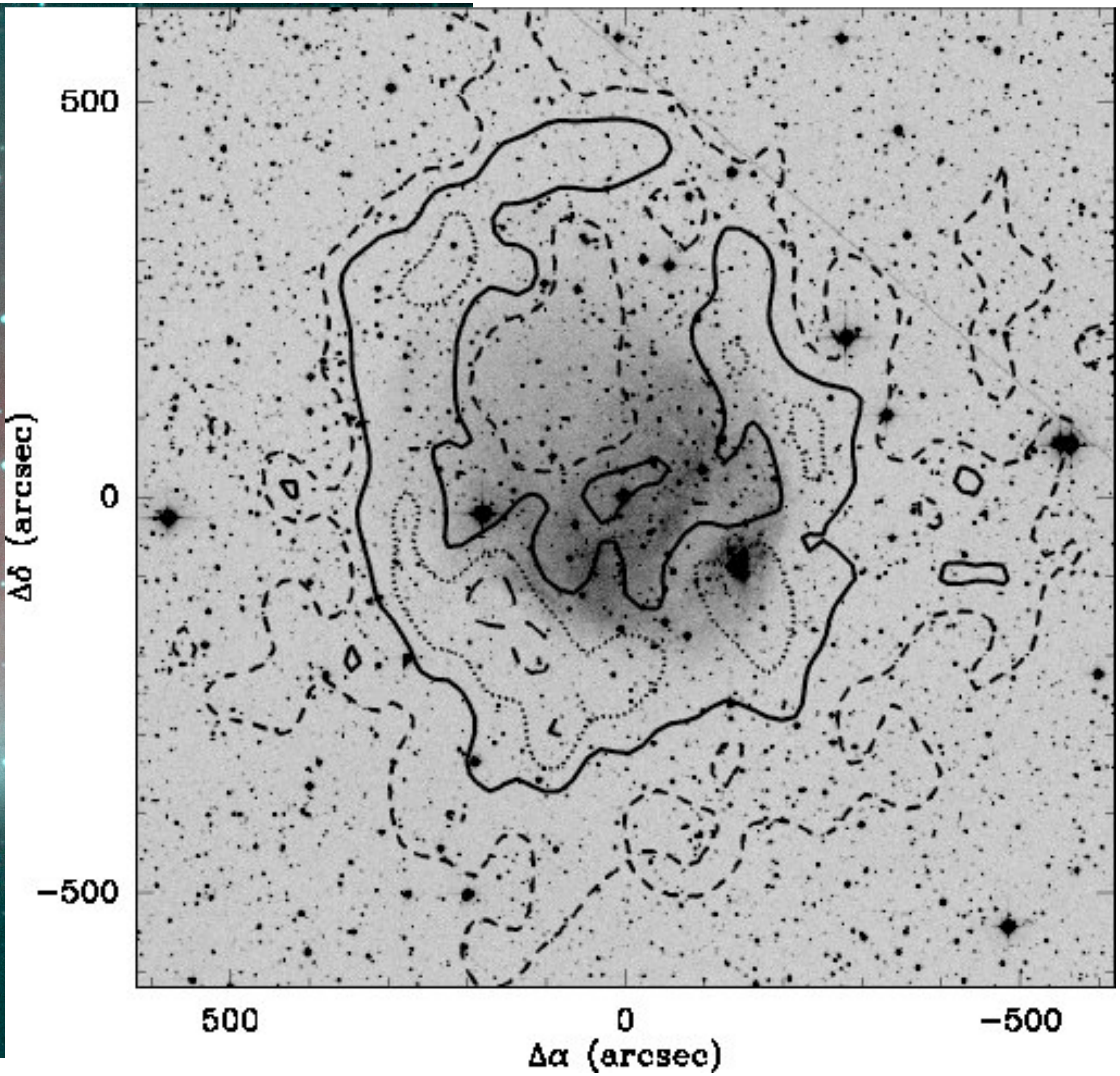

Brand et al. 2009 in prep.

Interstellar Molecules

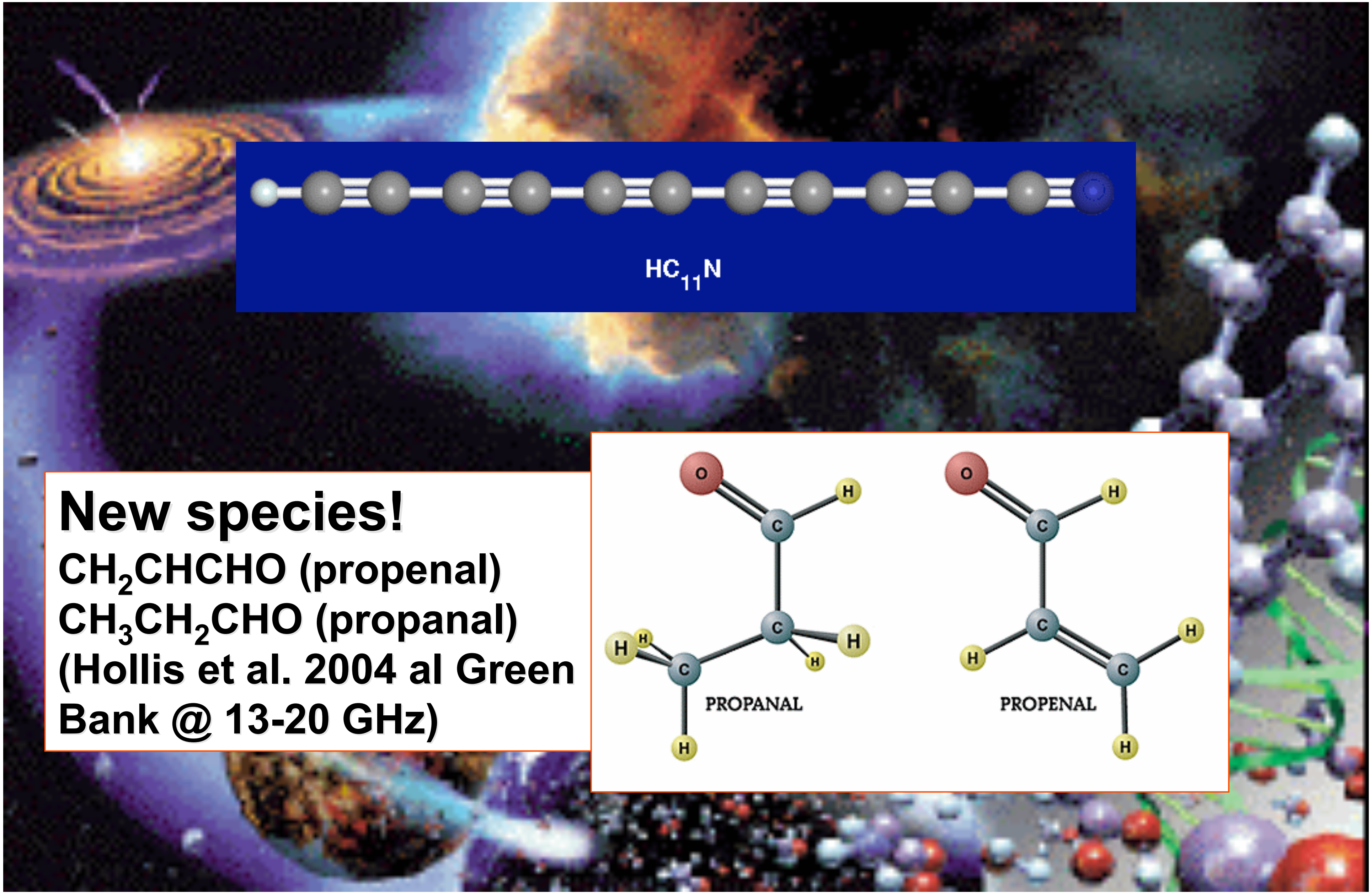

New species!

CH_2CHCHO (propenal)
CH_3CH_2CHO (propanal)
(Hollis et al. 2004 al Green Bank @ 13-20 GHz)

Circa 150 molecules have been detected in space

Page 1

Molecules in the Interstellar Medium or Circumstellar Shells (as of 09/2009)

2 atoms	3 atoms	4 atoms	5 atoms	6 atoms	7 atoms	8 atoms	9 atoms	10 atoms	11 atoms	12 atoms	13 atoms
H_2	C_3^*	c-C_3H	C_5^*	C_5H	C_6H 2008	CH_3C_3N	CH_3C_4H	CH_3C_5N	HC_9N	$C_6H_6^*$ (?)	$HC_{11}N$
AlF	C_2H	l-C_3H	C_4H	l-H_2C_4	CH_2CHCN 2008	$HC(O)OCH_3$	CH_3CH_2CN	$(CH_3)_2CO$	CH_3C_6H	$C_2H_5OCH_3$?	
AlCl	C_2O	C_3N	C_4Si	$C_2H_4^*$	CH_3C_2H	CH_3COOH	$(CH_3)_2O$	$(CH_2OH)_2$	C_2H_5OCHO 2009	n-C_3H_7CN 2009	
C_2^{**}	C_2S	C_3O	l-C_3H_2	CH_3CN	HC_5N	C_7H	CH_3CH_2OH	CH_3CH_2CHO			
CH	CH_2	C_3S	c-C_3H_2	CH_3NC	CH_3CHO	H_2C_6	HC_7N				
CH^+	HCN	$C_2H_2^*$	H_2CCN	CH_3OH	CH_3NH_2	CH_2OHCHO	C_8H				
CN	HCO	NH_3	CH_4^*	CH_3SH	c-C_2H_4O	l-HC_6H^* (?)	$CH_3C(O)NH_2$				
CO	HCO^+	HCCN	HC_3N	HC_3NH^+	H_2CCHOH	CH_2CHCHO (?)	C_8H^-				
CO^+	HCS^+	$HCNH^+$	HC_2NC	HC_2CHO	C_6H^-	CH_2CCHCN	C_3H_6				
CP	HOC^+	HNCO	HCOOH	NH_2CHO		H_2NCH_2CN 2008					
SiC	H_2O	HNCS	H_2CNH	C_5N							
HCl	H_2S	$HOCO^+$ 2008	H_2C_2O	l-HC_4H^* (?)							
KCl	HNC	H_2CO	H_2NCN	l-HC_4N							
NH	HNO	H_2CN	HNC_3	c-H_2C_3O							
NO	MgCN	H_2CS	SiH_4^*	H_2CCNH (?)							

Ca. 150 mol's

Source: CDMS [Cologne Database for Molecular Spectroscopy]

2 atoms	3 atoms	4 atoms	5 atoms	6 atoms	7 atoms	8 atoms	9 atoms	10 atoms	11 atoms	12 atoms	13 atoms
NS	MgNC	H_3O^+	H_2COH^+	C_5N^- 2008							
NaCl	N_2H^+	c-SiC_3	C_4H^- 2008								
OH	N_2O	CH_3*	HC(O)CN 2008								
PN	NaCN	C_3N^- 2008									
SO	OCS	PH_3 ? 2008									
SO^+	SO_2	HCNO 2009									
SiN	c-SiC_2	HOCN ? 2009									
SiO	CO_2*	HSCN 2009									
SiS	NH_2										
CS	H_3^+*										
HF	H_2D^+, HD_2^+										
SH^+	SiCN										
HD	AlNC										
FeO ?	SiNC										
O_2	HCP										
CF^+	CCP 2008										
SiH ?											
PO											
AlO 2009											

Extragalactic Molecules (as of 01/2008)

2 atoms	3 atoms	4 atoms	5 atoms	6 atoms	7 atoms
OH	H_2O	H_2CO	c-C_3H_2	CH_3OH	CH_3CCH
CO	HCN	NH_3	HC_3N	CH_3CN	
H_2	HCO^+	HNCO	CH_2NH		
CH **	C_2H	H_2CS (?)	NH_2CN		
CS	HNC	$HOCO^+$			
CH^+ **	N_2H^+	C_3H			
CN	OCS	H_3O^+ 2008			
SO	HCO				
SiO	H_2S				
CO^+ (?)	SO_2				
NO	HOC^+				
NS	C_2S				

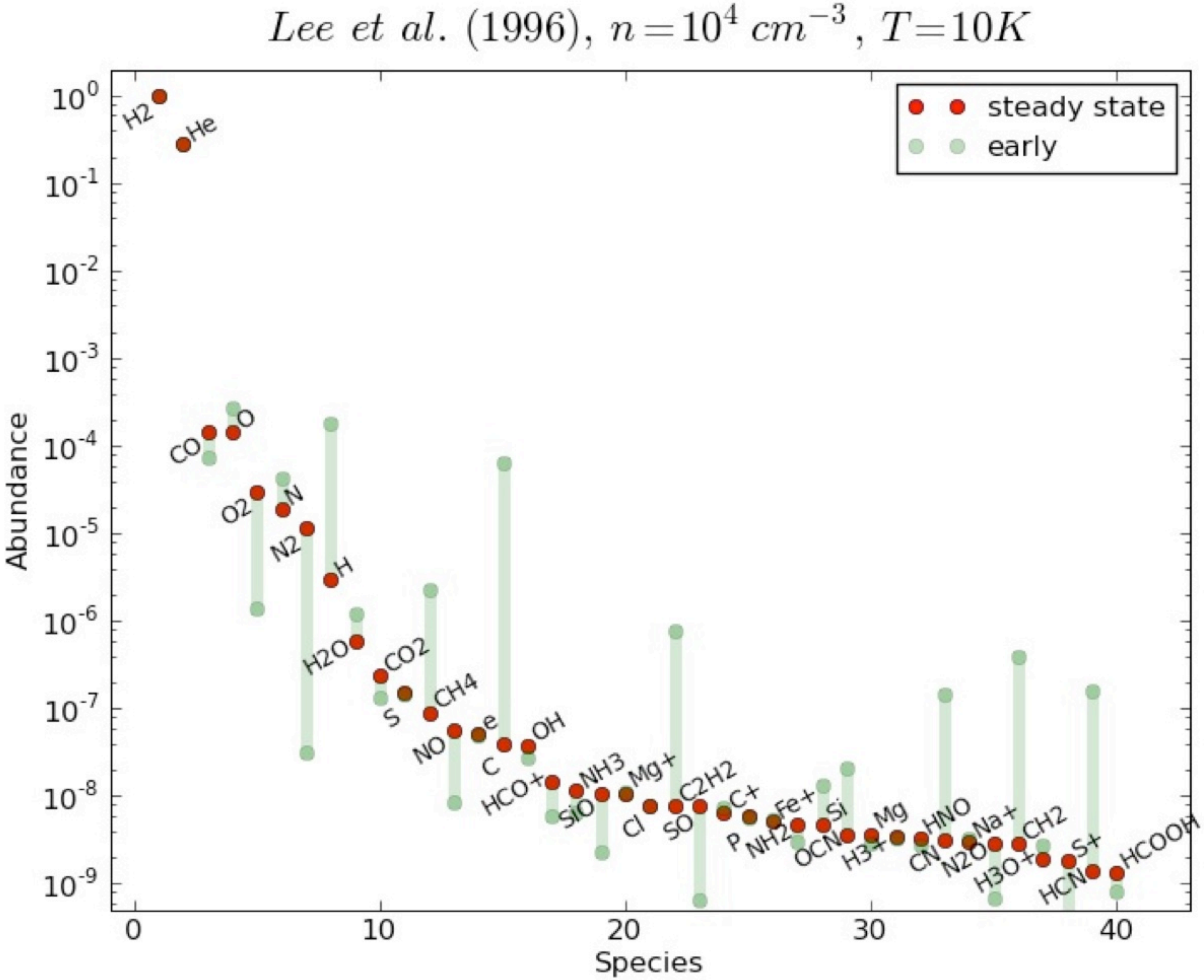

Lee et al. (1996), $n = 10^4\, cm^{-3}$, $T = 10K$
steady state
early
Abundance
Species
H2
He
CO
O
O2
N
N2
H
H2O
CO2
S
CH4
NO
e
C
OH
HCO+
SiO
NH3
Mg+
Cl
SO
C2H2
P
C+
NH2
Fe+
OCN
Si
H3+
Mg
CN
HNO
N2O
Na+
H3O+
CH2
HCN
S+
HCOOH

Astrochemistry. I.

- **Formation of H_2** (Gould & Salpeter 1963; Hollenbach & Salpeter 1970; Pirronello et al. 1999; Katz et al. 1999; Cazaux & Tielens 2002; Habart et al. 2003)

$R \sim 10^{-17}\ cm^3\ s^{-1}$

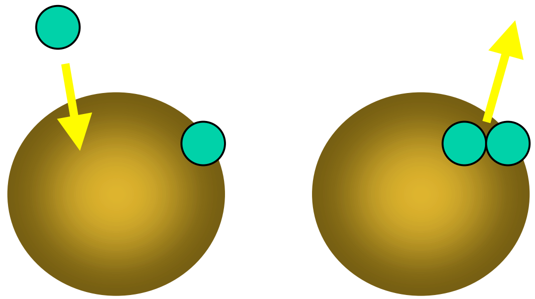

In gas phase:

$H^- + H \Rightarrow H_2 + e \quad R \sim 10^{-21} - 10^{-20}\ cm^3\ s^{-1}$

$H + H \Rightarrow H_2 + h\nu \quad R \sim 10^{-29} - 10^{-31}\ cm^3\ s^{-1}$

In molecular clouds: ion-neutral reactions

$C^+ + H_2 \Rightarrow CH_2^+ +$

$CH_2^+ + e^- \Rightarrow CH + H$

$CH + O \Rightarrow CO + H$

Astrochemistry. II.

- **Complex organic molecules** are easily observed near young stellar objects (e.g. Charnley et al. 1992; Caselli et al. 1993)

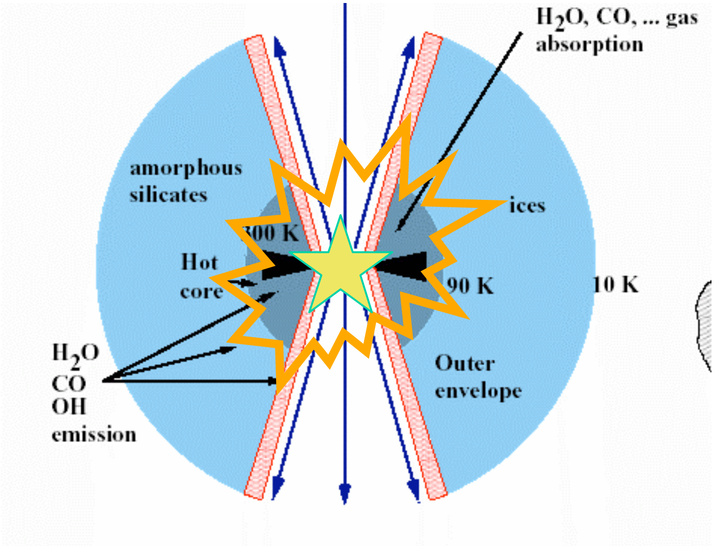

H-rich complex N-bearing and O-bearing molecules: CH_3CN, CH_2CHCN, CH_3CH_2CN, CH_3OCH_3, $HCOOCH_3$, C_2H_5OH.. (e.g. Blake et al. 1987)

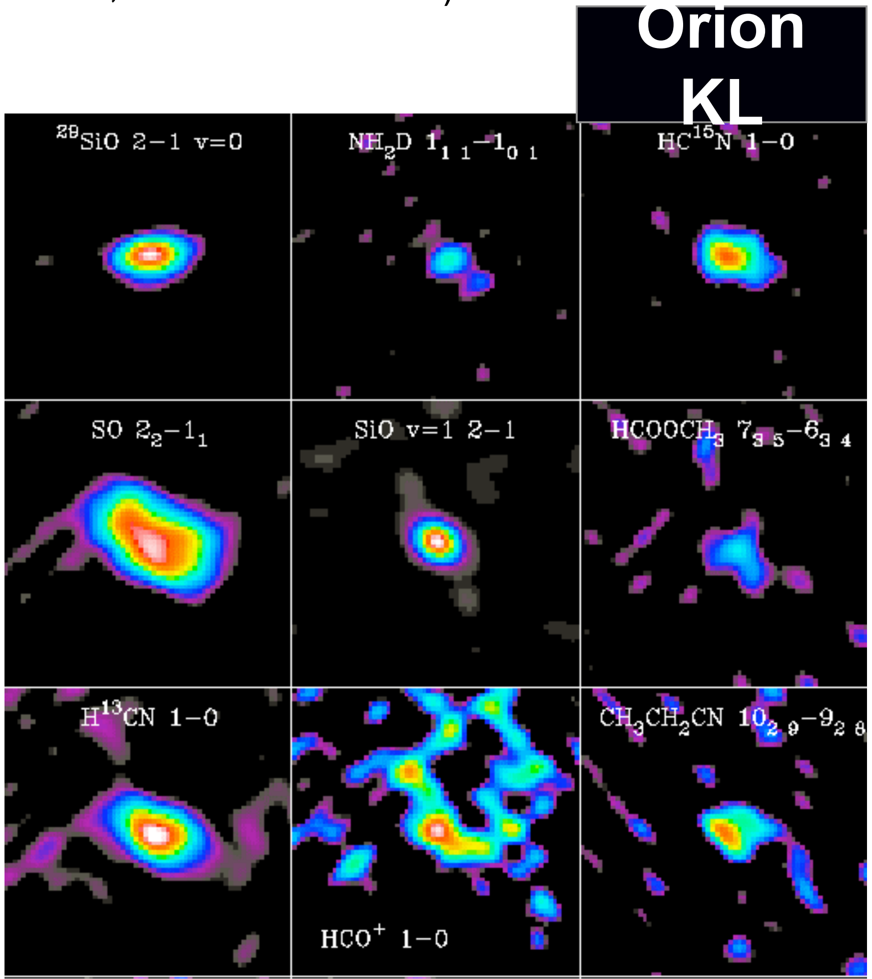

Astrochemistry. III.

- **To understand the distribution of the various molecular species to study the physical and kinematical properties of molecular clouds and of star formation.**
- Example: CO, typically used to determine the mass of molecular clouds, disappears from the gas phase at densities n(H2) > 10^4 cm^{-3} and T < 20 K.

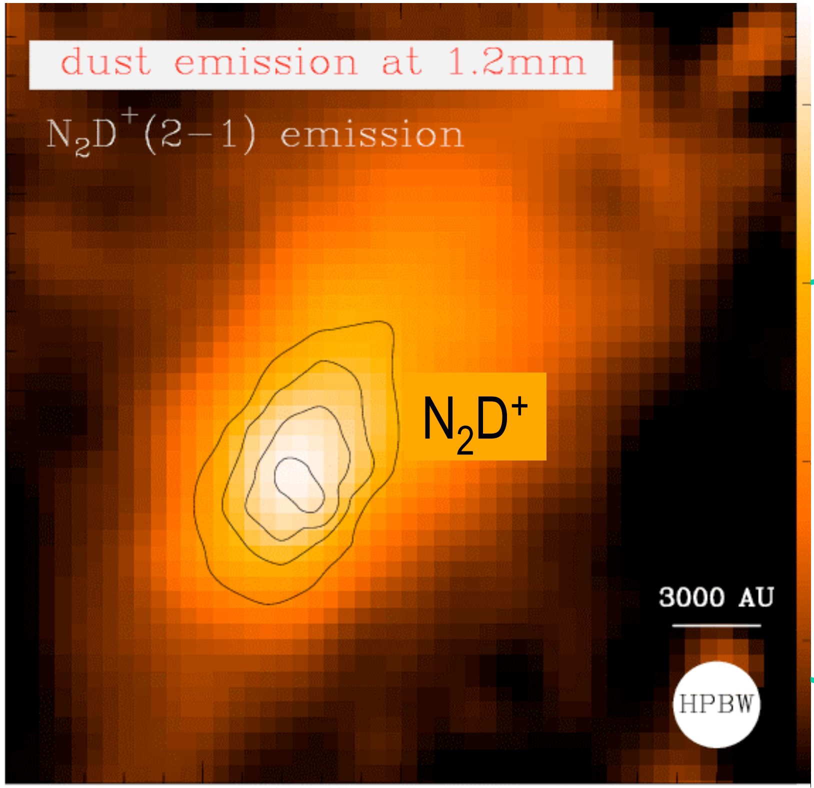

CO disappears from gas phase at R < 7000 AU

N_2 remains in the gas phase: more volatile than CO ?

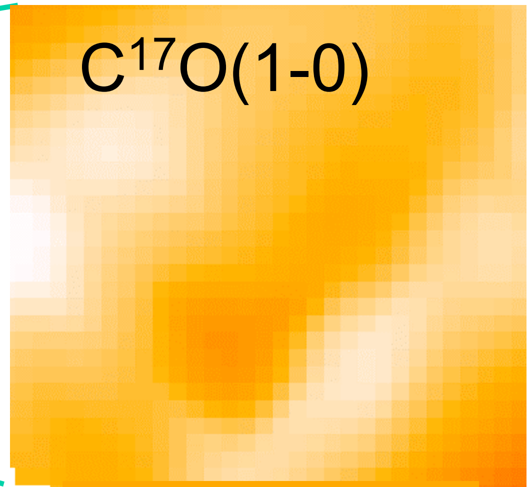

Caselli et al. 1999

L1517B: a low-mass pre-stellar core with depletion

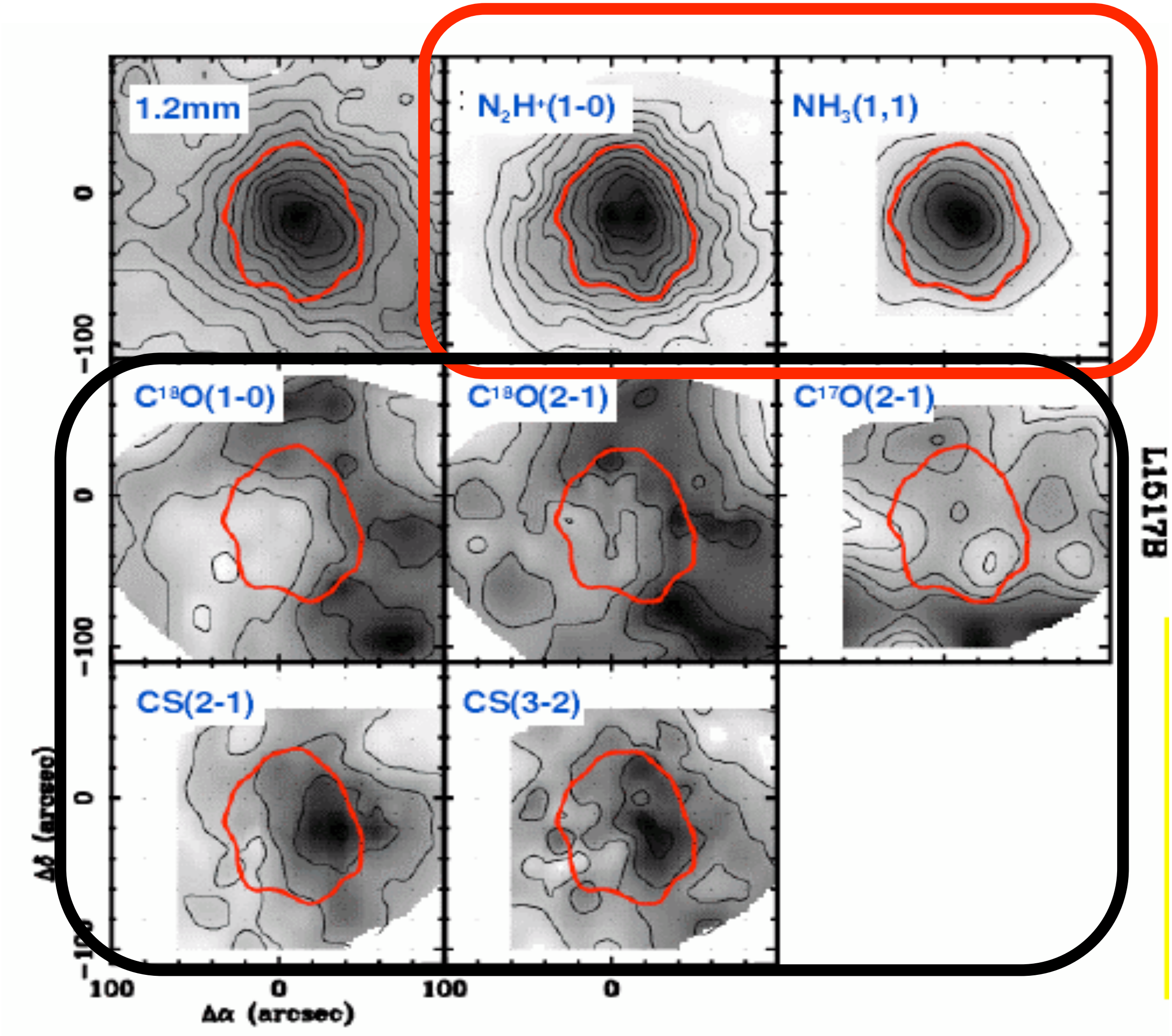

On the other hand, N-bearing species well trace the density profile seen in the dust continuum emission

C-bearing species completely miss the central density peak

Tafalla et al. 2004

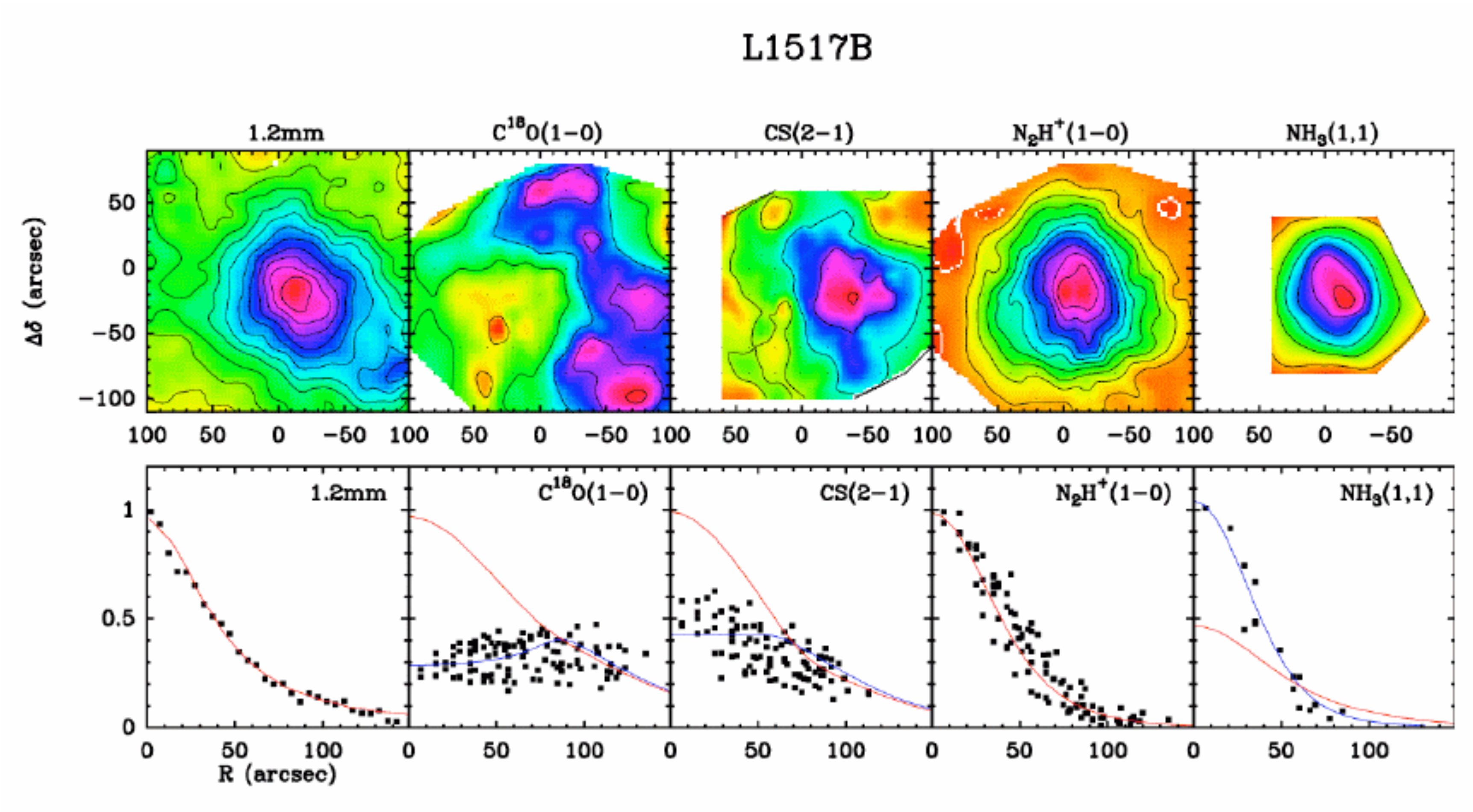

Cores have order-of-magnitude radial CS and CO abundance gradients

Shock-chemistry!

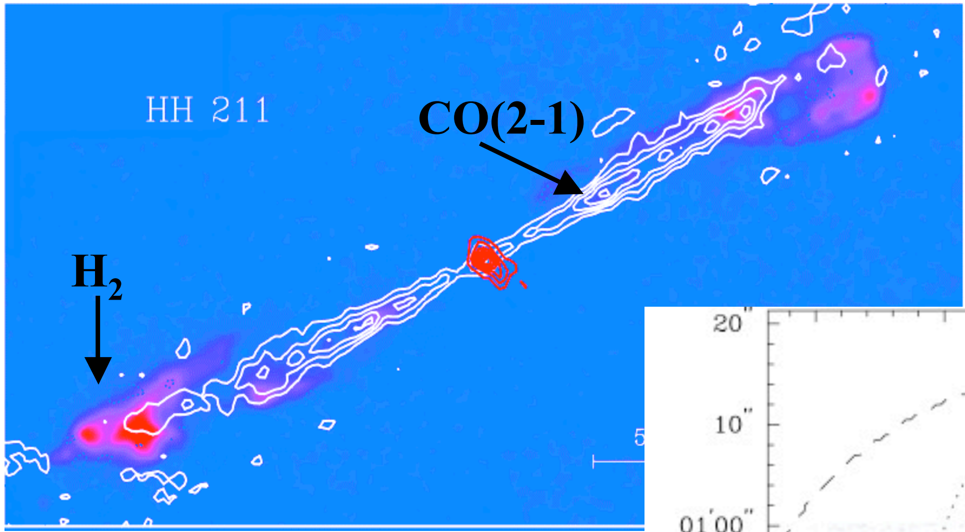

Gueth & Guilloteau (1999)

HH211

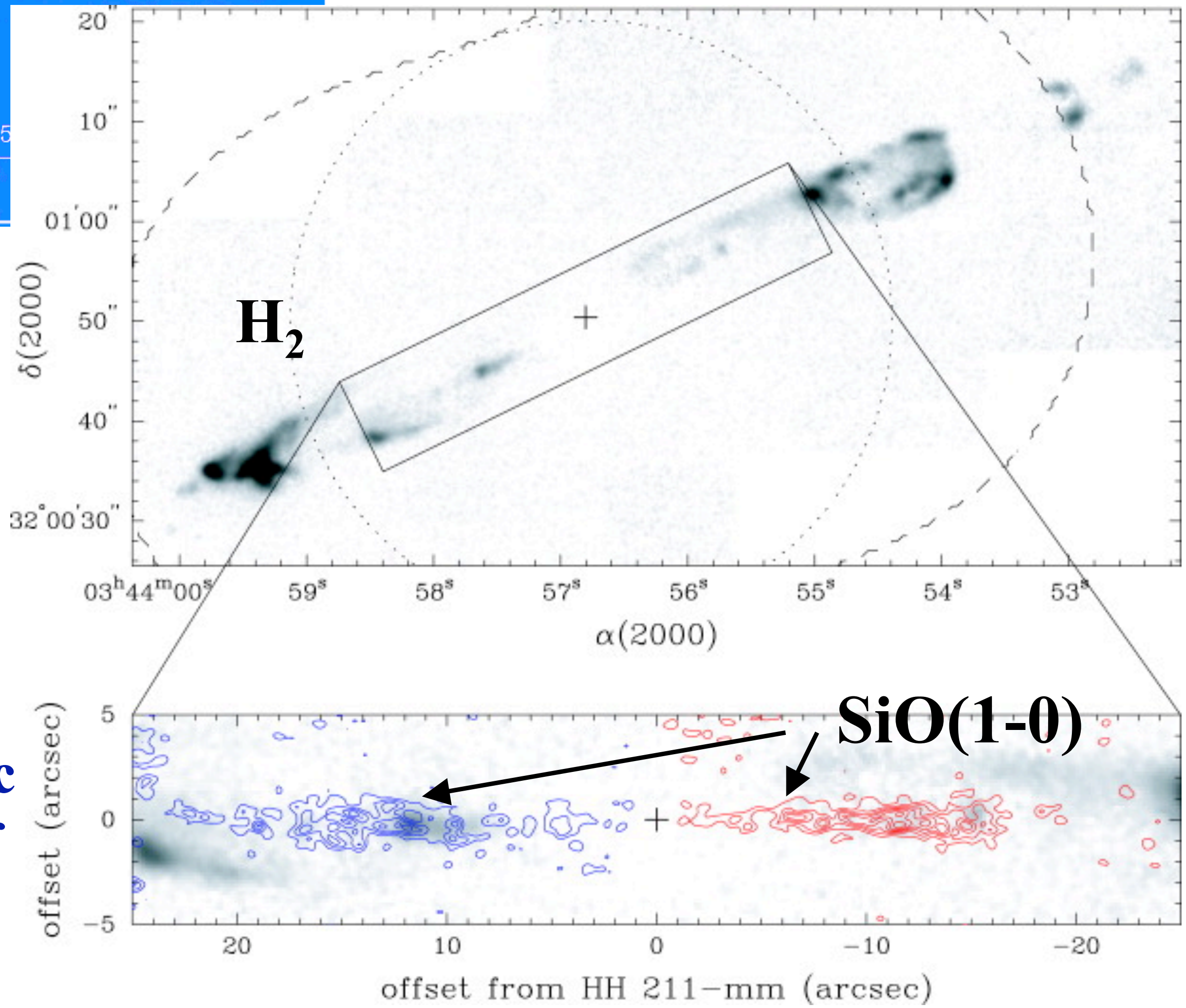

Chandler & Richer (2001)

The heating and compression caused by shocks gives rise to dramatic effects in the chemical composition of the surrounding cloud. Dissociation, endothermic reactions, sublimation of ices and disruption of grains lead to a shock-chemistry.

Chemically rich outflows

Shock tracers:
CH_3OH, SiO, H_2O, S-bearing species, H_2CO……

Bachiller & Tafalla (2000): an empirical time sequence of low-mass outflows?

1st stage (Class 0): jet-like, HV bullets;
2nd stage (Class 0): no bullets, rich chemistry;
3rd stage (Class I): shell structure, evacuated cavity.

L1157

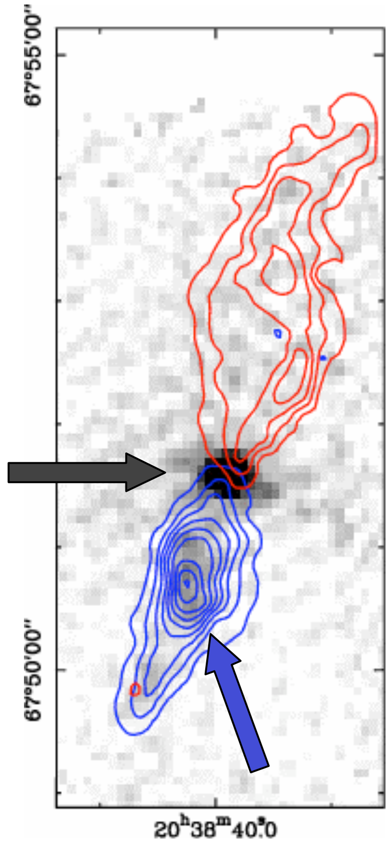

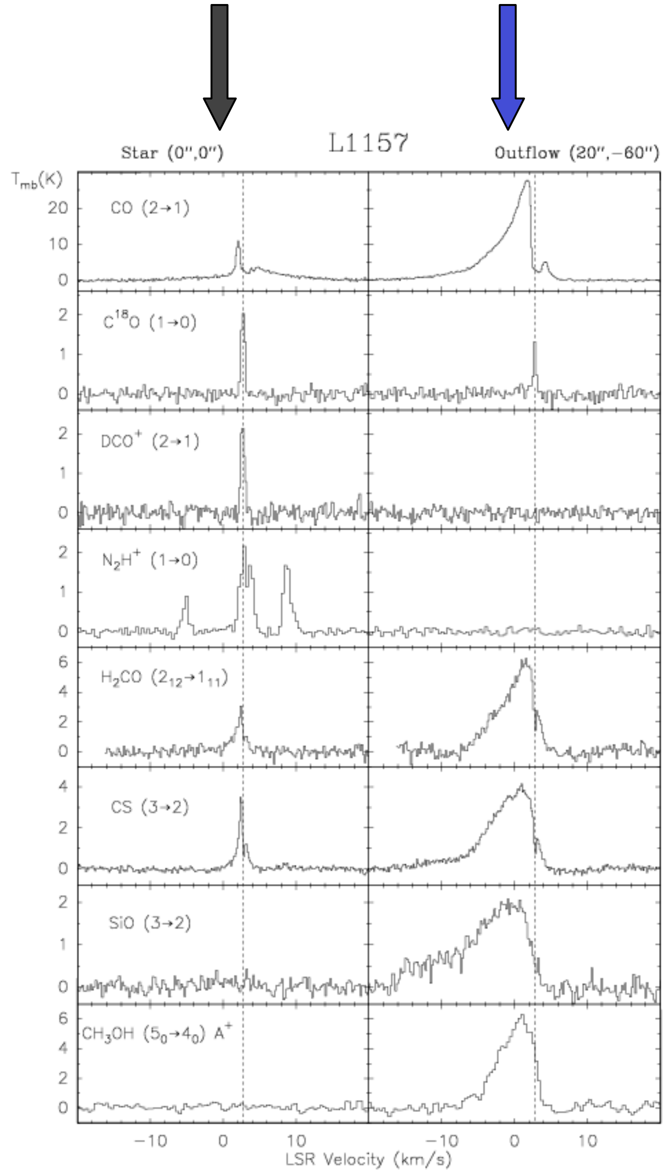

Bachiller et al. (2001)

Shock-enhanced abundances in outflows

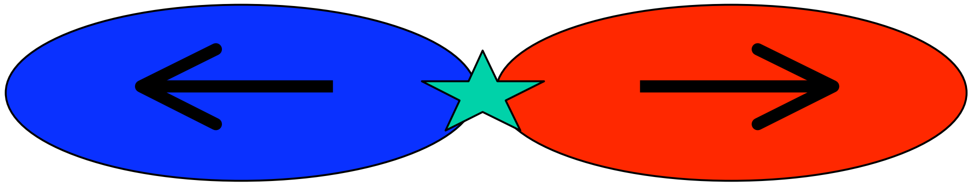

SiO	10^{-10} - 10^{-6}	< 10^{-12}
CH_3OH	10^{-7} - 10^{-5}	~ 10^{-9}
NH_3	~ 10^{-6}	~ 10^{-8}
H_2CO	~ 10^{-7}	~ 10^{-8}
HCN	~ 10^{-7}	~ 10^{-8}
SO	~ 10^{-7}	~ 5×10^{-9}

(with respect to H_2)

PROPERTIES
OF
MOLECULAR CLOUDS

Typical properties GMCs

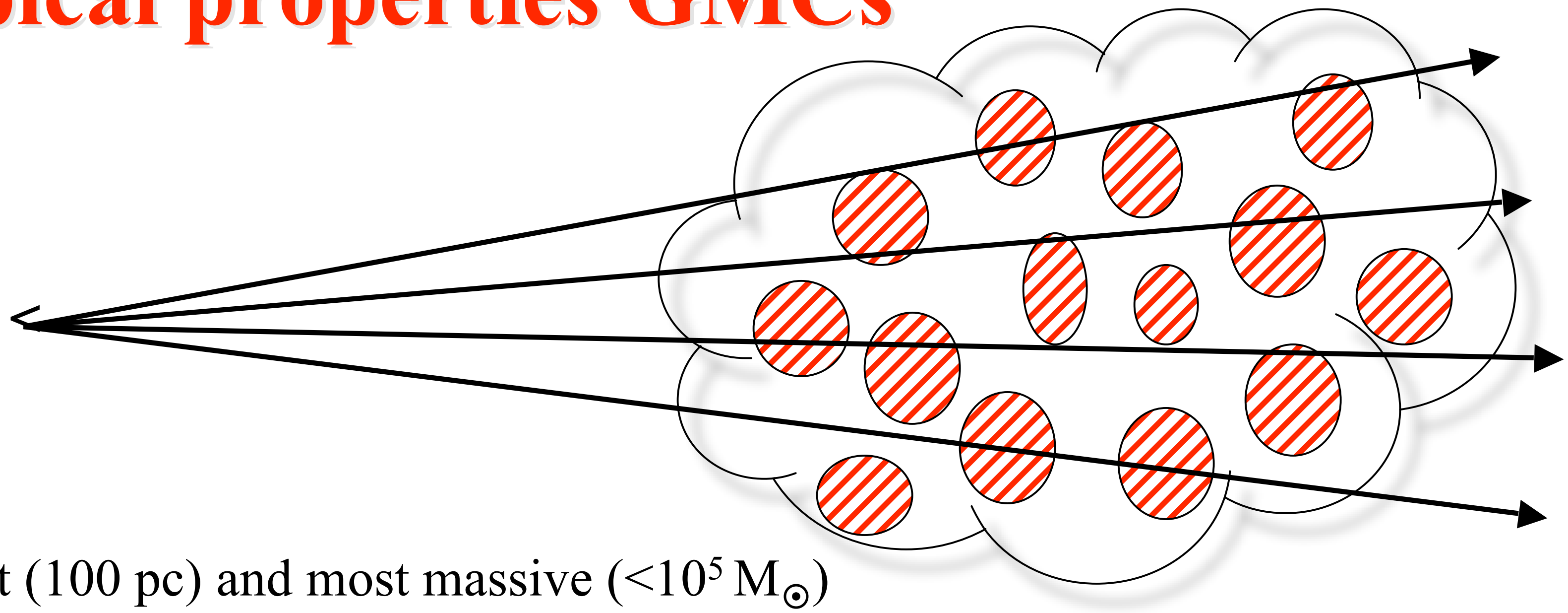

- Largest (100 pc) and most massive ($<10^5 M_\odot$) objects in Galaxy
- Not uniform: volume f.f.<<1
  surface f.f. ≈ 1
  (≥ 1 clump along the l.o.s.)
- $\Delta V_{obs} >> \Delta V_{therm} \approx (8\ln 2\ kT/\mu m_H)^{0.5}$
  line profile determined by velocity field of clumps: bulk motions.
- Gravitationally bound
  $P_{int}/k \sim 10^5$ Kcm^{-3} >>
  $< P_{ism}/k > \sim 10^4$ Kcm^{-3}

- All OB stars form in GMCs
- Strong confinement to spiral arms
  (contrast arm-interarm > 28:1)
- ΔV(cloud-cloud) ≈ 3-9 km/s (median 4.2)
  ≠ f(M) ≠ f(R)
- GMCs are young (< few 10^7 yr)
- Material stays locked up in stars: replenishment needed
  (SFR ~ 2-4 $M_\odot$/yr, return ~ 0.8 $M_\odot$/yr

Molecular clouds: elongated

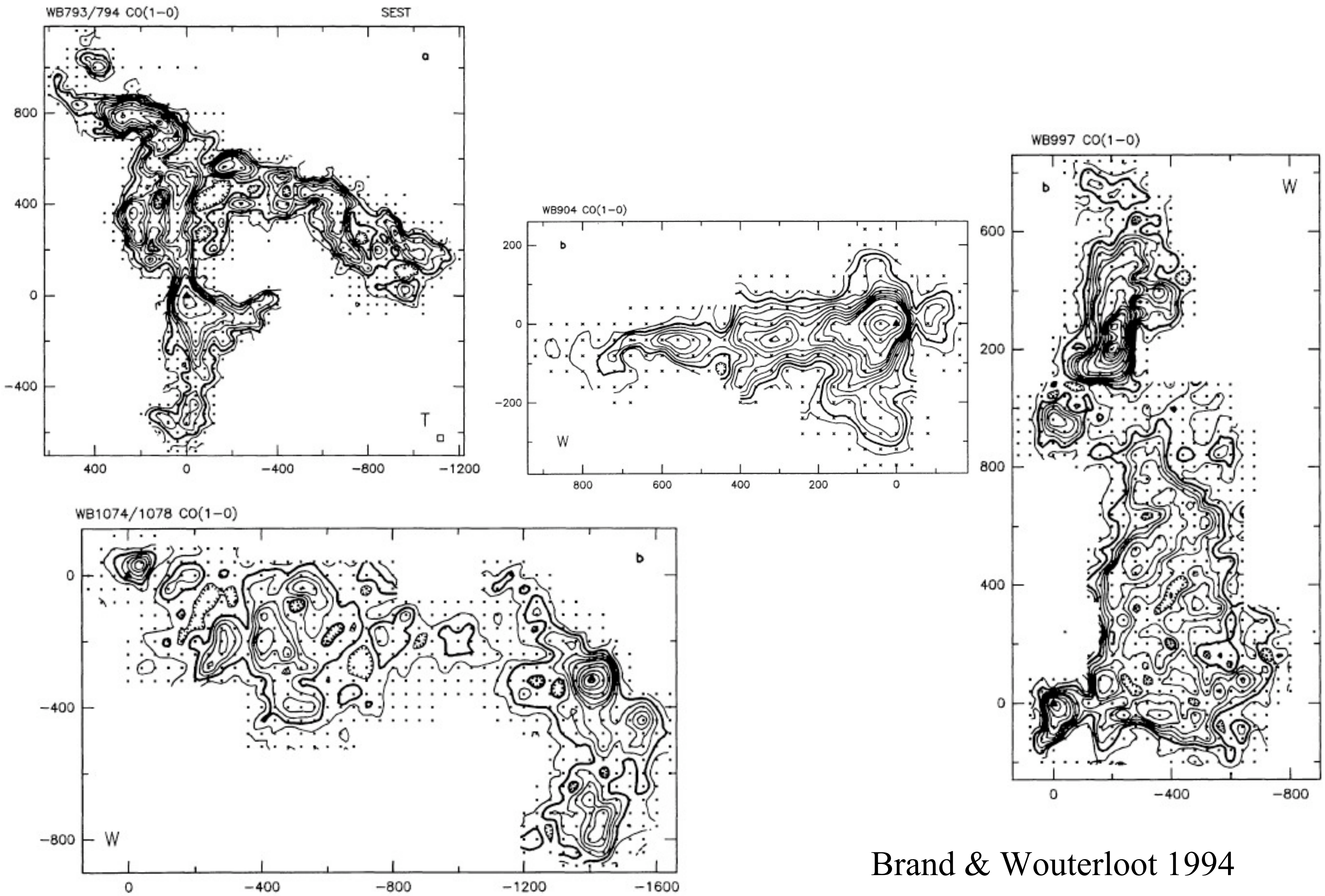

Brand & Wouterloot 1994

Orion A **^{13}CO 220 GHz = 1.3 mm**

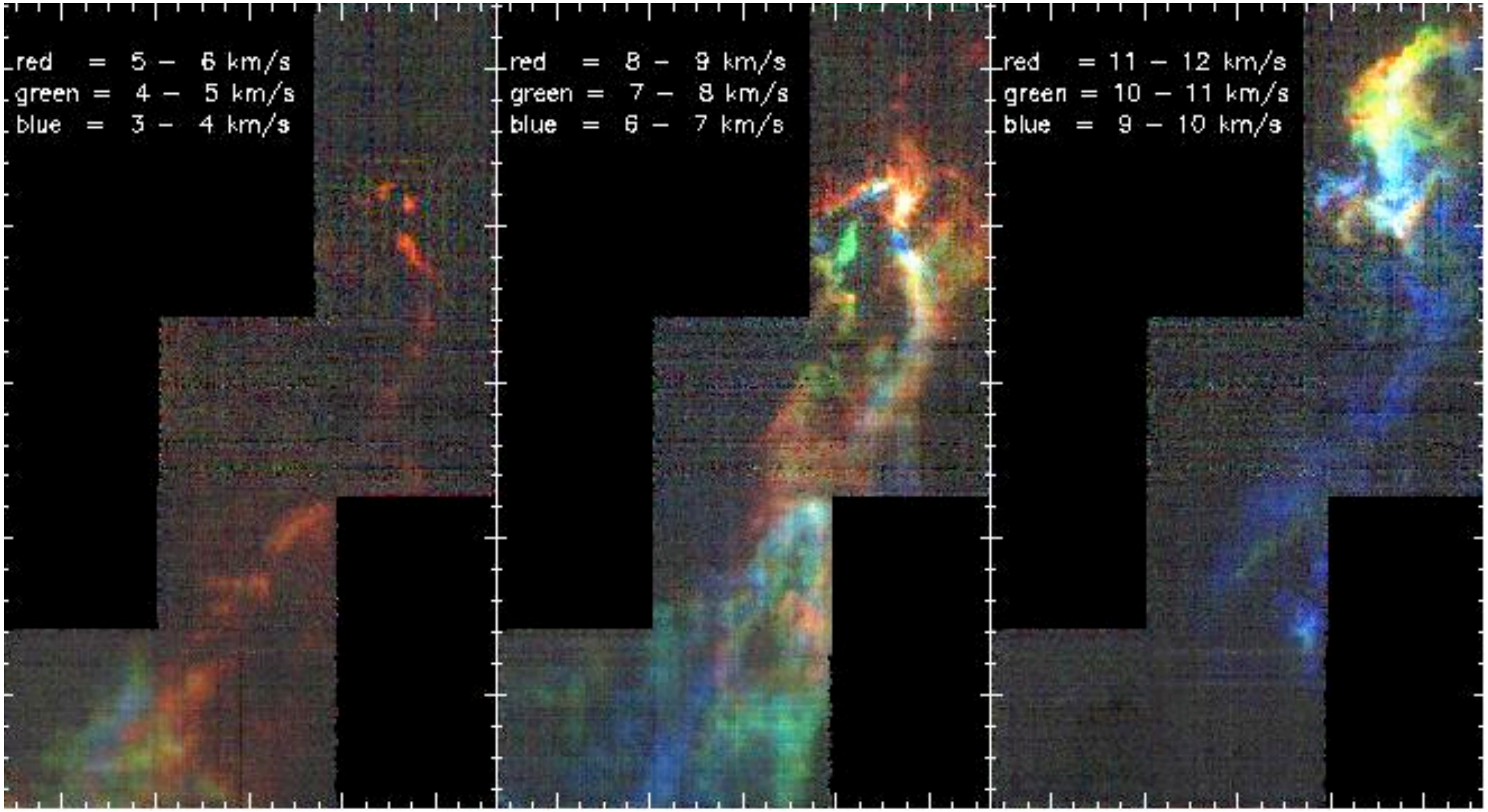

Sheets and filaments

J. Bally (IAU227)

Masses and mass-ratios

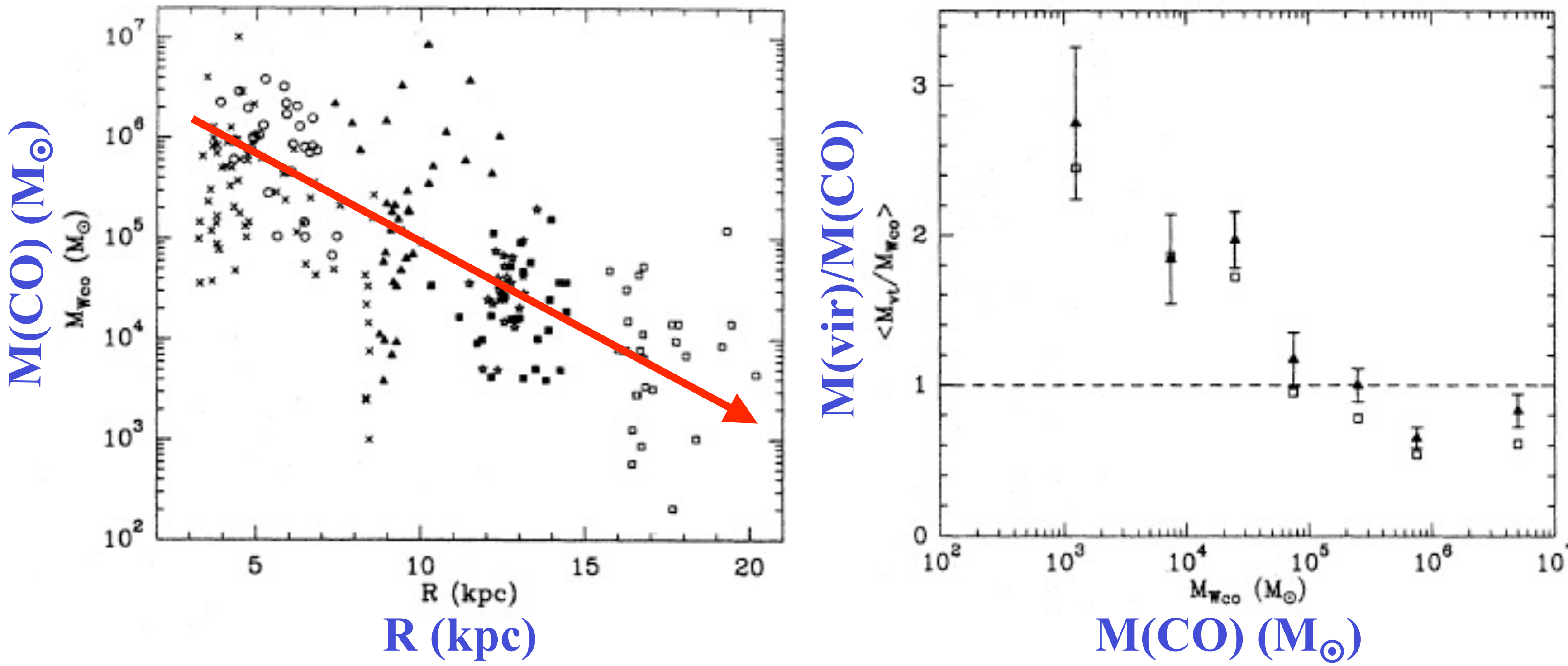

Brand & Wouterloot 1995

Molecular clouds – virial- and pressure equilibrium

$$4\pi\, r^3\, P_{ext} = M(\sigma_{3D})^2 - \frac{3}{5}\frac{GM^2}{r} \qquad \Rightarrow \frac{\Delta v^2}{r} = \frac{[fac1 * P_{ext}/k + fac2 * N(H_2)^2]}{[fac3 * N(H_2)]}$$

P_{ext} dominates: $\frac{\Delta v^2}{r} \propto N(H_2)^{-1}$

Self-grav. dominates: $\frac{\Delta v^2}{r} \propto N(H_2)$

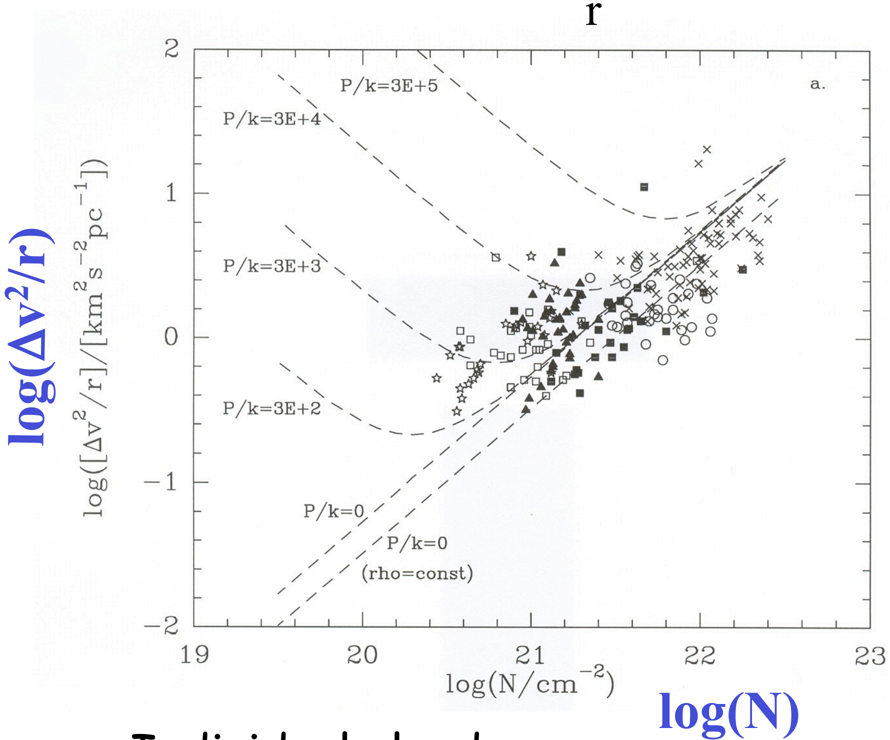

Individual clouds

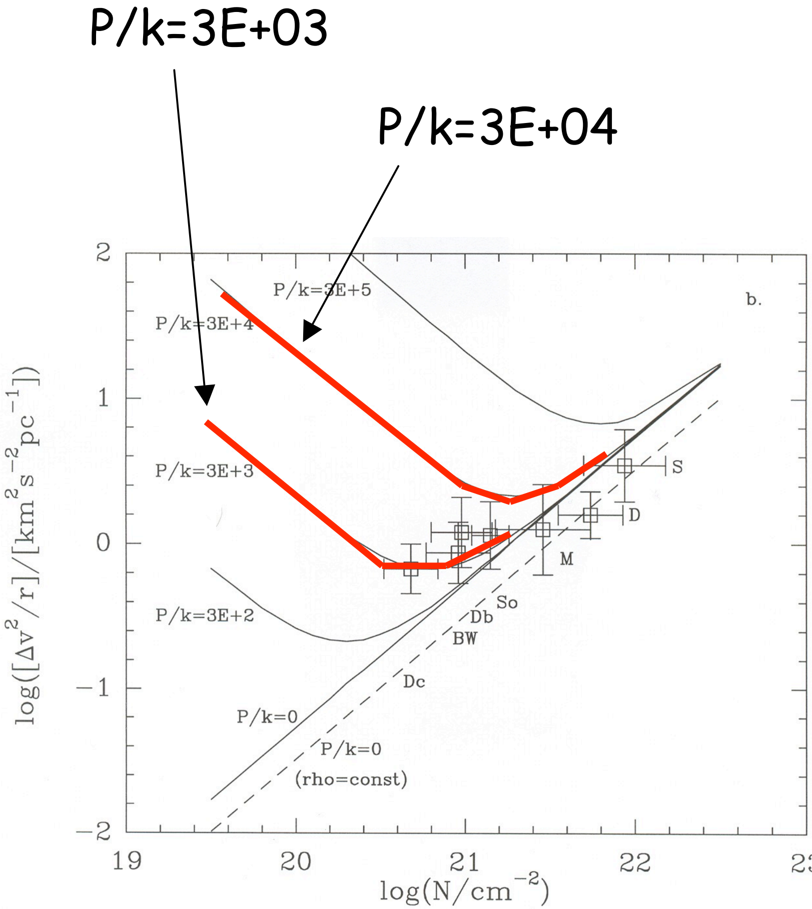

Sample averages

Brand & Wouterloot 1995

Molecular clouds & star formation

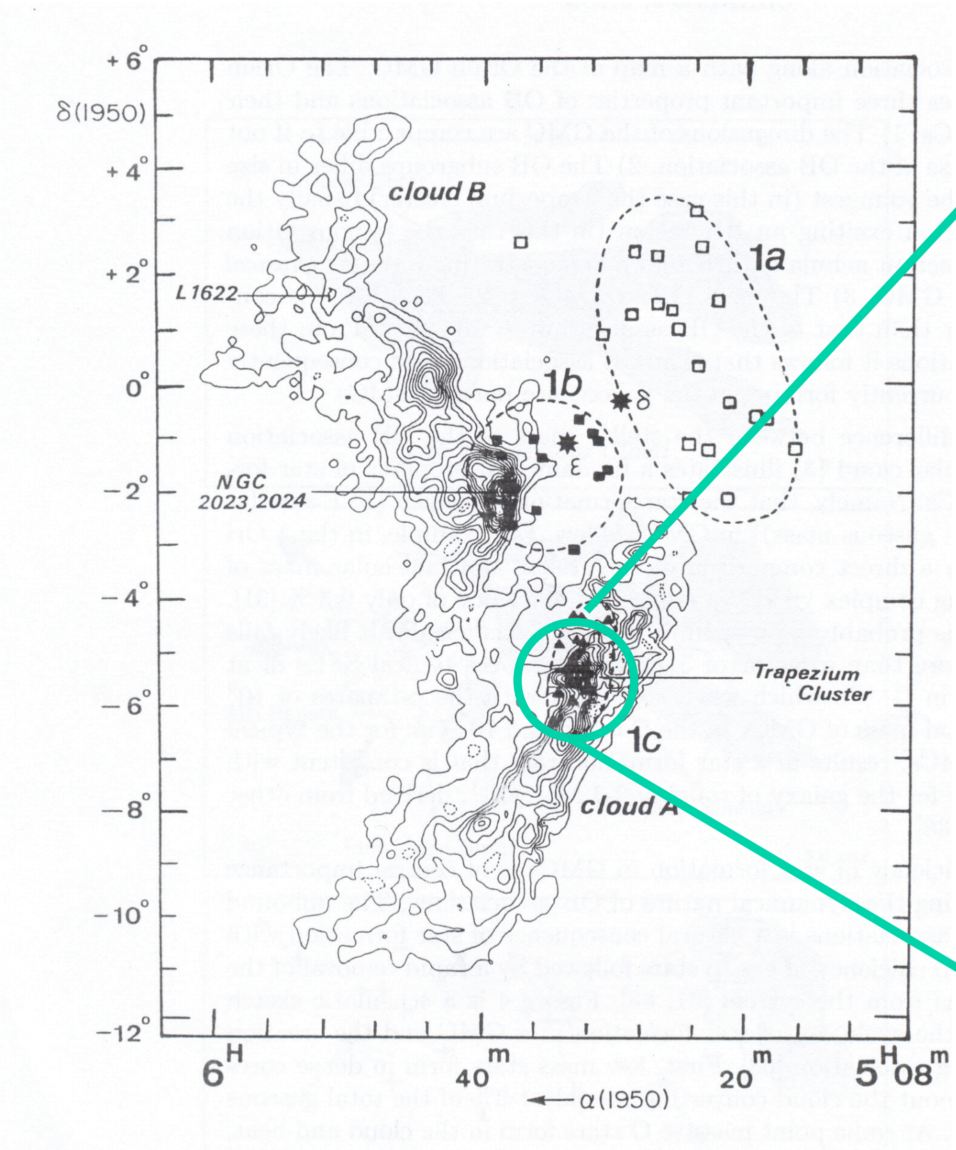

Molecular clouds & star formation

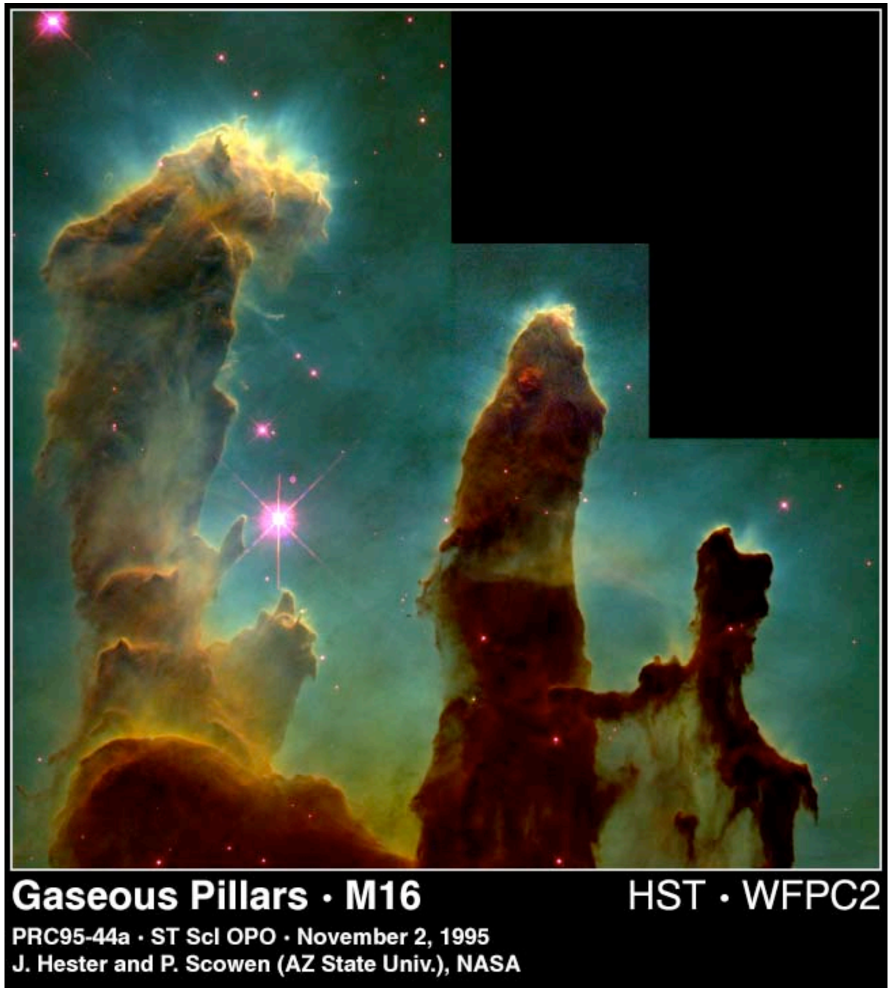

HST: NGC3603

Star formation sites in outer Galaxy

Projected distribution
WB89-clouds
Wouterloot & Brand
1989 A&AS 80, 149
(WB89)

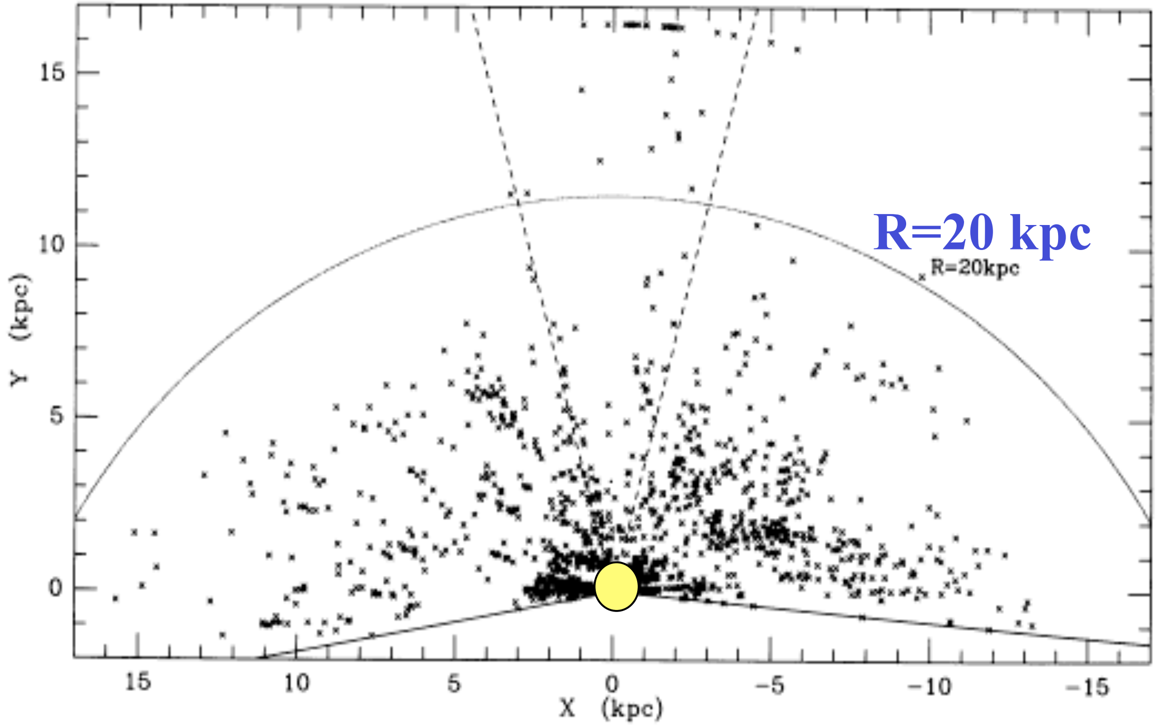

R=20 kpc

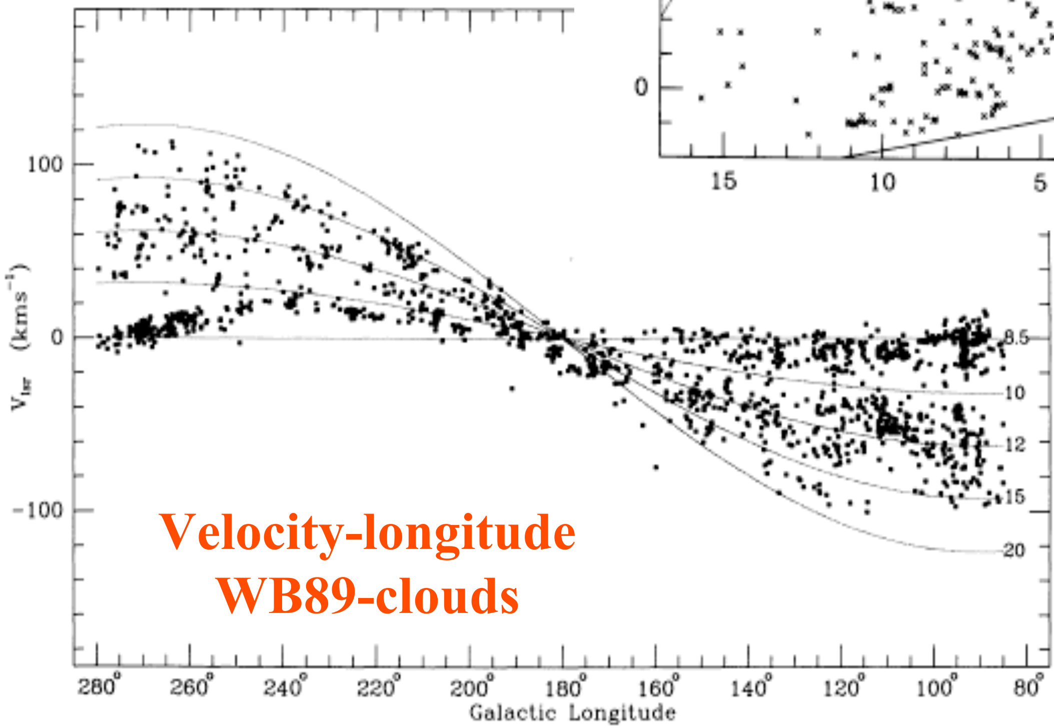

Velocity-longitude
WB89-clouds

Fig. Distribution of IRAS sources with colours of star-forming regions; shows there IS star formation out to the edge of the galactic molecular disk.

Embedded clusters I

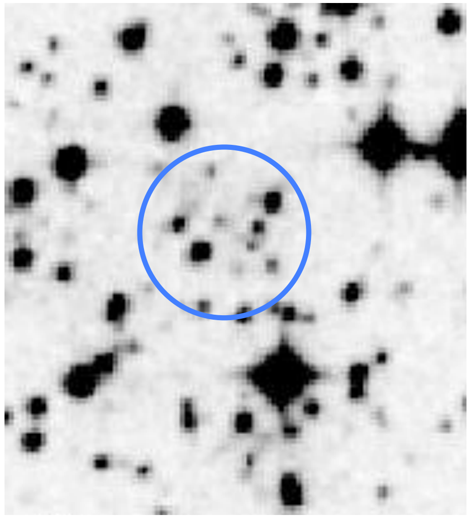

DSS-optical

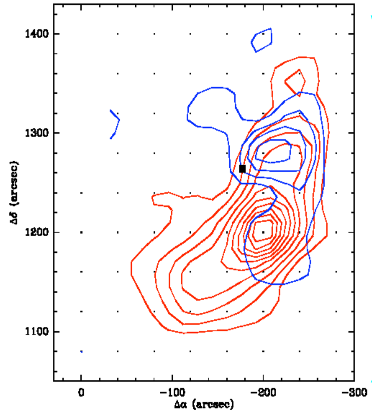

Outflow in $^{12}CO(1-0)$ (SEST)

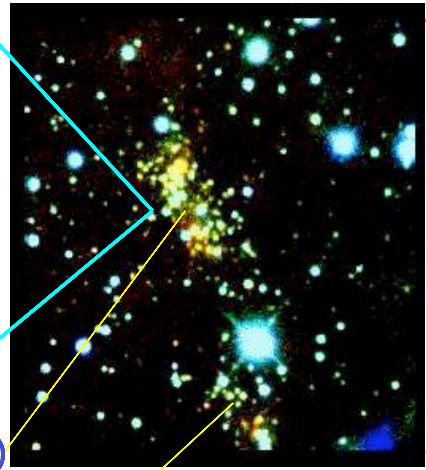

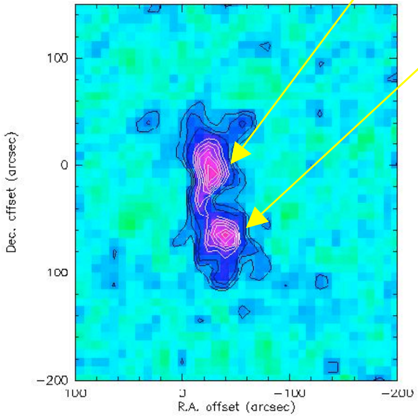

1.2 mm continuum (SEST/SIMBA)

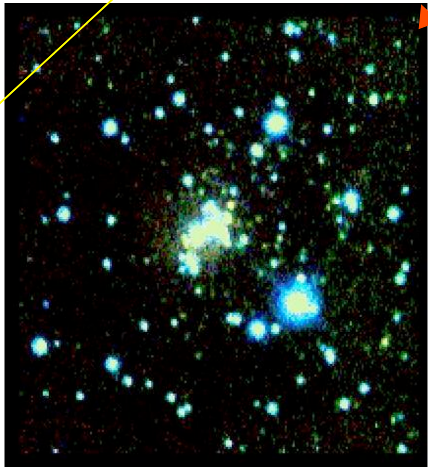

JHK-composite
~ 1'.7x1'.7

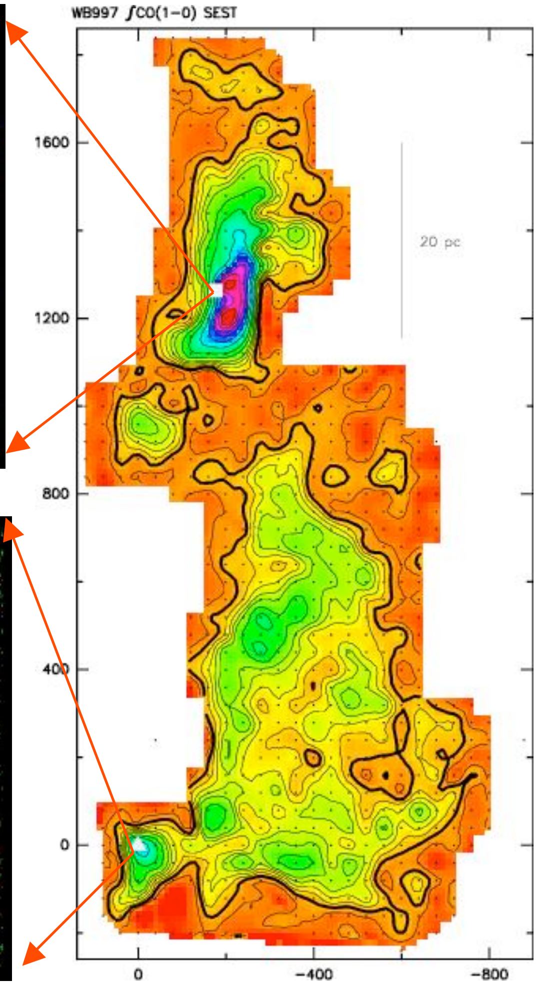

Cloud: M=6.0 × 10^4 $M_{\odot}$
d, R = 9.3, 15.7 kpc

IRAS07255-2012
IRAS07257-2033

Brand & Wouterloot 2003 & in prep.

Embedded clusters II

Brand & Wouterloot, A&A 2007

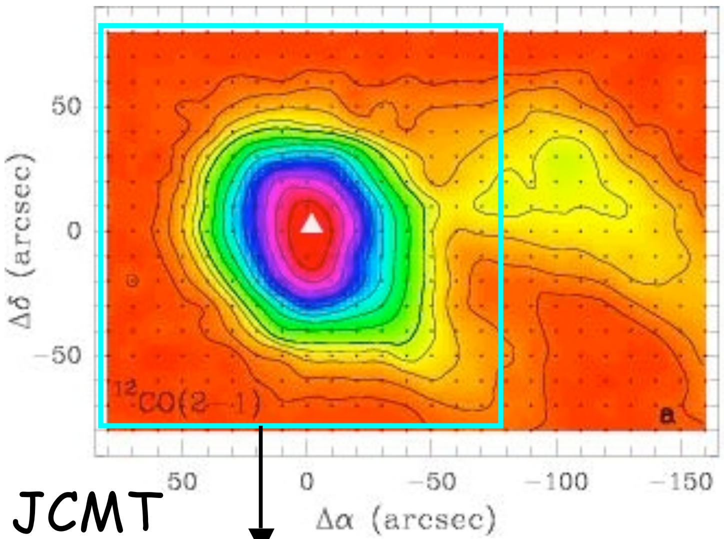

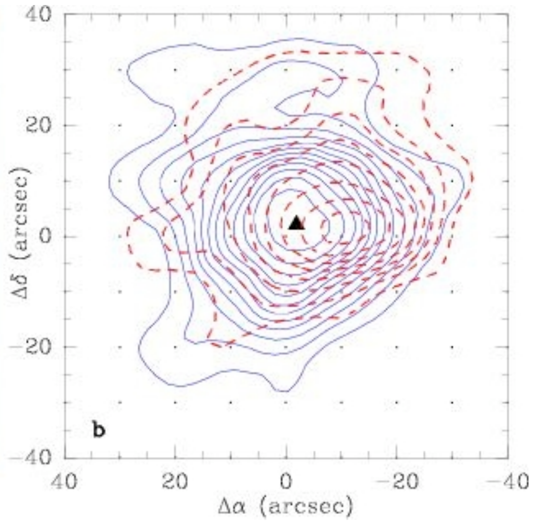

△: dust core

White contour: half of the peak value

JCMT

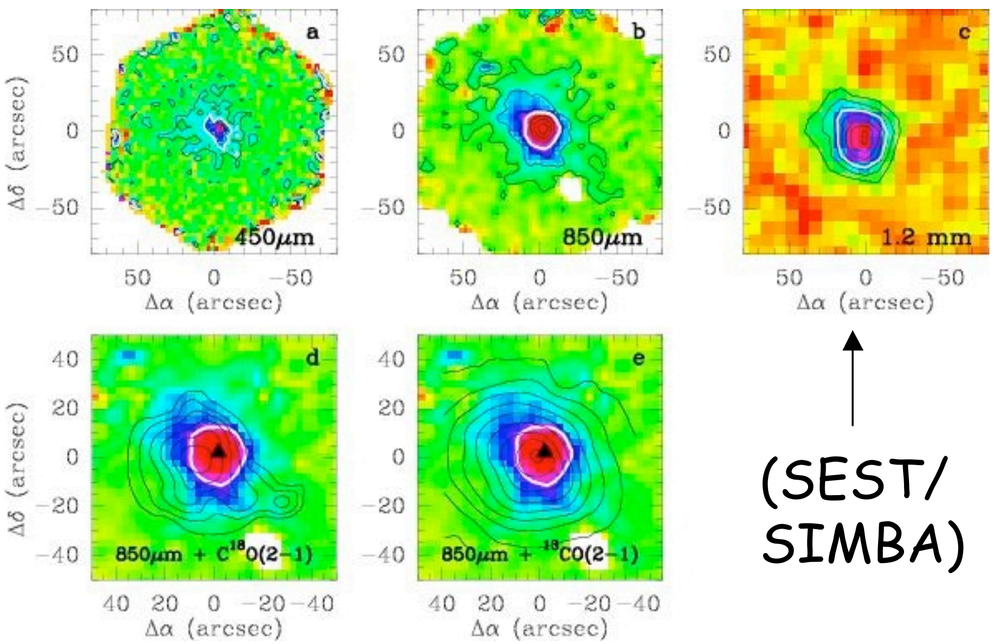

(SEST/ SIMBA)

R, d = 20.2, 11.9 kpc

$M_{cloud} \approx 5 \times 10^3\ M_\odot$ (CO);

M_{vir}(core) $\approx 400\ M_\odot$ (CS);

$M_{dust} \approx 10\ M_\odot$ (SED-fit; $T_{dust} \approx 22$ K).

$M_{outflow} \approx 12\ M_\odot$ (CO); $t_{dyn} \approx 4 \times 10^4$ yrs.

Brand & Wouterloot, A&A 2007

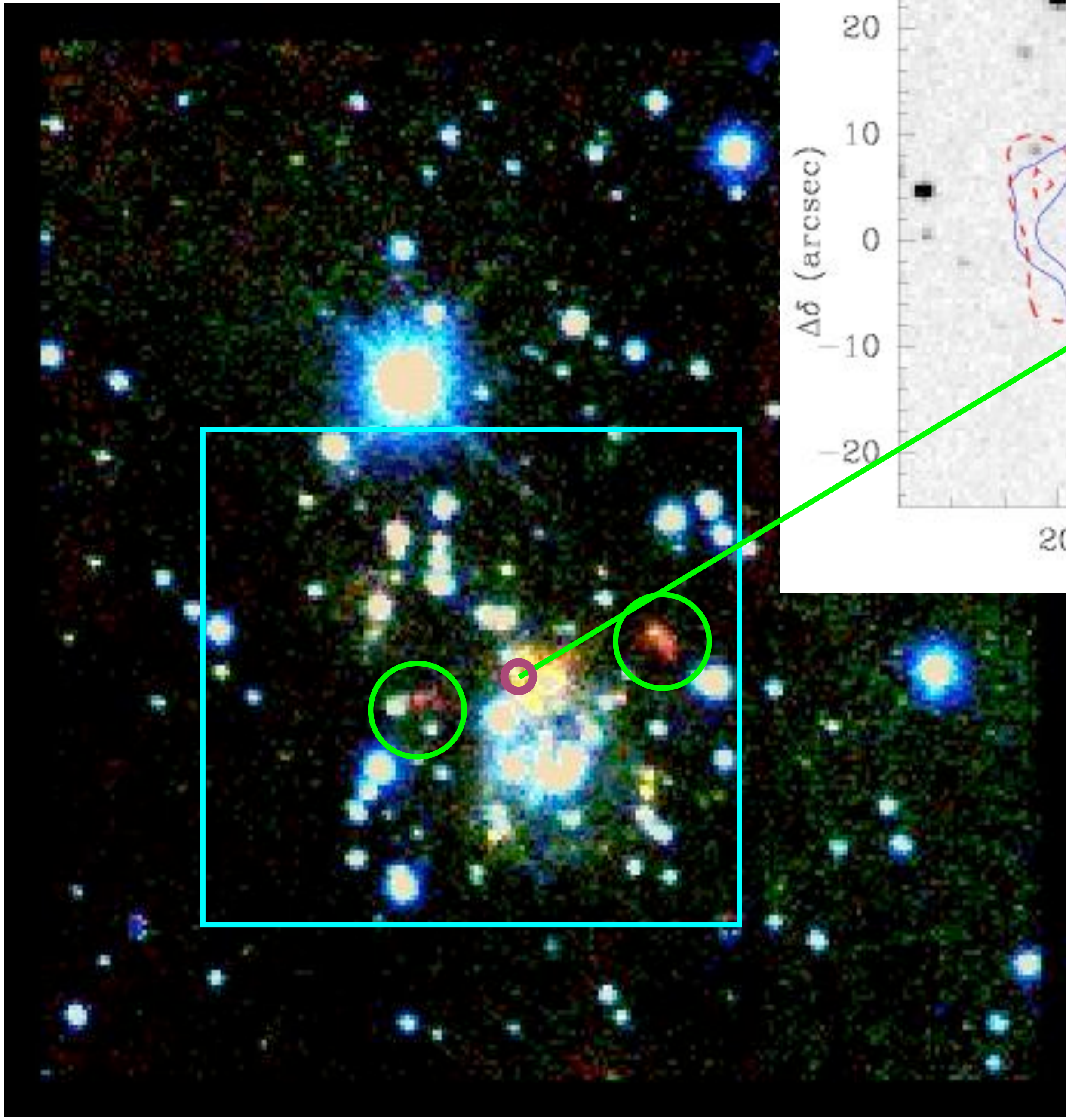

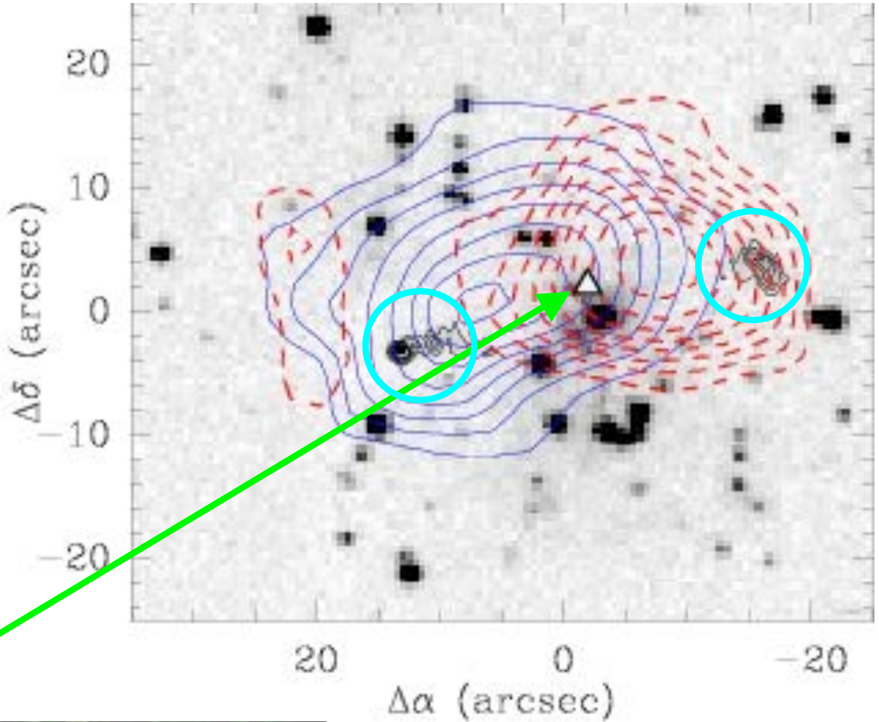

JCMT data.
∫T[CO(3-2)]dV
+
K-frame (ESO)

ESO-data

JHK-combined

A cloud without star formation

G216-2.5: “Maddalena’s Cloud”

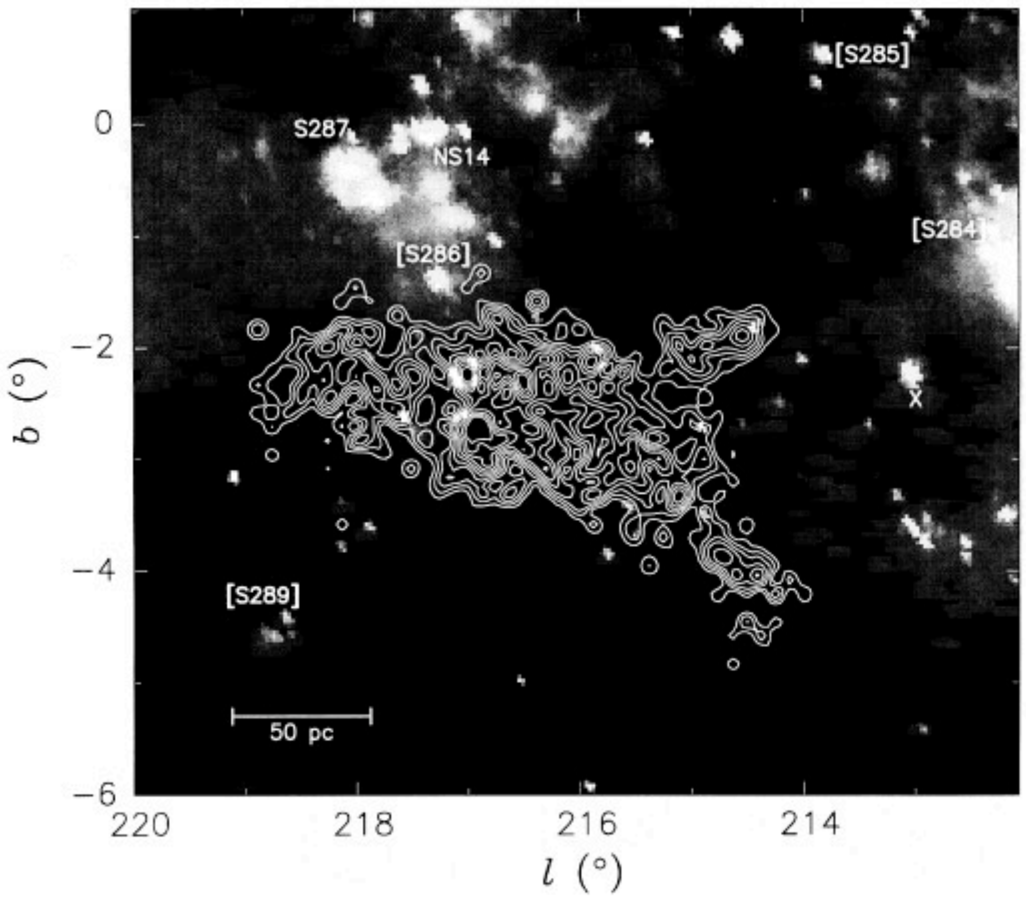

$L_{IR}/M_{cloud} < 0.07\ L_{\odot}/M_{\odot}$

while typically
$L_{IR}/M_{cloud} \sim 1\ L_{\odot}/M_{\odot}$

DERIVING
FUNDAMENTAL PROPERTIES

Typical energies involved in molecular transitions

- Electronic transitions

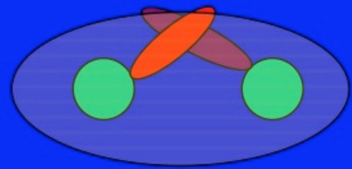

- Vibrational transitions

stretching

bending

- Rotational transitions

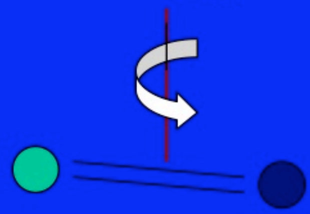

- Electronic/nuclear Spin interactions

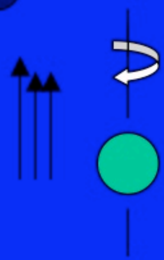

energy level separations

low-energy rotational transitions of small molecules lie at mm wavelength

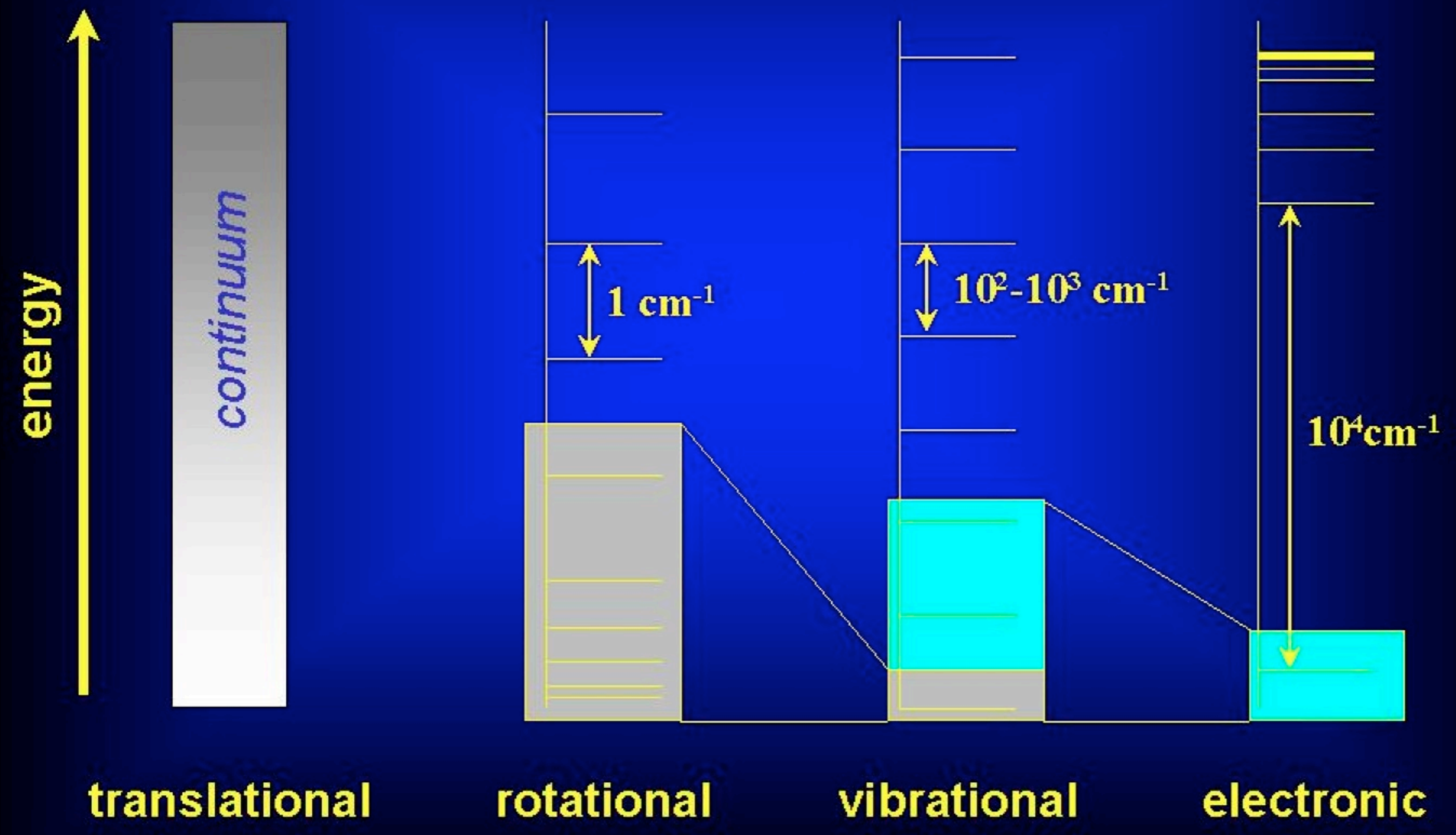

Observing molecular clouds at large

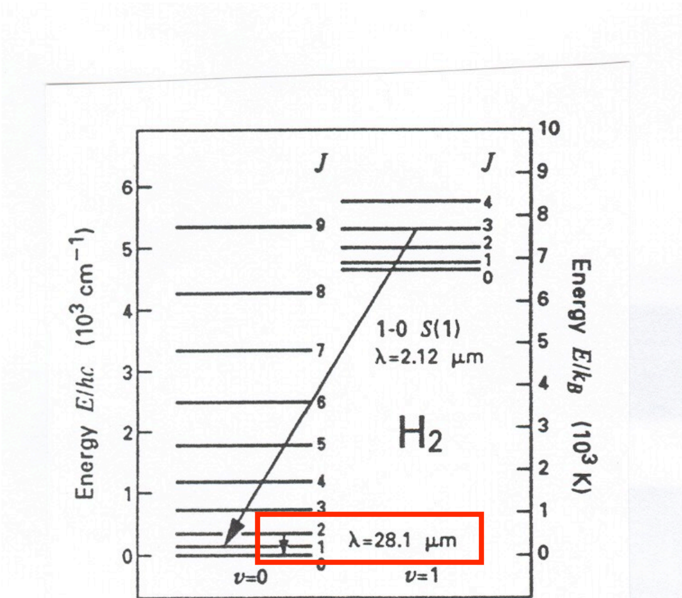

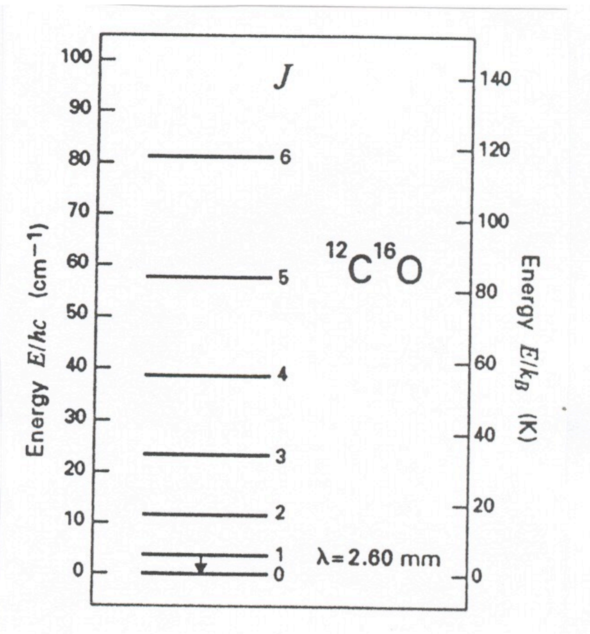

Lowest allowed (J=2-0)
ΔE = 510 K

H_2 smallest diatomic molecule: widely-spaced energy levels
Even lowest excited rot. levels too far above ground state
to be easily populated at normal molecular cloud T.
no dipole moment, hence quadrupole radiation (slow)

CO: more closely-spaced energy levels; easily populated also at low T

Two-level system

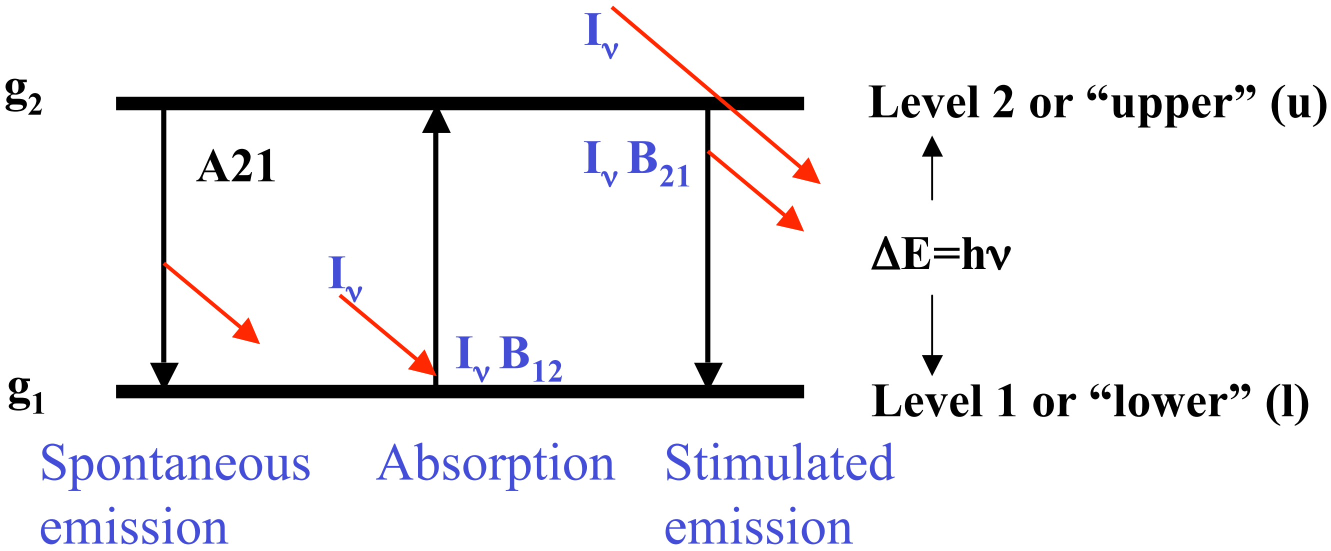

$$g_1 B_{12} = g_2 B_{21} \ ; \ A_{21} = (2h\nu^3/c^2)\, B_{21}$$

$$n_2 / n_1 = (g_2 / g_1) \exp(- \Delta E / kT_{ex})$$

Boltzmann equation

Statistical equilibrium: in=out, regardless of process:

$$dn_1/dt = (A_{21} + IB_{21} + C_{21})n_2 - (IB_{12} + C_{12})n_1 \ = 0 \text{ for each level}$$

Example: CO. In molecular cloud, excitation J=1 level through collisions with H_2.

If n_{tot} low, each upward transition followed by spontaneous emission of photon (rate = $n_1 A_{10}$).

If n_{tot} high, excited CO loses energy in collisions with H_2, without emission photon. Two regimes are separated at critical density $A_{10}/\gamma_{10} = 3 \times 10^3$ cm^{-3}.

$$n_1 / n_0 = (g_1 / g_0) \exp(- \Delta E/kT_{ex})$$

$n_{tot} << n_{crit}$: n_1 / n_0 small and $\propto n_{tot}$, $T_{ex} < T_{kin}$

$n_{tot} >> n_{crit}$: CO in LTE and $T_{ex} = T_{kin}$

NH_3(1,1)	$n_{crit} = 1.9 \times 10^4$ cm^{-3}.
CS	$n_{crit} = 4.2 \times 10^5$ cm^{-3}.
H_2O (thermal emission)	$n_{crit} = 1.7 \times 10^7$ cm^{-3}.

Radiation transport I

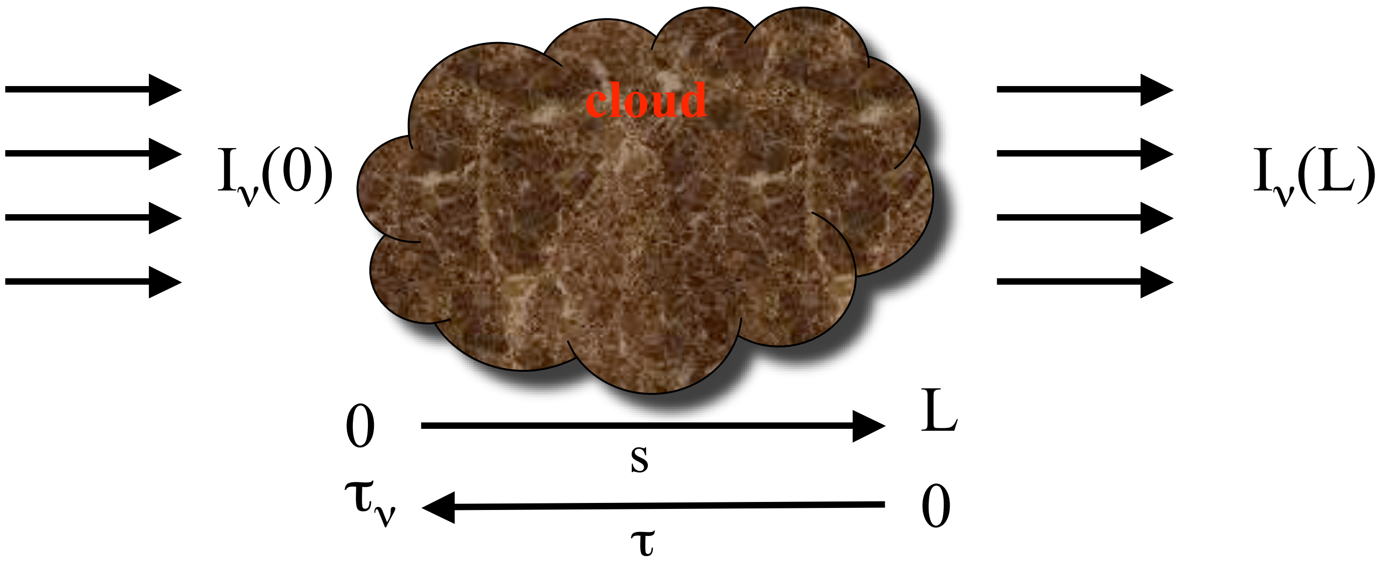

$dI_\nu = -k_\nu I_\nu \, ds + j_\nu ds$ $\qquad$ $d\tau_\nu \equiv -k_\nu ds$

$dI_\nu = I_\nu \, d\tau_\nu + (j_\nu / k_\nu) \, d\tau_\nu$ $\qquad$ (j_ν / k_ν) = source function S_ν

$$j_\nu = (h\nu/4\pi) n_u A_{ul} \phi(\nu)$$
$$k_\nu = (h\nu/4\pi)(n_l B_{lu} - n_u B_{ul})\phi(\nu)$$

TE at temperature T: $S_\nu = B_\nu(T_{ex})$: Planck function. Then:

$$I_\nu = I_\nu(0) e^{-\tau_\nu} + B_\nu(T_{ex})(1 - e^{-\tau_\nu})$$

Radiation transport II

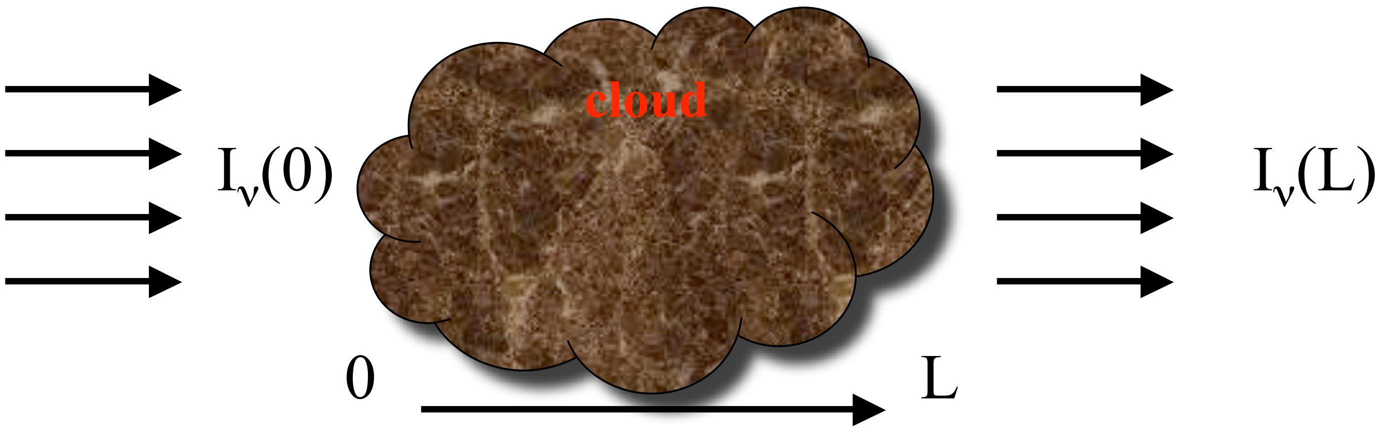

So we have: $I_\nu = I_\nu(0)e^{-\tau_\nu} + B_\nu(T_{ex})(1- e^{-\tau_\nu})$

Define $T_A(\nu) \equiv I_\nu /[2k\nu^2 c^{-2}]$, $T_A(0) = T_{bg}$, and define $J_\nu(T) = (h\nu/k)(e^{h\nu/kT} - 1)^{-1}$
(Note: in Rayleigh-Jeans limit $h\nu/kT << 1$ and $J_\nu(T) = T$)

Then: $T_A = J(T_{ex})(1- e^{-\tau_\nu}) + J(T_{bg})\, e^{-\tau_\nu}$ → **Detection equation**

in Rayleigh-Jeans limit: $T_A = T_{ex}(1- e^{-\tau_\nu}) + T_{bg}\, e^{-\tau_\nu}$
In practice one measures $\Delta T_A = T_A - T_{bg}$ (ON-OFF) $= (T_{ex} - T_{bg})(1- e^{-\tau_\nu})$

1) $\tau_\nu \ll 1$: $\Delta T_A \approx T\, \tau_\nu$ measure column density. All photons escape.
2) $\tau_\nu \gg 1$: $\Delta T_A \approx T$ measure kinetic temperature, but independent of col. dens.
Only photons at cloud surface ($\tau_\nu \leq 1$) escape.

T_{ex}, τ, and column density in LTE

For an optically thick line, e.g. CO(1-0): $\tau_\nu \gg 1$; the detection equation yields:

$T_{ex} = (h\nu/k)\ \ln^{-1}(h\nu/k\ [T_A + J(T_{bg})\ ]^{-1} + 1)$
$\quad\ = 5.532\ \ln^{-1}(5.532[T_A + 0.818\ ]^{-1} + 1)$

For an optically thin line, e.g. ^{13}CO(1-0): $\tau_\nu \ll 1$; it follows that:

$\tau_\nu = -\ln[1 - T_A/(J(T_{ex}) - J(T_{bg}))]^{-1}$

Column density – derived from transition between levels J and J-1.
Detection equation: $T_A = J(T_{ex})\ (1- e^{-\tau_\nu}) + J(T_{bg})\ e^{-\tau_\nu}$ and $\tau_\nu \ll 1$, solve for τ_ν.
From definition of T_{ex}, the definitions of the Einstein-coefficients, the equation for the absorption coefficient, and the definition of τ

$$N_{tot} = \left(\frac{3h}{8\pi^3\mu^2}\right)\left(\frac{Z}{J}\right)e^{\frac{h\nu}{kT_{ex}}}\left[1 - e^{-\frac{h\nu}{kT_{ex}}}\right]^{-1}\left[J(T_{ex}) - J(T_{bg})\right]\int T_A\,dv$$

with Z the partition function (linking N_l to N_{tot}).

or: $N_{tot} = f(T_{ex}) \int T_A\ dv$

Total column density

$$N_{tot} = f(T_{ex}) \int T_A \, dv$$

For $^{13}CO(1\text{-}0)$ and $C^{18}O(1\text{-}0)$ and $T_{ex} \approx 5 - 20$ K:

$$f(T_{ex}) \approx (1.1 \pm 0.2) \times 10^{15} \text{ cm}^{-2} / (\text{Kkm/s})$$

Hence:

$N_{tot} = (1.1 \pm 0.2) \times 10^{15} \int T_A \, dv \text{ cm}^{-2} \Rightarrow$ Mass!

If $\tau_\nu \leq 2$ then correction factor $\tau_0 / [1 - \exp(-\tau_0)]$, with τ_0 the opt. depth at line center $\tau_0 = -\ln(1-1/R)$ and $R = T_A(^{12}CO) / T_A(^{13}CO)$.

Therefore:

$$N_{tot} = (1.1 \pm 0.2) \times 10^{15} \times \tau_0 / [1 - \exp(-\tau_0)] \times \int T_A \, dv \text{ cm}^{-2}$$

Mass follows via abundances: $N(^{12}CO)/N(^{13}CO) \sim 90$ and $N(^{12}CO)/N(H_2) \sim 1 \times 10^{-4}$

Typical medium Temperature

Critical density proportional to A

Table 2. Parameters of the commonly observed short cm/mm molecular lines

Chemical[a] formula	Molecule name	Transition	ν/GHz	E_u/K[b]	A_{ij}/s^{-1}[c]
H_2O	ortho-water*	$J_{K_a K_c} = 6_{16} - 5_{23}$	22.235253	640	1.9×10^{-9}
NH_3	para-ammonia	$(J, K) = (1,1) - (1,1)$	23.694506	23	1.7×10^{-7}
NH_3	para-ammonia	$(J, K) = (2,2) - (2,2)$	23.722634	64	2.2×10^{-7}
NH_3	ortho-ammonia	$(J, K) = (3,3) - (3,3)$	23.870130	122	2.5×10^{-7}
SiO	silicon monoxide*	$J = 1 - 0, v = 2$	42.820587	3512	3.0×10^{-6}
SiO	silicon monoxide*	$J = 1 - 0, v = 1$	43.122080	1770	3.0×10^{-6}
SiO	silicon monoxide	$J = 1 - 0, v = 0$	43.423858	2.1	3.0×10^{-6}
CS	carbon monosulfide	$J = 1 - 0$	48.990964	2.4	1.8×10^{-6}
DCO^+	deuterated formylium	$J = 1 - 0$	72.039331	3.5	2.2×10^{-5}
SiO	silicon monoxide*	$J = 2 - 1, v = 2$	85.640456	3516	2.0×10^{-5}
SiO	silicon monoxide*	$J = 2 - 1, v = 1$	86.243442	1774	2.0×10^{-5}
$H^{13}CO^+$	formylium	$J = 1 - 0$	86.754294	4.2	3.9×10^{-5}
SiO	silicon monoxide	$J = 2 - 1, v = 0$	86.846998	6.2	2.0×10^{-5}
HCN	hydrogen cyanide	$J = 1 - 0, F = 2 - 1$	88.631847	4.3	2.4×10^{-5}
HCO^+	formylium	$J = 1 - 0$	89.188518	4.3	4.2×10^{-5}
HNC	hydrogen isocyanide	$J = 1 - 0, F = 2 - 1$	90.663574	4.3	2.7×10^{-5}
N_2H^+	diazenylium	$J = 1 - 0, F_1 = 2 - 1, F = 3 - 2$	93.173809	4.3	3.8×10^{-5}
CS	carbon monosulfide	$J = 2 - 1$	97.980968	7.1	2.2×10^{-5}
$C^{18}O$	carbon monoxide	$J = 1 - 0$	109.782182	5.3	6.5×10^{-8}
^{13}CO	carbon monoxide	$J = 1 - 0$	110.201370	5.3	6.5×10^{-8}
CO	carbon monoxide	$J = 1 - 0$	115.271203	5.5	7.4×10^{-8}
$H_2{}^{13}CO$	ortho-formaldehyde	$J_{K_a K_c} = 2_{12} - 1_{11}$	137.449959	22	5.3×10^{-5}
H_2CO	ortho-formaldehyde	$J_{K_a K_c} = 2_{12} - 1_{11}$	140.839518	22	5.3×10^{-5}
CS	carbon monosulfide	$J = 3 - 2$	146.969049	14.2	6.1×10^{-5}
$C^{18}O$	carbon monoxide	$J = 2 - 1$	219.560319	15.9	6.2×10^{-7}
^{13}CO	carbon monoxide	$J = 2 - 1$	220.398714	15.9	6.2×10^{-7}
CO	carbon monoxide	$J = 2 - 1$	230.538001	16.6	7.1×10^{-7}
CS	carbon monosulfide	$J = 5 - 4$	244.935606	33.9	3.0×10^{-4}
HCN	hydrogen cyanide	$J = 3 - 2$	265.886432	25.5	8.5×10^{-4}
HCO^+	formylium	$J = 3 - 2$	267.557625	25.7	1.4×10^{-3}
HNC	hydrogen isocyanide	$J = 3 - 2$	271.981067	26.1	9.2×10^{-4}

Choose molecular species depending on n, T of gas you want to probe. Also must consider expected strength of line, depends on intrinsic strength (prop to A) + chemical abundance. Must be strong enough to detect, but may want to avoid being optically thick

TABLE 1 Properties of density probes

Molecule	Transition	ν (GHz)	E_{up} (K)	n_c(10 K) (cm^{-3})	n_{eff}(10 K) (cm^{-3})	n_c(100 K) (cm^{-3})	n_{eff}(100 K) (cm^{-3})
CS	$J = 1 \rightarrow 0$	49.0	2.4	4.6×10^4	7.0×10^3	6.2×10^4	2.2×10^3
CS	$J = 2 \rightarrow 1$	98.0	7.1	3.0×10^5	1.8×10^4	3.9×10^5	4.1×10^3
CS	$J = 3 \rightarrow 2$	147.0	14	1.3×10^6	7.0×10^4	1.4×10^6	1.0×10^4
CS	$J = 5 \rightarrow 4$	244.9	35	8.8×10^6	2.2×10^6	6.9×10^6	6.0×10^4
CS	$J = 7 \rightarrow 6$	342.9	66	2.8×10^7	...	2.0×10^7	2.6×10^5
CS	$J = 10 \rightarrow 9$	489.8	129	1.2×10^8	...	6.2×10^7	1.7×10^6
HCO^+	$J = 1 \rightarrow 0$	89.2	4.3	1.7×10^5	2.4×10^3	1.9×10^5	5.6×10^2
HCO^+	$J = 3 \rightarrow 2$	267.6	26	4.2×10^6	6.3×10^4	3.3×10^6	3.6×10^3
HCO^+	$J = 4 \rightarrow 3$	356.7	43	9.7×10^6	5.0×10^5	7.8×10^6	1.0×10^4
HCN	$J = 1 \rightarrow 0$	88.6	4.3	2.6×10^6	2.9×10^4	4.5×10^6	5.1×10^3
HCN	$J = 3 \rightarrow 2$	265.9	26	7.8×10^7	7.0×10^5	6.8×10^7	3.6×10^4
HCN	$J = 4 \rightarrow 3$	354.5	43	1.5×10^8	6.0×10^6	1.6×10^8	1.0×10^5
H_2CO	$2_{12} \rightarrow 1_{11}$	140.8	6.8	1.1×10^6	6.0×10^4	1.6×10^6	1.5×10^4
H_2CO	$3_{13} \rightarrow 2_{12}$	211.2	17	5.6×10^6	3.2×10^5	6.0×10^6	4.0×10^4
H_2CO	$4_{14} \rightarrow 3_{13}$	281.5	30	9.7×10^6	2.2×10^6	1.2×10^7	1.0×10^5
H_2CO	$5_{15} \rightarrow 4_{14}$	351.8	47	2.6×10^7	...	2.5×10^7	2.0×10^5
NH_3	(1,1)inv	23.7	1.1	1.8×10^3	1.2×10^3	2.1×10^3	7.0×10^2
NH_3	(2,2)inv	23.7	42	2.1×10^3	3.6×10^4	2.1×10^3	4.3×10^2

... means no value; inv means inversion transition.

Evans 1999, Ann. Rev. A&A 37

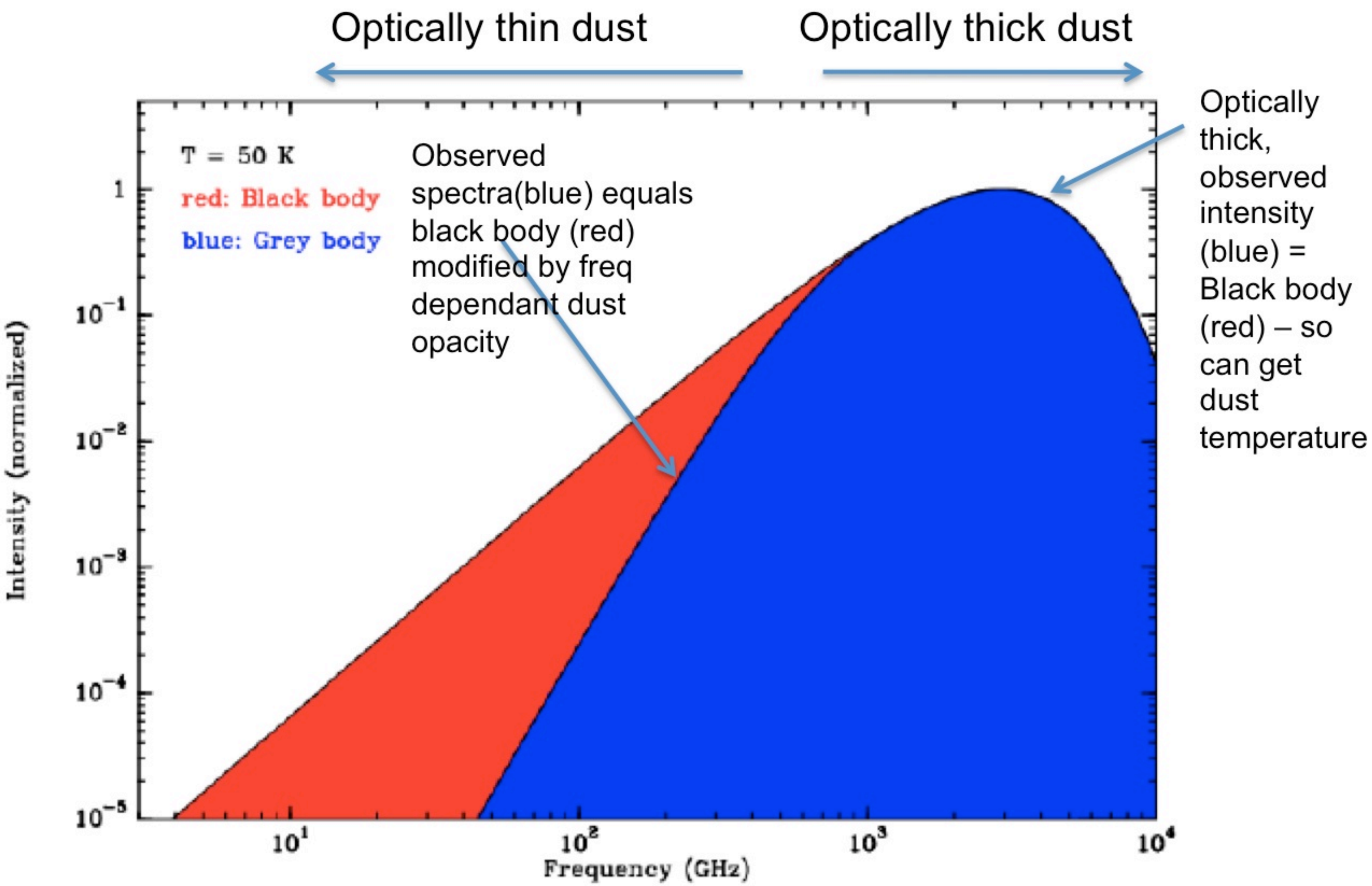

λ ~ 100-500 μm good diagnostic T_d

λ ~ 800 μm - 3 mm good tracer of mass

$$M_d = \frac{S_\nu d^2}{B_\nu(T_d)\kappa_d}$$

$$\kappa_d = \kappa_0 \left(\frac{\nu}{230GHz}\right)^\beta cm^2 g^{-1}$$

Deriving $N(H_2)$, total mass

1. Lines (Planck & Boltzmann)

Detection eqn., LTE, $\tau(^{12}CO) \gg 1$ ($\Rightarrow T_{ex}$), $\tau(^{13}CO) \ll 1$

$N(^{13}CO) = f(\tau_{13}, T_{ex}, \Delta v_{13}) + [H_2]/[^{13}CO] = \ldots. \Rightarrow N(H_2)_{LTE}$

$^{12}C/H$, $^{12}C/^{13}C$ gradients $\Rightarrow [H_2]/[^{13}CO] = f(R)$

Non-LTE transitions: LVG model (full radiation transport eqns.)

2. Lines (empirical)

$N(H_2)/\int T_{12}\,dv \equiv X \Rightarrow N(H_2)_{Wco}$

X = constant or $f(R)$? Works better for ensembles than for individual clouds

3. Virial theorem

Cloud radius (r), linewidth (Δv), assumptions about density distribution. For spherical cloud, $n \propto r^{-2} \Rightarrow M_{vir} = 126\, r\, \Delta v^2$

Exclude non-bound motions (e.g. outflows); actual density distribution?

4. Dust continuum

$M = (gS_\nu d^2)/\kappa_\nu B(T_{dust})$

κ_ν, T-structure, gas-to-dust ratio (g) uncertain

Results of molecular cloud mapping

Type	**R (pc)**	**n (cm^{-3})**	**M ($M_\odot$)**	**ΔV (km/s)**	**T (K)**	**Cores & stars**
Diffuse	0.3-3	30-500	$0.5\text{-}10^2$	0.7-1.5	10?	Low-mass
Dark	3-10	$10^{2\text{-}3}$	$10^{3\text{-}4}$	1-3	10	Low-mass
Giant	20-100	10-300	$10^{5\text{-}6}$	5-15	10-20	High-mass (+Low-mass)

Total molecular mass in Galaxy ~ 2-4 x 10^9 $M_\odot \approx$ M(HI)

CLUMPY STRUCTURE
AND
MASS DISTRIBUTIONS

Our Galaxy at 115 GHz

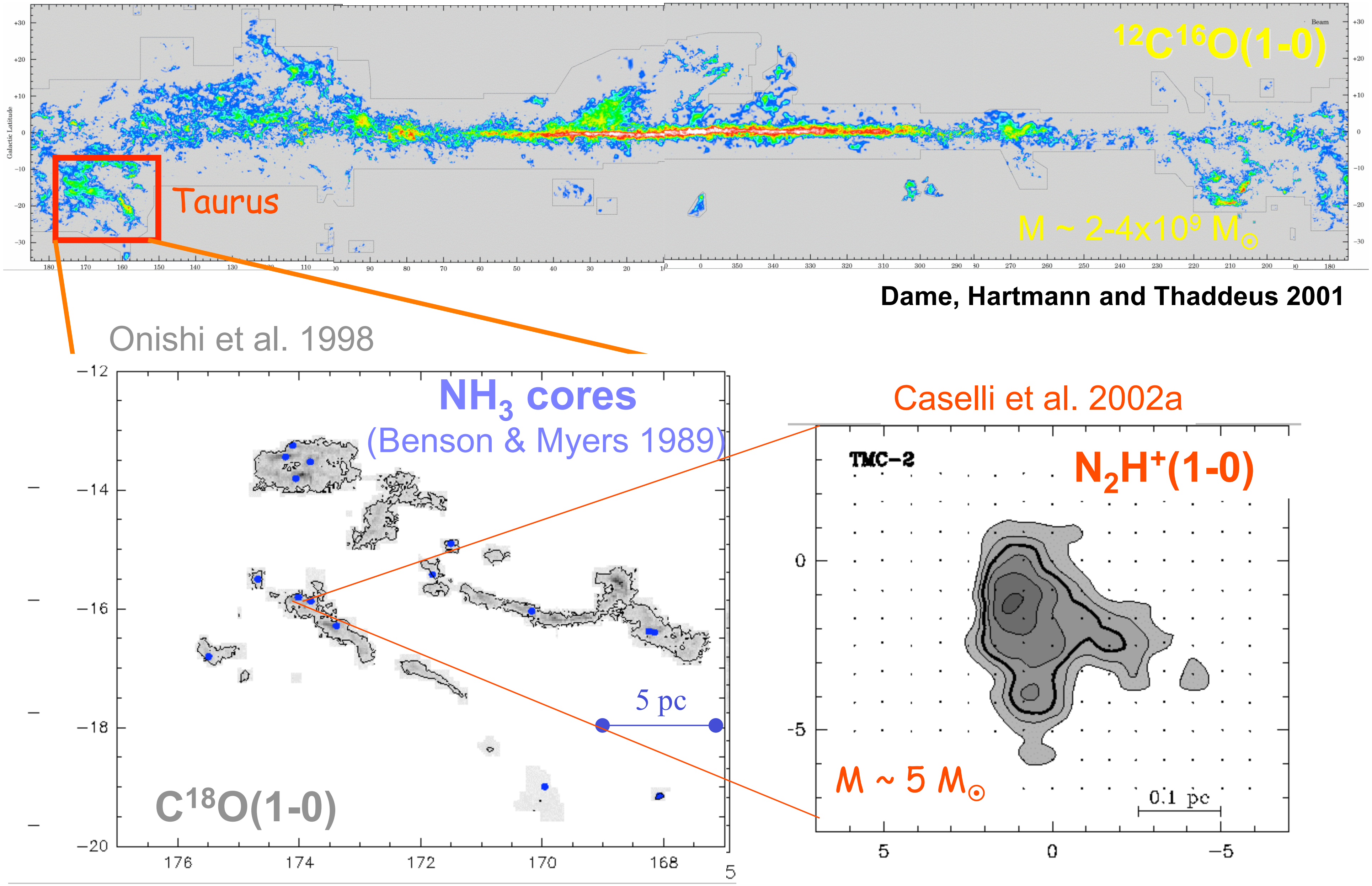

Clumpy structure - Self-similarity

CO [∅ ≈8’≈1 pc]

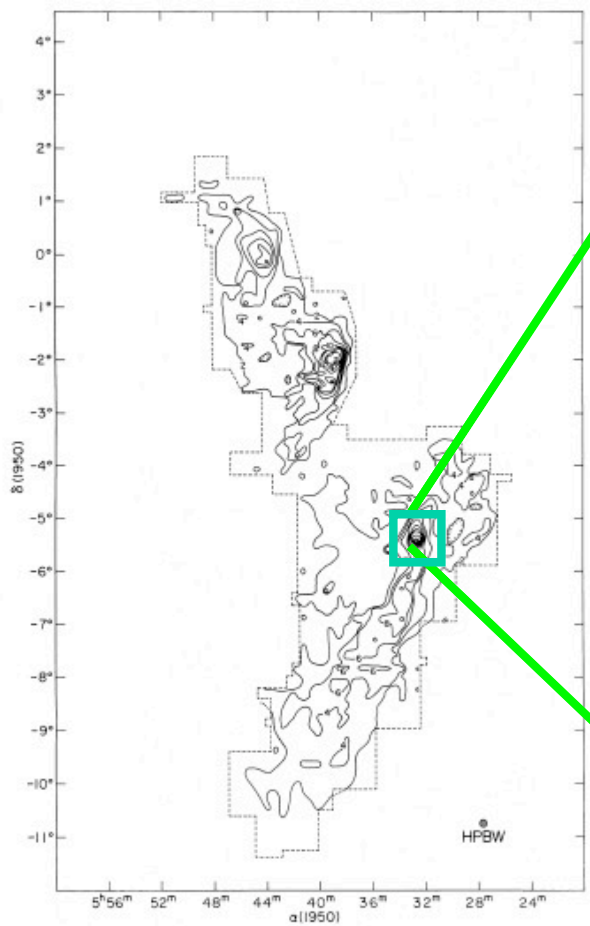

Kutner et al. 1977

NH_3 [∅ ≈43”≈0.1 pc]

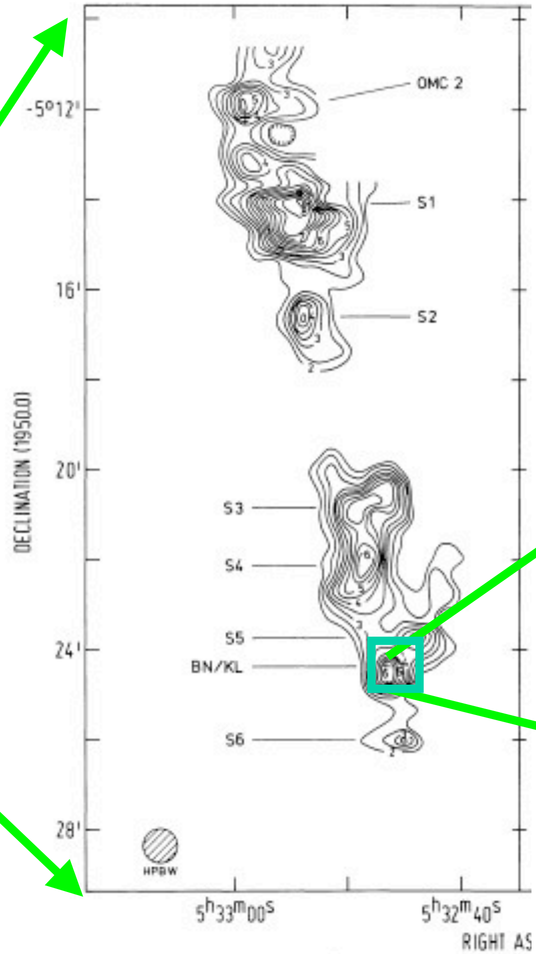

Batrla et al. 1983

NH_3 [∅ ≈1”.5x2”.2 ≈ 4 10^{-3} pc]

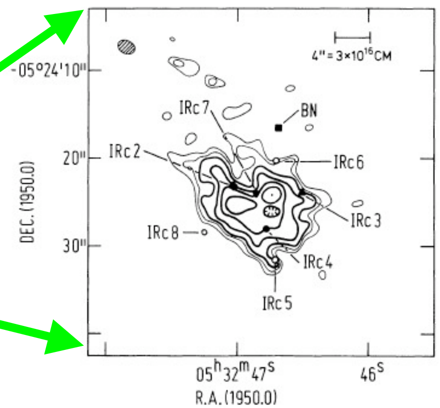

Pauls et al. 1983

Cloud structure

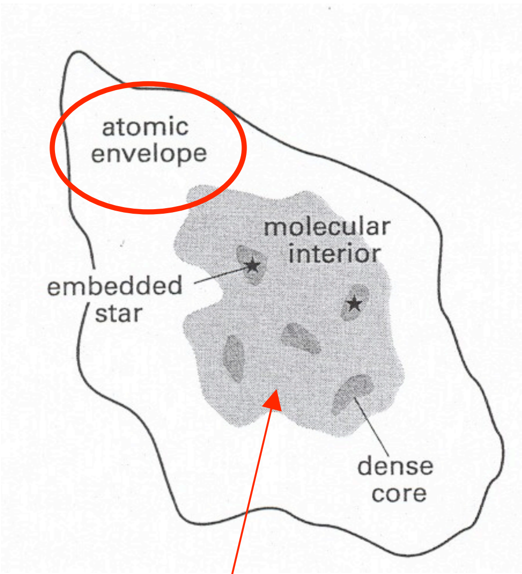

Interclump gas: predominantly atomic

Self-similar, fractal structure

Cloud , clump, core

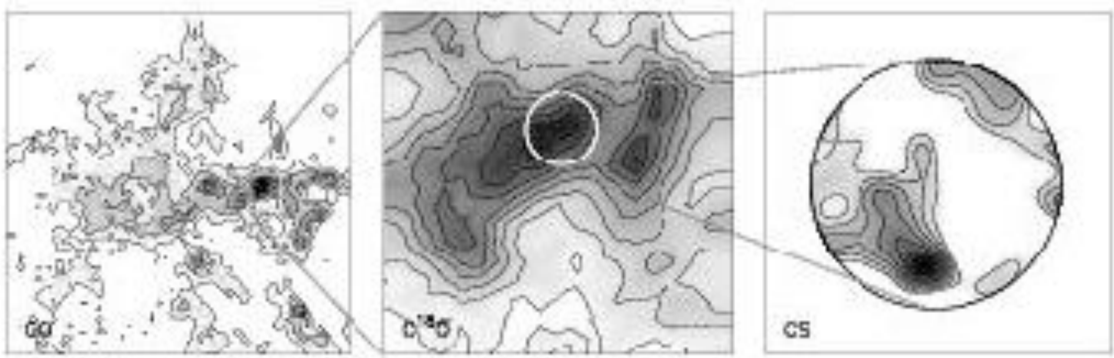

Figure 4. Hierarchical cloud structure. The three panels show a representative view from cloud to clump to core. The bulk of the molecular gas (cloud; left panel) is best seen in CO which, although optically thick, faithfully outlines the location of the H_2. Internal structure (clumps; middle panel) is observed at higher resolution in an optically thin line such as $C^{18}O$. With a higher density tracer such as CS, cores (right panel) stand out. The observations here are of the Rosette molecular cloud and are respectively, Bell Labs (90"), FCRAO data (50"), and BIMA data (10").

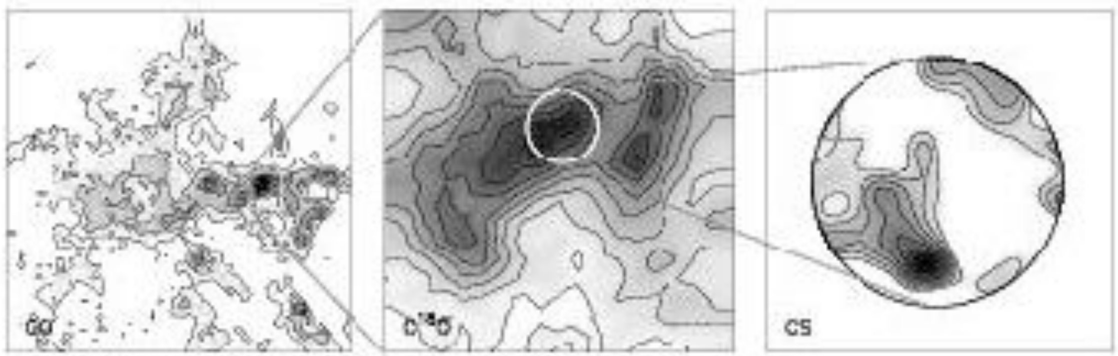

Clouds	clumps	cores
D ≥ 10 pc	D ≈ 1 pc	D ≈ 0.1 pc
$n(H_2) \approx 10^2$-10^3 cm^{-3}	$n(H_2) \approx 10^5$ cm^{-3}	$n(H_2) \approx 10^7$ cm^{-3}
$M \geq 10^4$ $M_\odot$	$M \approx 10^3$ $M_\odot$	$M \approx 10$-10^3 $M_\odot$
T ≈ 10 K	T ≈ 50 K	T ≈ 100 K
CO, ^{13}CO	CS, $C^{34}S$	NH_3, CH_3CN
$N(CO)/N(H_2) \approx 10^{-4}$	$N(CS)/N(H_2) \approx 10^{-8}$	$N(CH_3CN)/N(H_2) \approx 10^{-10}$

Typical clump properties

(based on a study of the RMC – Rosette Molecular Cloud)

- 60 –90% of H_2 in clumps

- $<n> \sim 10^3$ cm^{-3}; $<n_{vol}> \sim 25$ cm^{-3} . Thus: volume filling factor ~ 2.5%
  Hence: n(interclump) ~ 2.5-12.5 cm^{-3}

- $\Sigma(r) \propto r^{-1}$, i.e. $\rho(r) \propto r^{-2}$

- Mass spectrum $dN/dM \propto M^{\alpha}$, $\alpha = -1.4$ to -1.7 for M = 1-3000 $M_{\odot}$.
  Idem for clouds as a whole

Self-similarity – Clump mass distribution

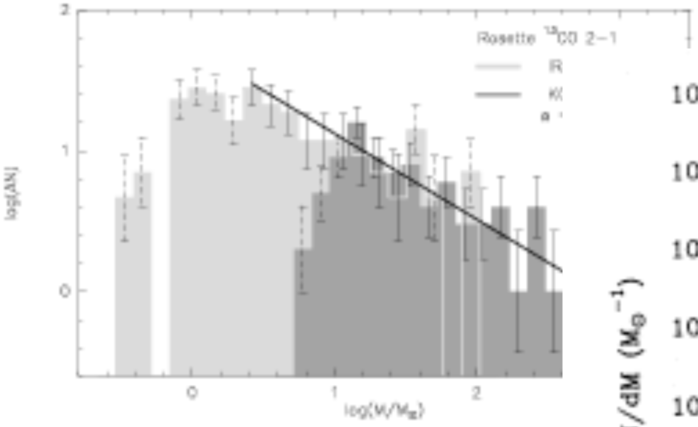

Fig. 16. Clump mass spectrum derived from ^{13}CO J=2→1 ... with KOSMA (85 clumps) and IRAM. The continuous li... a fit to the power law function $dN/dM \propto M^{-\alpha}$. The re... is α=1.61. The dashed lines of the error bars mark the... beyond the turnover points and the IRAM high-mass e... not included in the fit.

Rosette Molecular Cloud
Schneider et al. 1998

Kramer et al. 1998

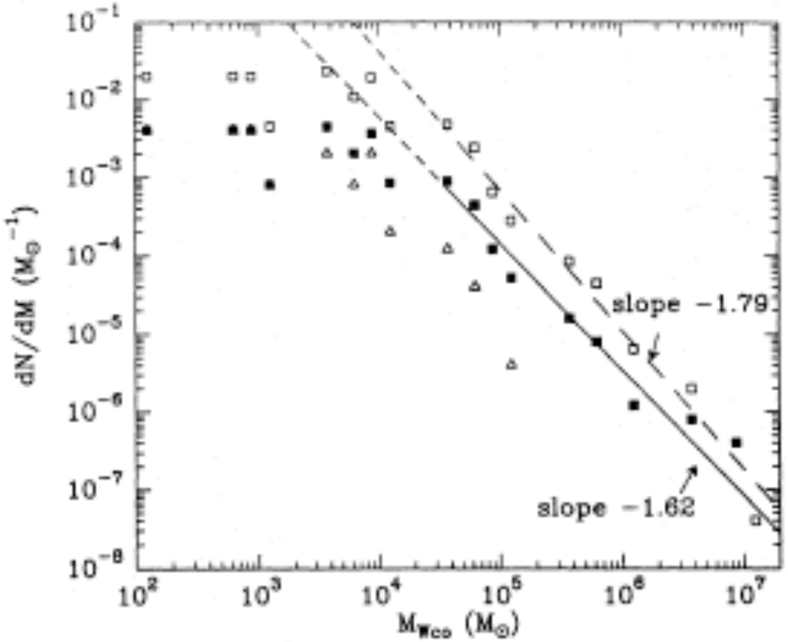

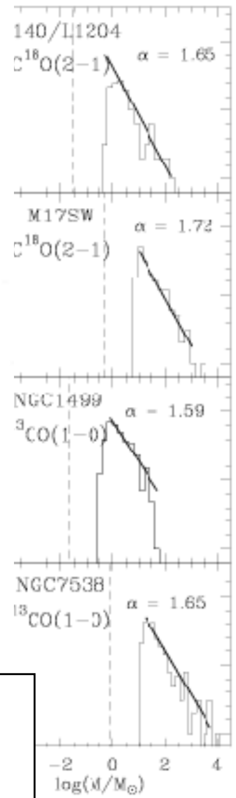

Power-law mass distribution 10 ... 1

Most clumps at low-mass end, ... ss clumps

204 clouds between R=2-25kpc: same slope!

Mass distribution of sample of GMCs has **same slope**

Brand & Wouterloot 1995

Simba results 1

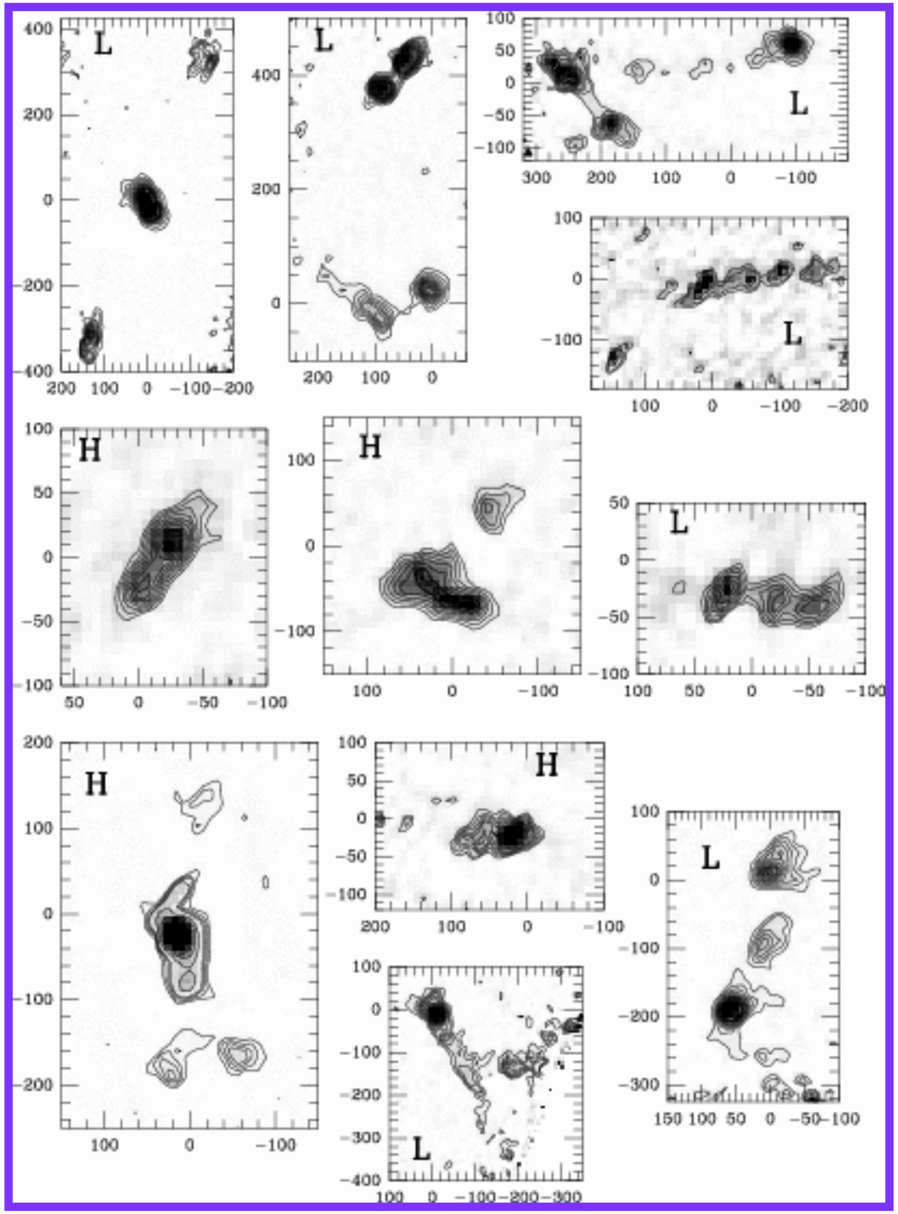

Multiple cores & chains

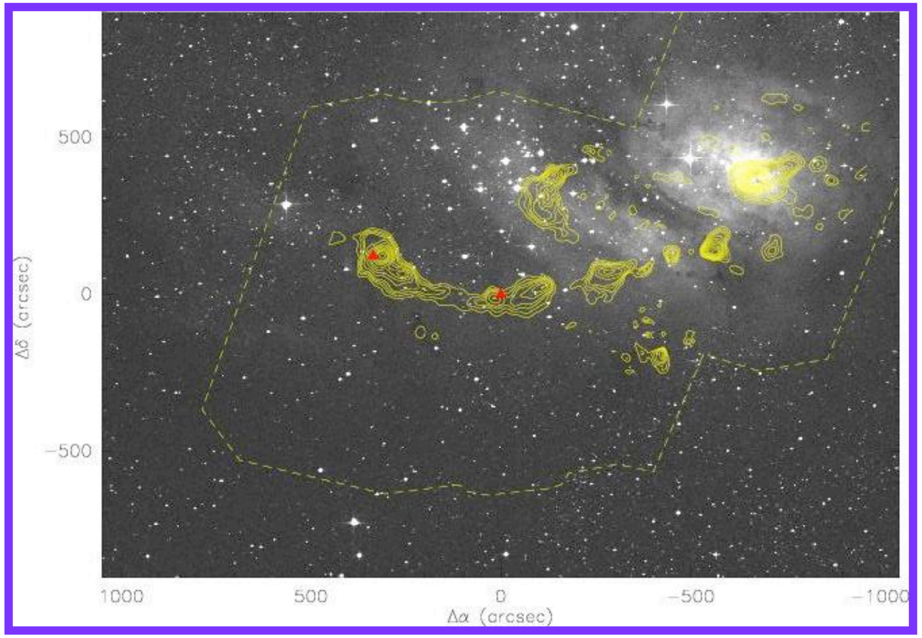

DSS + SIMBA (1.2-mm cont.)

AND: 95 pre-stellar or pre-cluster cores!

Beltran, Brand, Cesaroni et al. 2006

Simba results 2: clump mass function

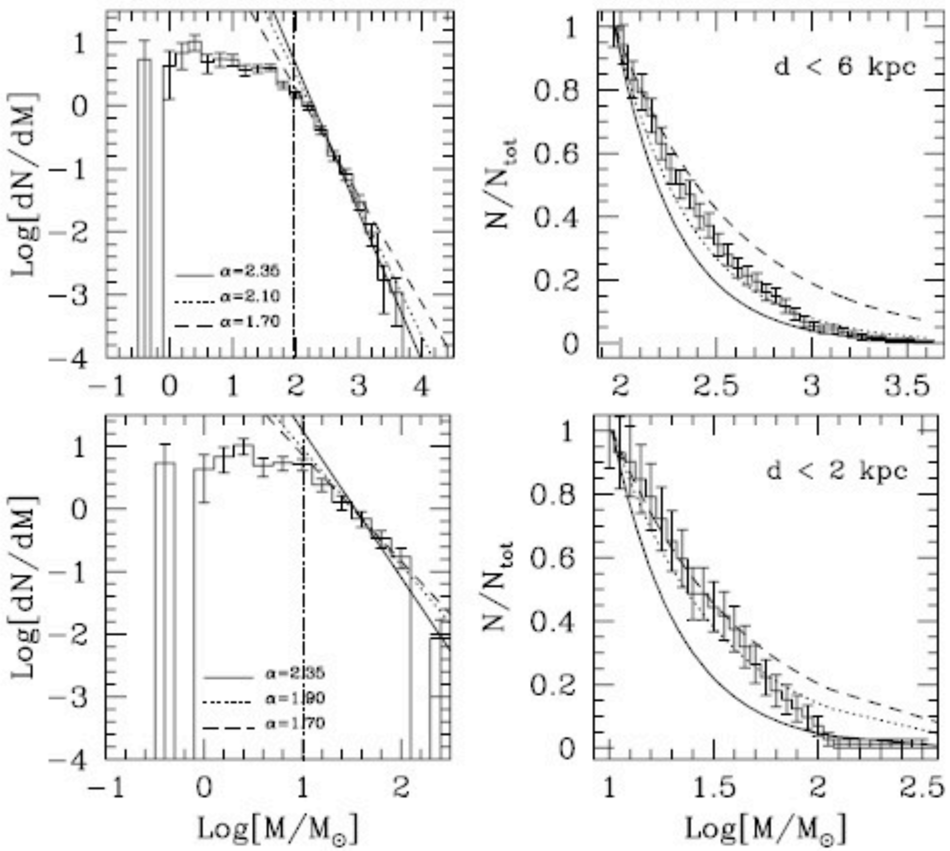

Fig. 10. *Left top panel*: the mass spectrum of the 1.2 mm clumps detected at a distance <6 kpc. The solid line represents the Salpeter IMF, $dN/dM \propto M^{-2.35}$; the dotted line is a −2.1 power law, obtained from the least square fit to the data, and the dashed line is a −1.7 power law. The vertical dot-dashed line indicates the completeness limit at 6 kpc. *Right top panel*: the normalized cumulative mass distribution of clumps with masses above the completeness limit at 6 kpc. The solid, and dashed lines are the same as in the left panel, and the dotted line is a −1.9 power law, obtained from the least square fit to the data. *Left bottom panel*: same as above for clumps detected at a distance <2 kpc. The vertical dot-dashed line indicates the completeness limit at 2 kpc. *Right bottom panel*: same as above for clumps with masses above the completeness limit at 2 kpc.

Slope 10-100 $M_\odot$: -(1.5-1.9); >100 $M_\odot$: -2.1

Beltran, Brand, Cesaroni et al. 2006

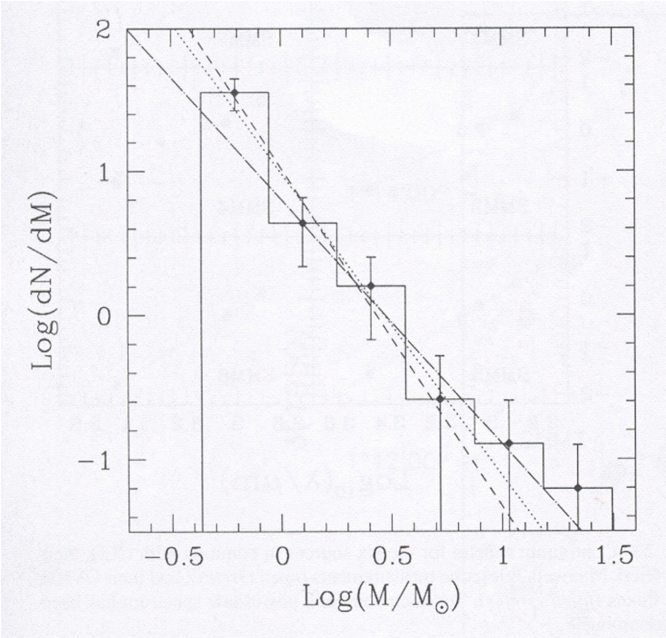

Serpens: Testi & Sargent 1998

26 pre-stellar clumps
Slope -2.1

IMF:
Salpeter: -2.5 for M= 1-10 $M_\odot$.
Miller-Scalo: -1.5 for M < 1 $M_\odot$.

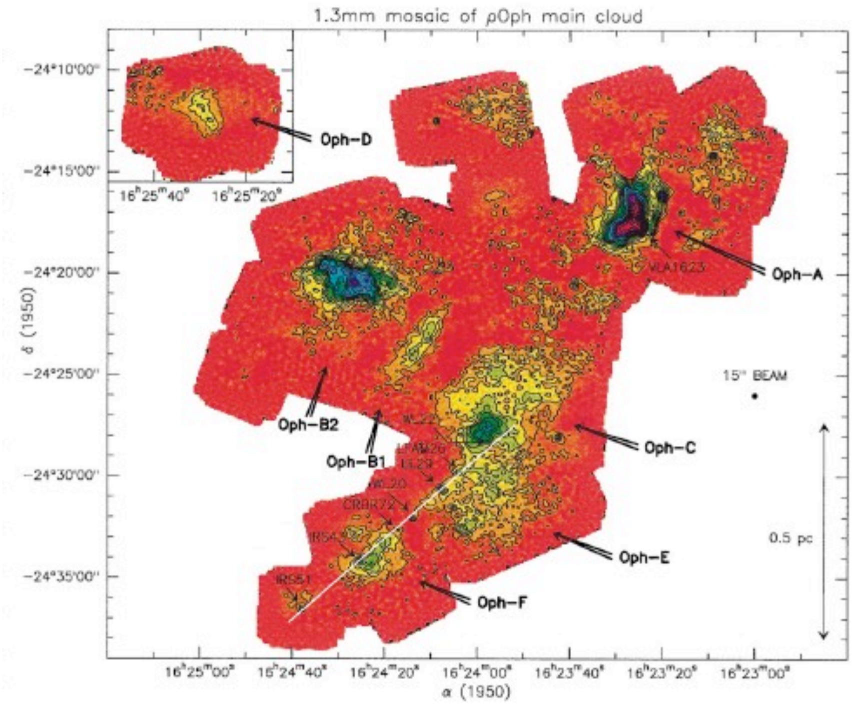

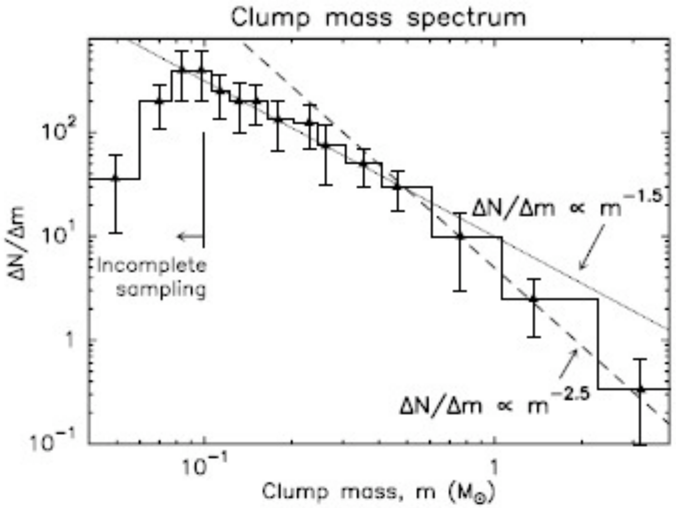

60 pre-stellar clumps in ρ Oph
Slope -1.5 for M= 0.1-0.5 $M_\odot$.
-2.5 0.5-3 $M_\odot$.

Ophiuchus: Motte et al. 1998

Typical clump properties

(based on a study of the RMC – Rosette Molecular Cloud; Blitz et al.)

- 60 –90% of H_2 in clumps

- $\langle n \rangle \sim 10^3$ cm^{-3}; $\langle n_{vol} \rangle \sim 25$ cm^{-3}. Thus: volume filling factor ~ 2.5%
  Hence: n(interclump) ~ 2.5-12.5 cm^{-3}

- $\Sigma(r) \propto r^{-1}$, i.e. $\rho(r) \propto r^{-2}$

- Mass spectrum $dN/dM \propto M^{\alpha}$, $\alpha = -1.4$ to -1.7 for M = 1-3000 $M_{\odot}$.
  Idem for clouds as a whole

- Most clumps not gravitationally bound, but most mass is in clumps that are.
  Yet clumps are not expanding: pressure-confinement

- Inside clump: $P_{int}/k \sim 6\text{-}12 \times 10^4$ Kcm^{-3} (bulk gas motions)
  Inside GMC, due to gravity: $P_{grav}/k \sim 8 \times 10^4$ Kcm^{-3}
  $P_{HI}/k \sim 10 \times 10^4$ Kcm^{-3}
  $\Rightarrow$ clumps confined by interclumps gas (which is HI)

MOLECULAR GAS KINEMATICS
rotation curve and kinematic distances

The observed velocity field

(Brand & Blitz 1993)

Radial velocity as a function of distance

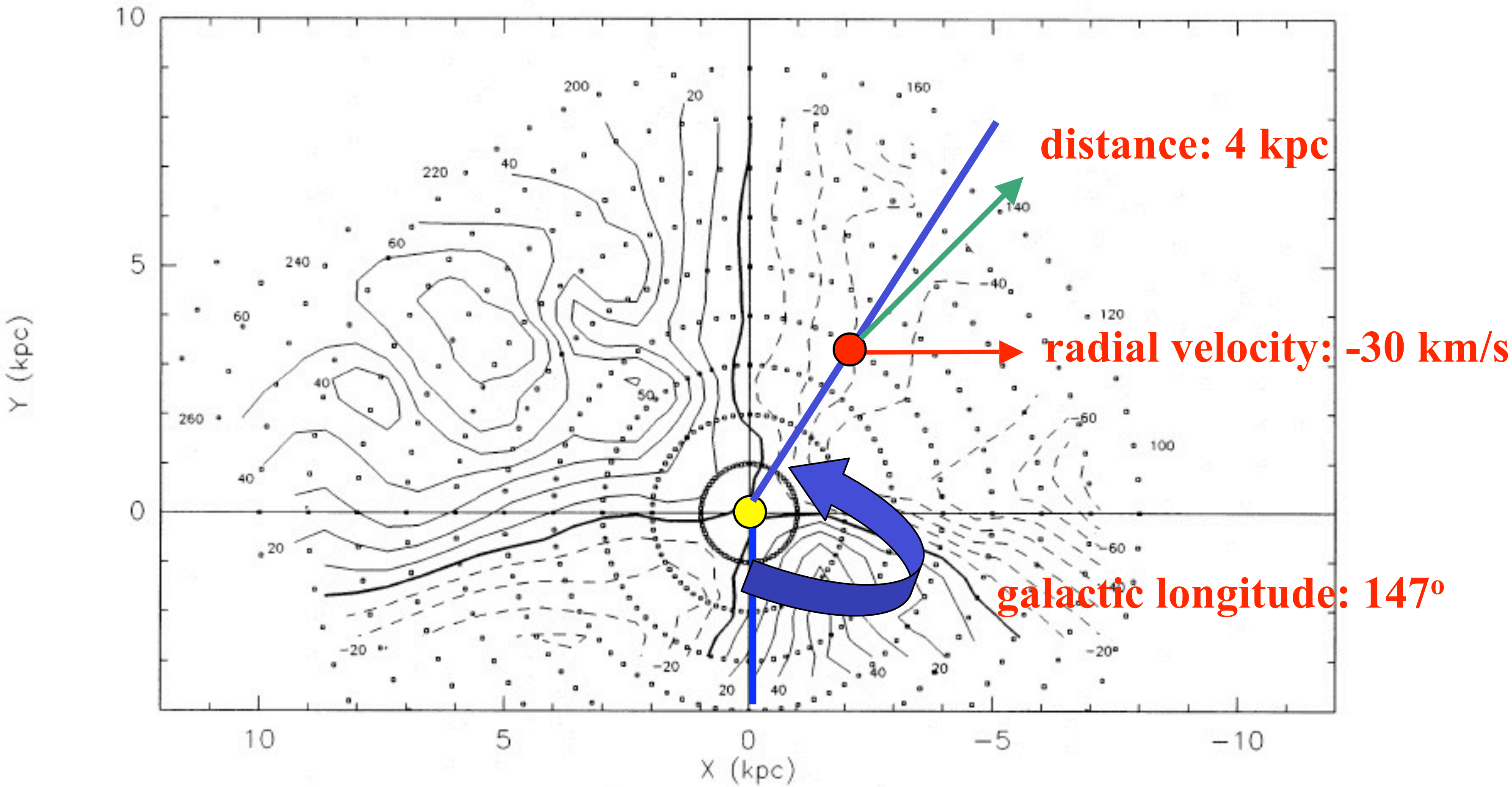

Kinematic distances I

Observed velocity field is useful to determine kinematic distances, but its range of use is limited (e.g., <2 kpc from Sun in inner Galaxy)

Therefore: construct the rotation curve (Θ versus R)

Transform observed radial velocities and spectro-photometric distances into galactic rotation velocity Θ and galactocentric distance R:

$V_{lsr} = (\Theta R_0/R - \Theta_0) \sin l \cos b$ for circular rotation.
$\omega = \Theta / R$: angular rotation velocity $\Rightarrow V_{lsr} = R_0(\omega - \omega_0) \sin l \cos b \Rightarrow$
$\omega = V_{lsr}/(R_0 \sin l \cos b) + \omega_0$

$R = (d^2 \cos^2 b + R_0^2 - 2 R_0 d \cos b \cos l)^{1/2}$

Advantage: get distances everywhere.
Disadvantage: in some regions erroneous because streaming motions are not included.

Rotation curve from HI and CO

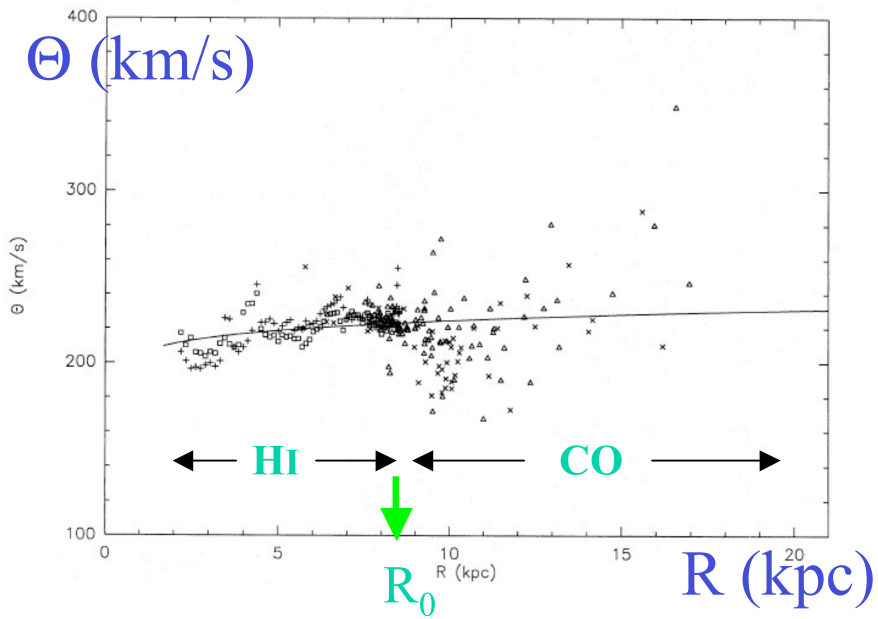

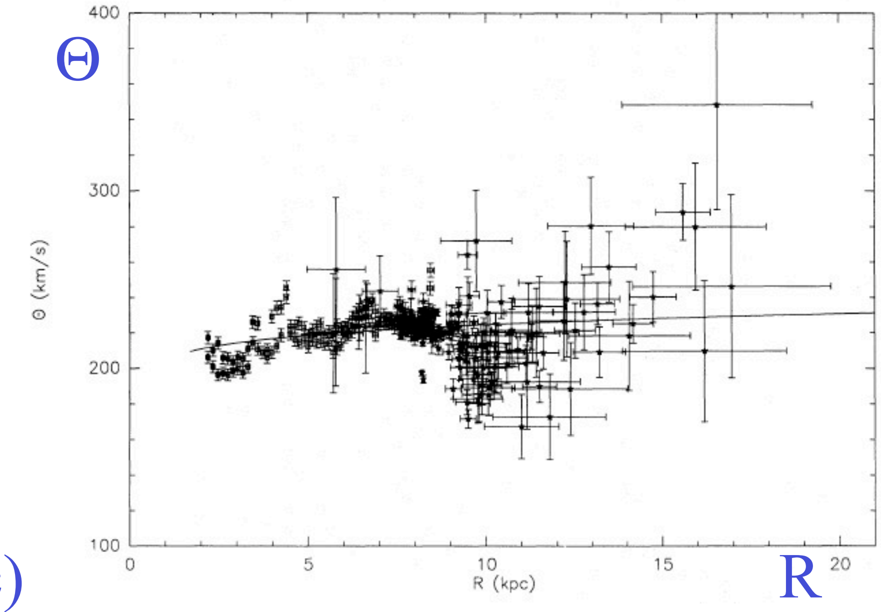

Fit a function of type:

$\omega/\omega_0 = a_1(R/R_0)^{a2-1} + a_3(R/R_0)$

Implying

$\Theta/\Theta_0 = a_1(R/R_0)^{a2} + a_3$

$a_1 = 1.0077$, $a_2 = 0.0394$, $a_3 = 0.00712$

(Brand & Blitz 1993)

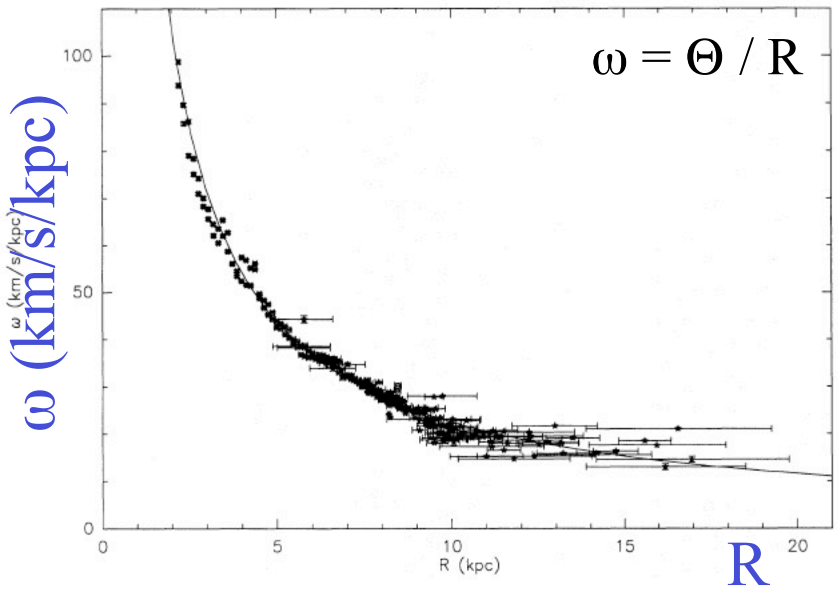

Kinematic distances II

Rotation curve: $\Theta = \Theta_0 \, (R/R_0)^a$ with $\Theta_0 = 220$ km/s, $R_0 = 8.5$ kpc

In general: $V_{lsr} = R_0(\omega - \omega_0) \sin l \cos b$, and $\omega = \Theta/R$.

It follows that:

$R = ([(V_{lsr} / \sin l \cos b) + \Theta_0] / \Theta_0 \, R_0^{1-a})^{1/(a-1)}$ and

$d = [R_0 \cos l \pm (R^2 - R_0^2 \sin^2 l)]^{0.5} / \cos b$

For outer Galaxy: choose '+'
For inner Galaxy, there are 2 solutions: distance ambiguity!

Distance ambiguity in inner Galaxy

Velocity field from rotation curve

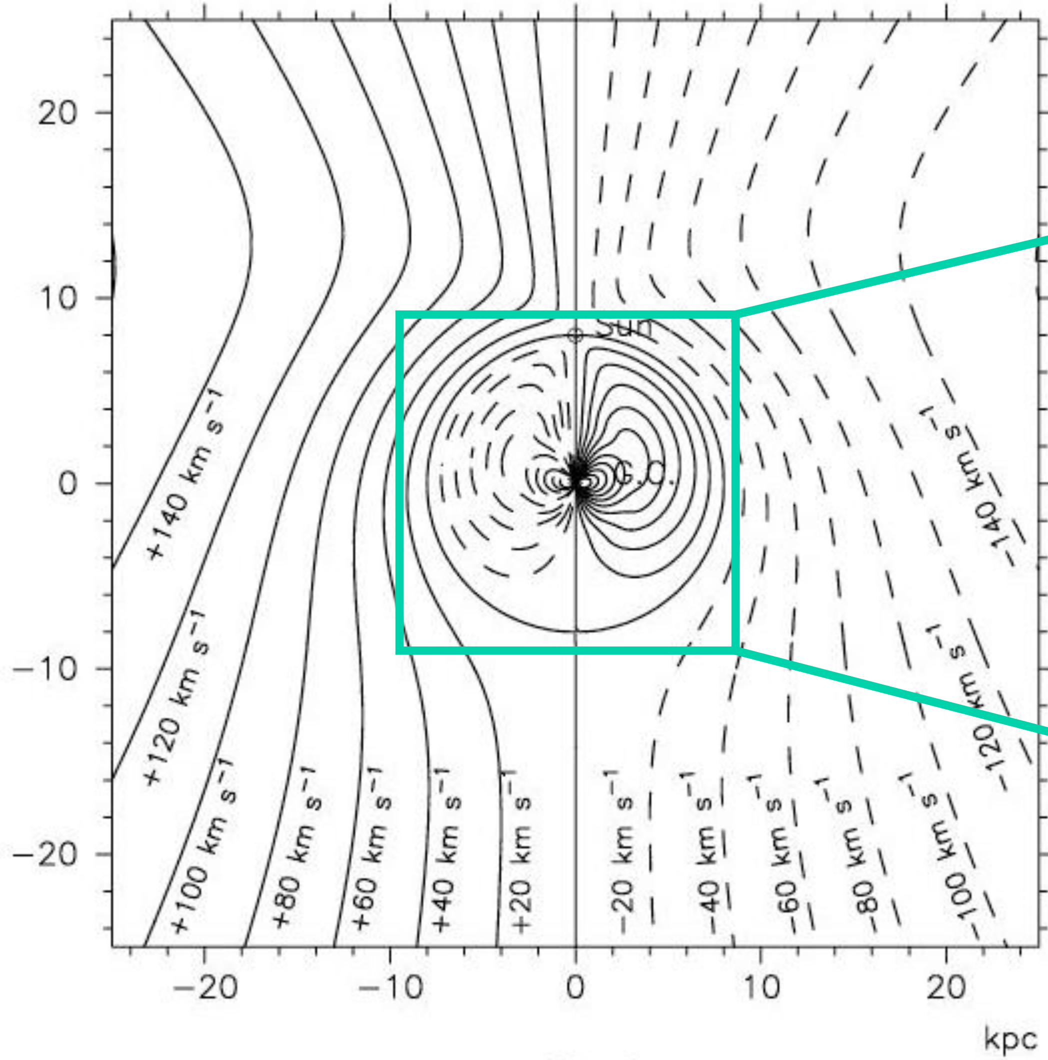

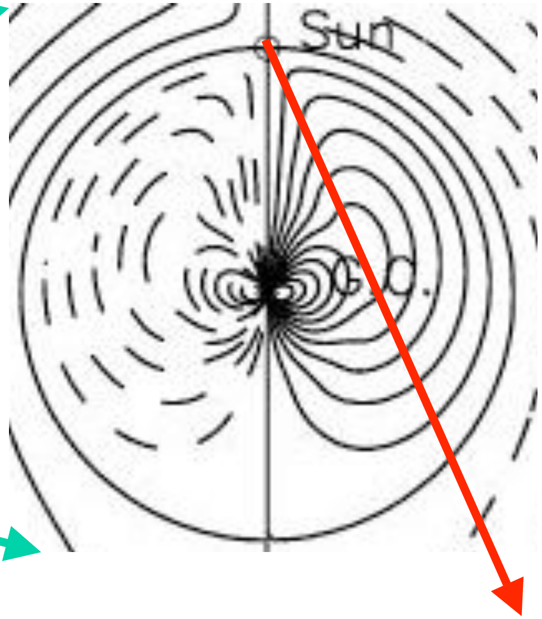

Nakanishi & Sofue 2003 PASJ

Two values for d at the same V_{lsr} : ambiguity

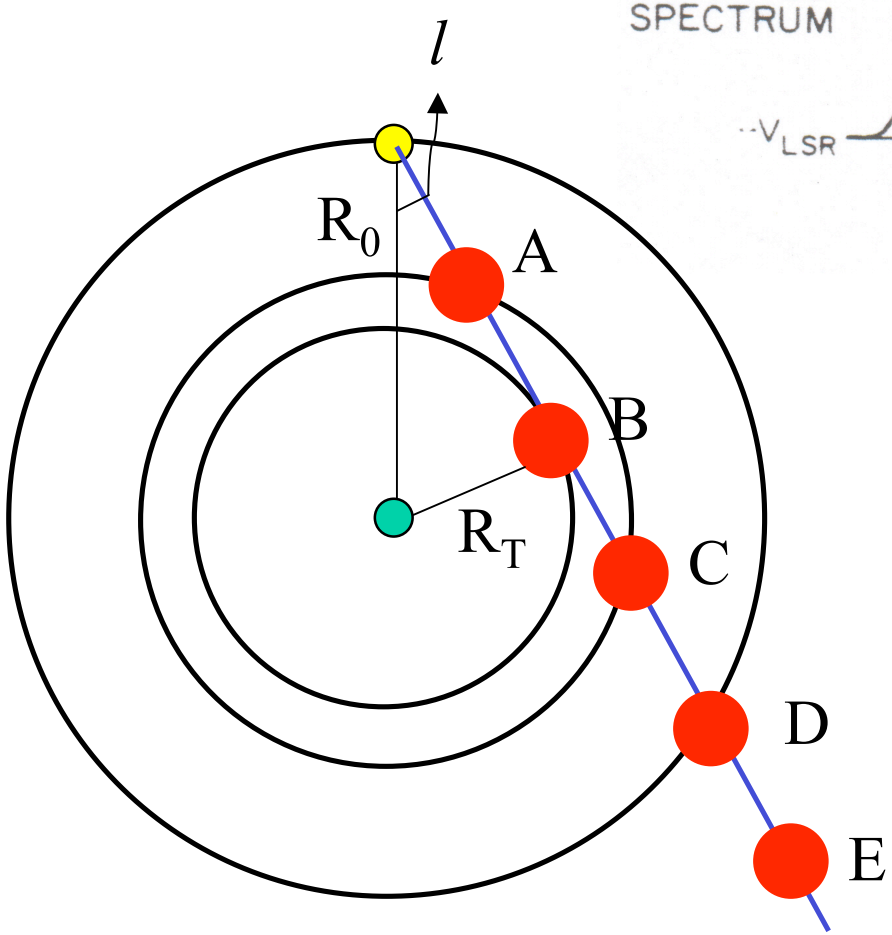

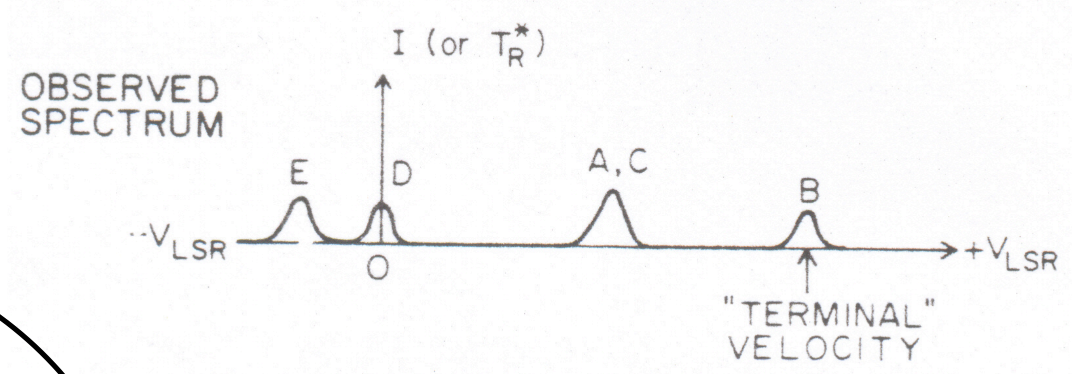

$R_T = R_0 \sin l$: subcentral (tangent) point. Maximum V_{lsr} long l.o.s.

Velocity crowding

Contours of dV/dr

Arched in green:
dV/dr ≤ 6 km/s/kpc

Artificial density structures

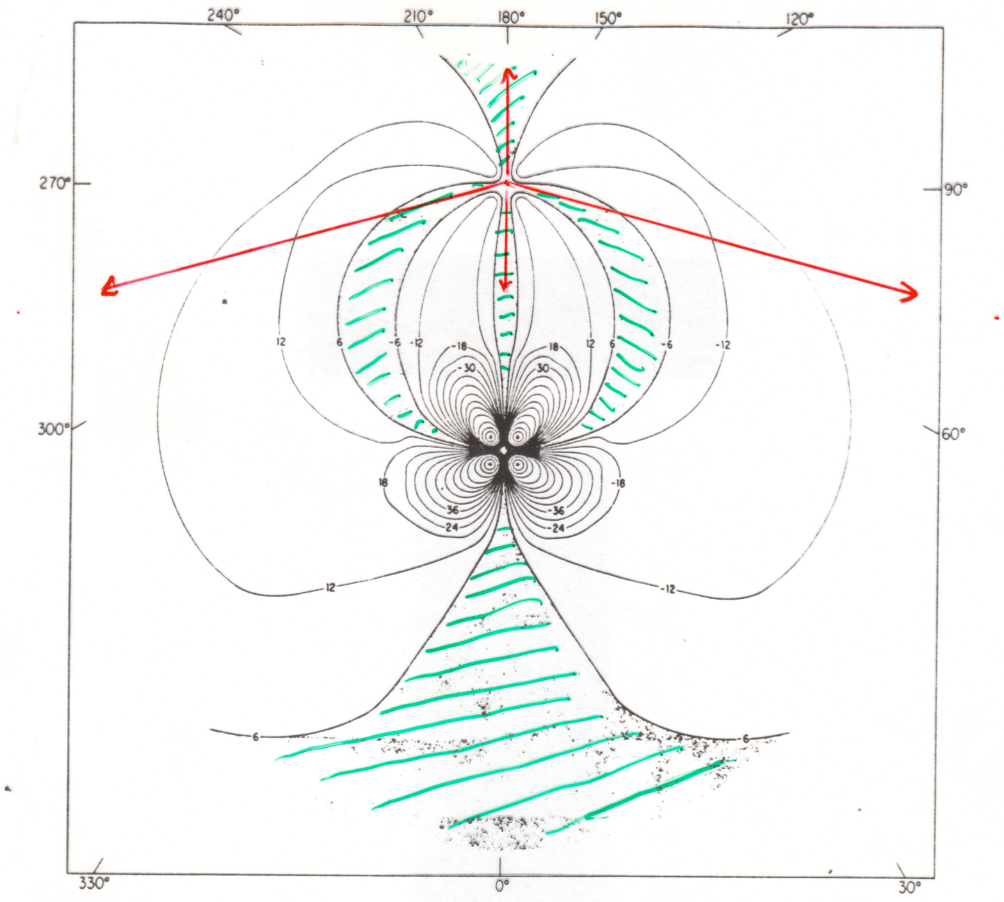

(Burton 1988)

HI: V-residuals

(Burton & Bania 1974)

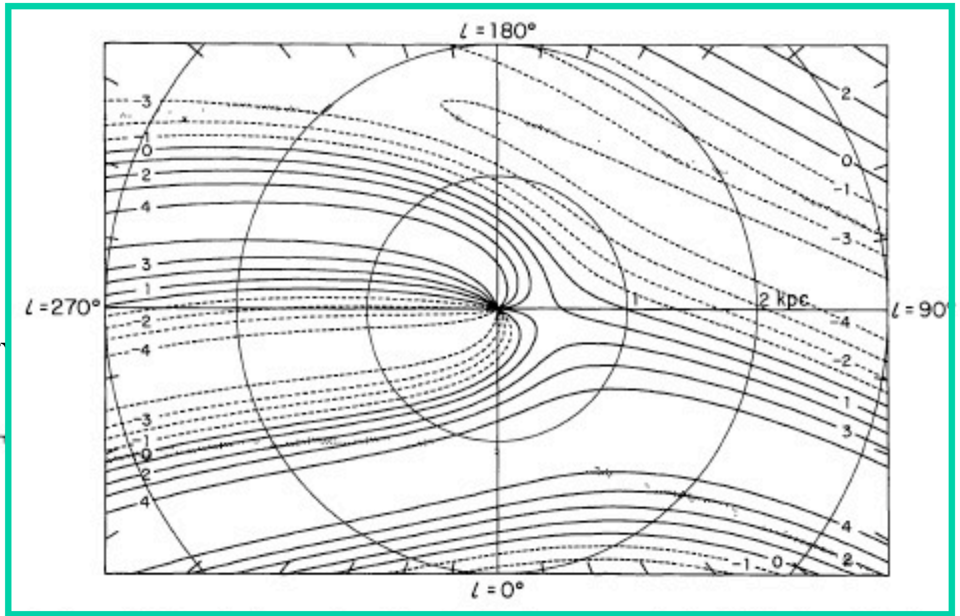

V_{lsr} - residuals: obser

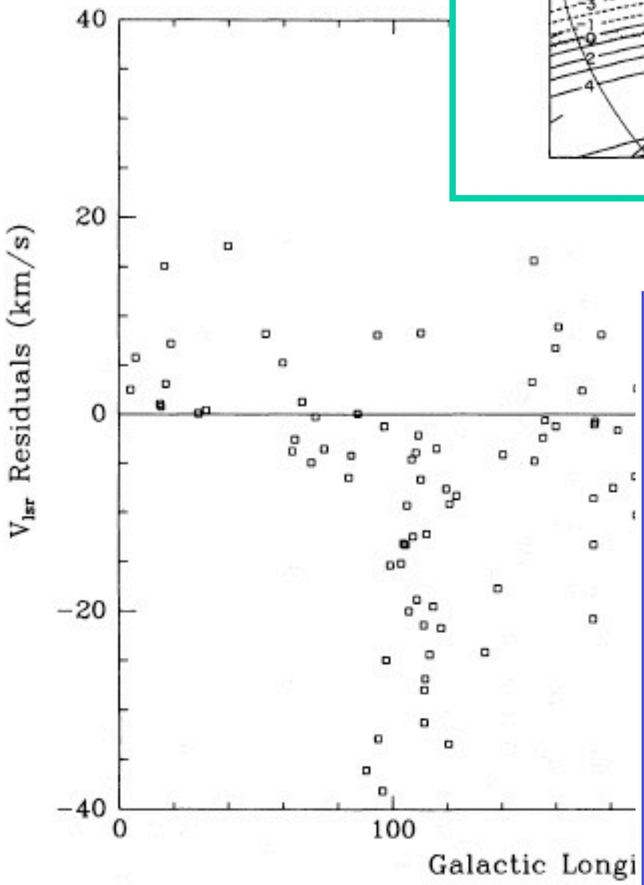

CO: Streaming motions pattern

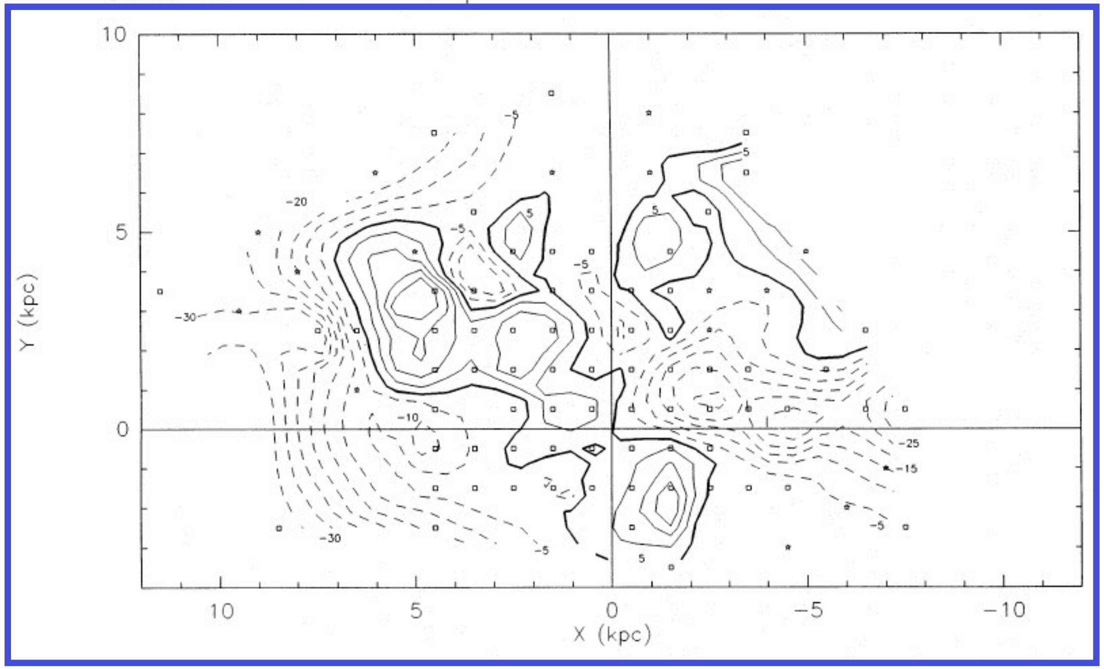

(Brand & Blitz 1993)

Trigonometric parallax

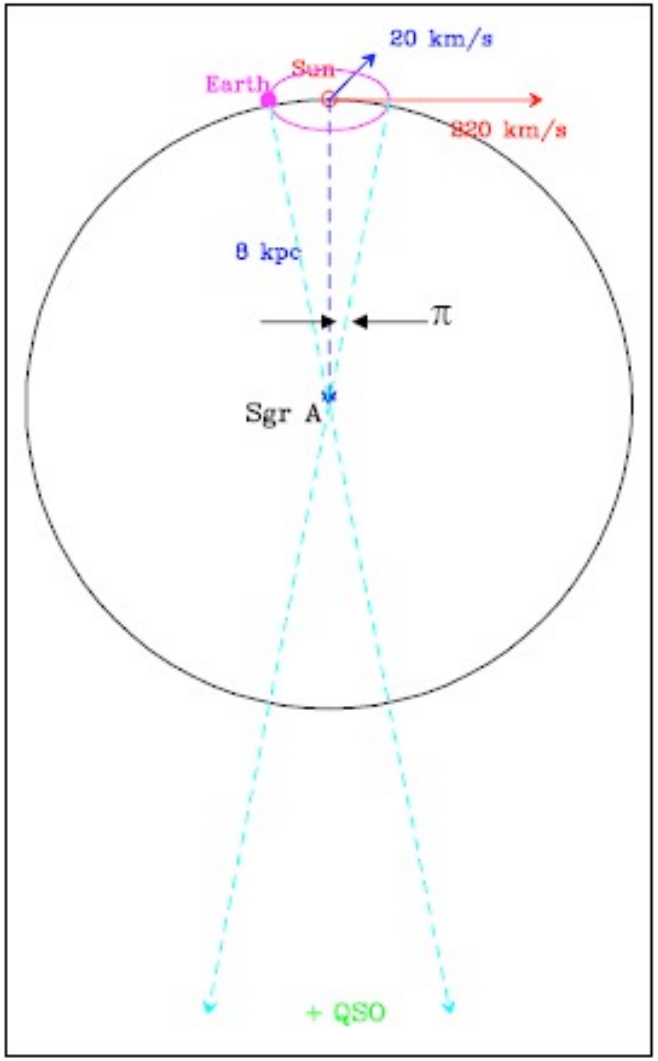

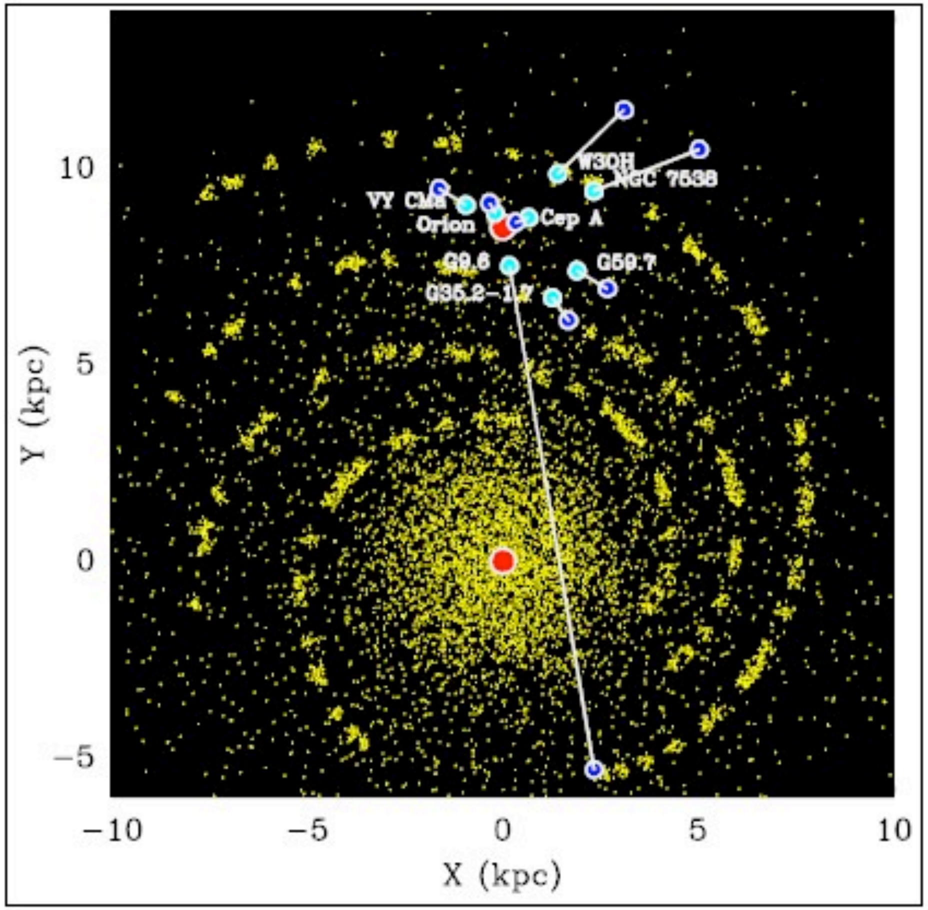

(Reid – IAU242, 2007; ApJ 700, 137 2009)

The new Galaxy

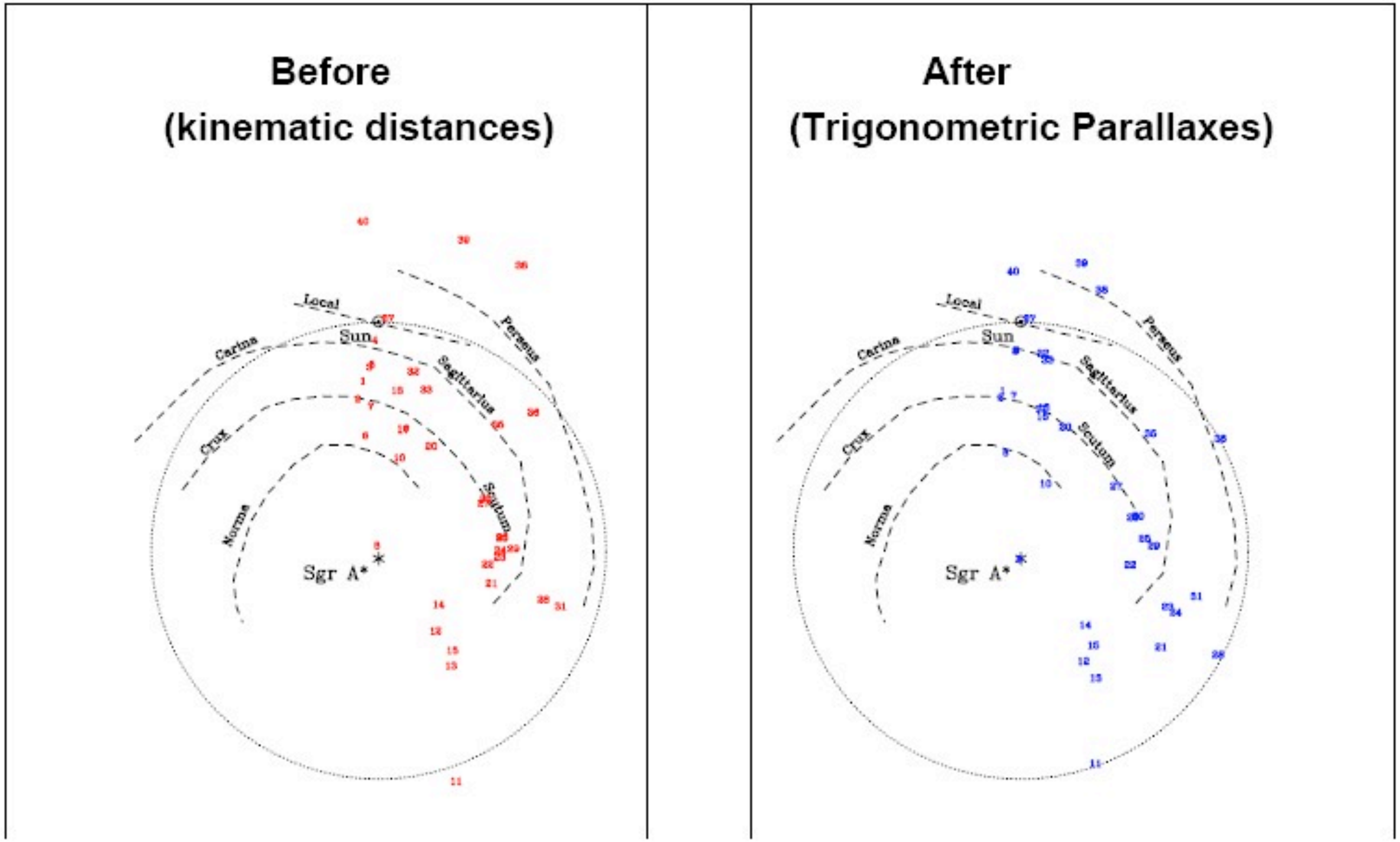

(Reid - IAU242, 2007; 2009)

STAR FORMATION

Star formation: in molecular clouds

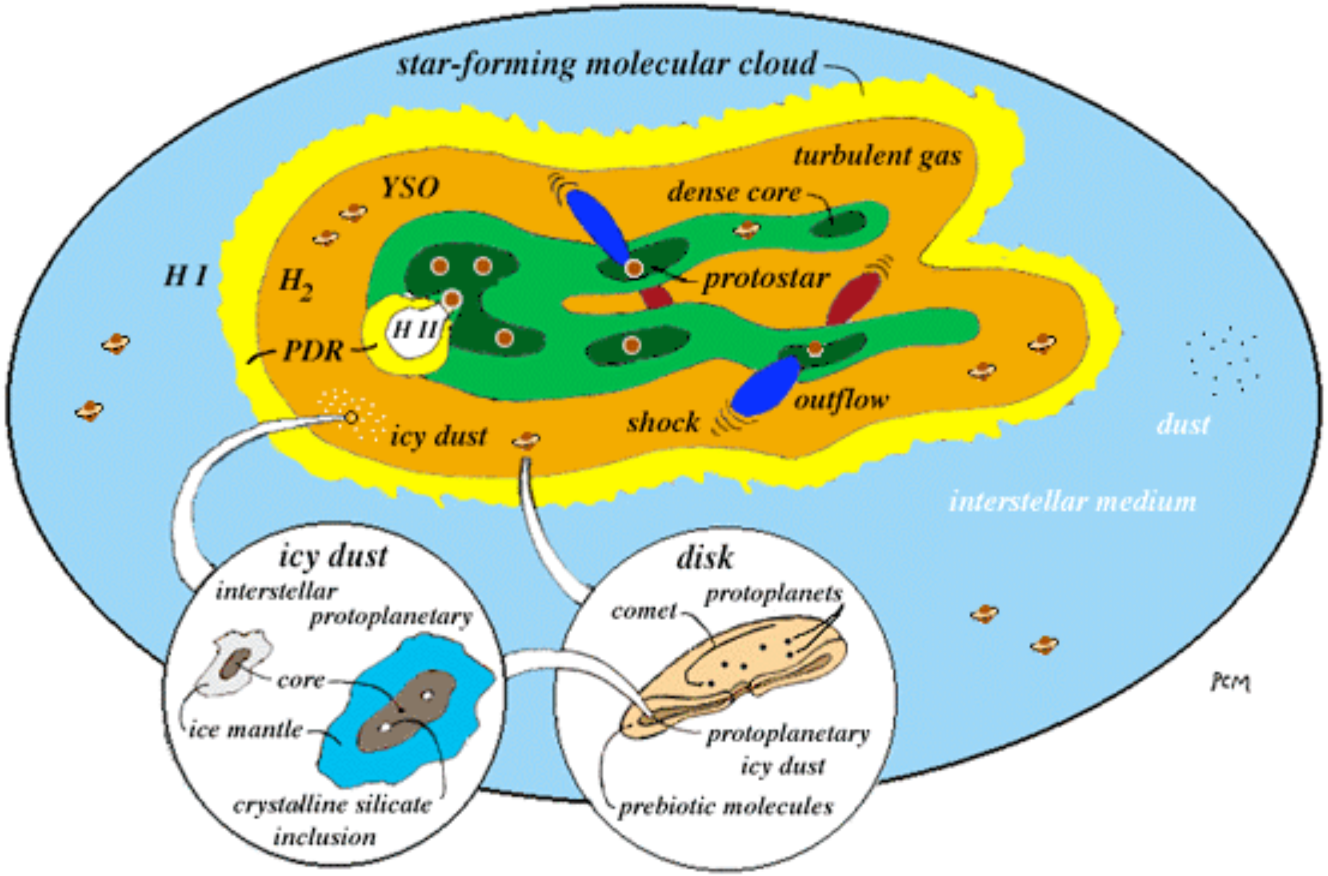

Star formation catastrophe?

$M_{cloud} \approx 10^{4\text{-}5}\, M_\odot \gg M_{Jeans} \approx 10^2\, M_\odot \Rightarrow$ collapse on

free-fall timescale $t_{ff} \approx \sqrt{(3\pi/32G\rho)} \approx 10^6$ yrs.

On galactic scale:

$SFR = M_{GMC}/t_{ff} \approx 10^9\, M_\odot / 10^6\, \text{yrs} \approx 10^3\, M_\odot\ /\text{yr}$

$\gg SFR_{obs} \approx 3\, M_\odot\ /\text{yr}$

Clouds are prevented from total collapse!

SFE: Star formation efficiency

TABLE 2 Star-formation efficiencies for nearby embedded clusters

Cluster name	Core mass ($M_\odot$)	Stellar mass ($M_\odot$)	SFE	References
Serpens	300	27	0.08	Olmi & Testi 2002
Rho Oph	550	53	0.09	Wilking & Lada 1983
NGC 1333	950	79	0.08	Warin et al. 1996
Mon R2	1000	341	0.25	Wolf et al. 1990
NGC 2024	430	182	0.33	E.A. Lada et al. 1991a,b
NGC 2068	266	113	0.30	E.A. Lada et al. 1991a,b
NGC 2071	456	62	0.12	E.A. Lada et al. 1991a,b

Lada & Lada 2003 ARAA 41

Cloud support

Virial theorem: $2T+2U+W+M=0$

Gravitational energy

Thermal energy (random motions): $U/W \approx 3\times10^{-3} \rightarrow$ irrelevant

Magnetic field term: $M/W = 0.3$

Kinetic energy (bulk motions, mostly from clumps): $T/W \approx 0.5$

Clouds are supported by turbulence and magnetic fields

B-field: Zeeman splitting

In presence of B-field, hyperfine splitting of levels is modified: spectral line splits in 2, centered on primary component, with opposing polarisations.

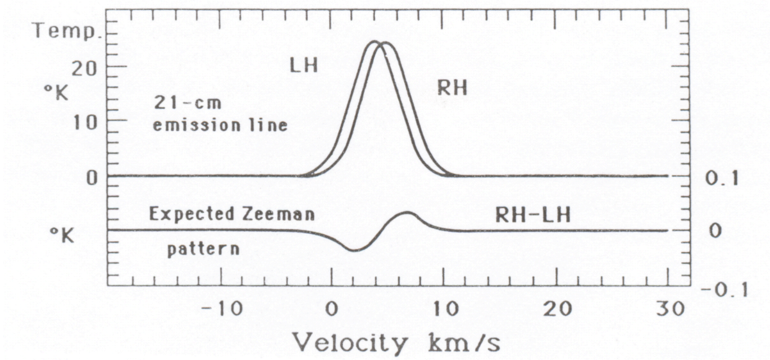

$$\frac{\Delta\nu_{\mathrm{mag}}}{\Delta\nu_{\mathrm{therm}}} \approx 10^{-3}\left(\frac{B}{\mu\mathrm{G}}\right)\left(\frac{T_k}{10\mathrm{K}}\right)^{-1/2}$$

3.27 Hz/μG OH @ 1665 MHz
1.96 Hz/μG OH @ 1665 MHz
7.2 10^{-4} Hz/μG NH_3 @ 22 GHz
2.3 10^{-3} Hz/μG H_2O @ 22 GHz

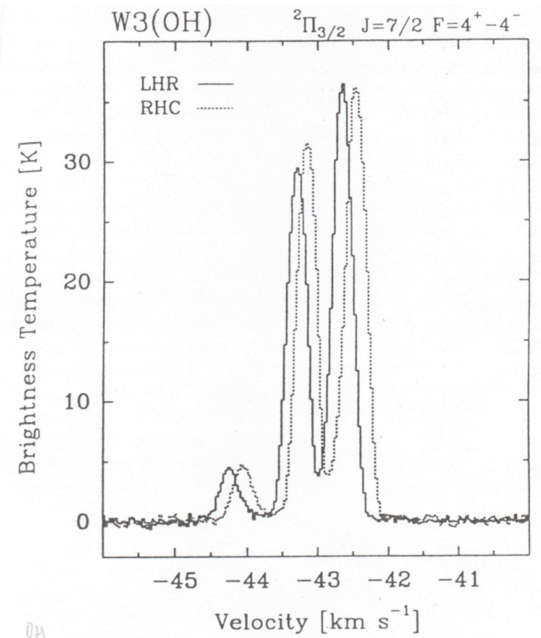

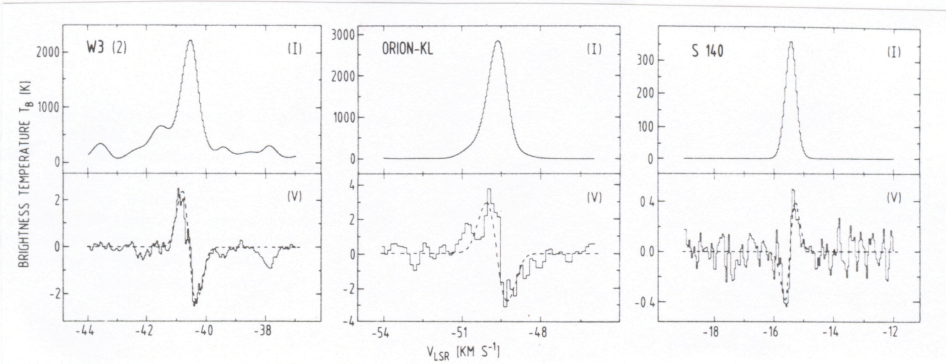

Güsten et al. 1994

B-field: Zeeman splitting

In presence of B-field, hyperfine splitting of levels is modified: spectral line splits in 2, centered on primary component, with opposing pol

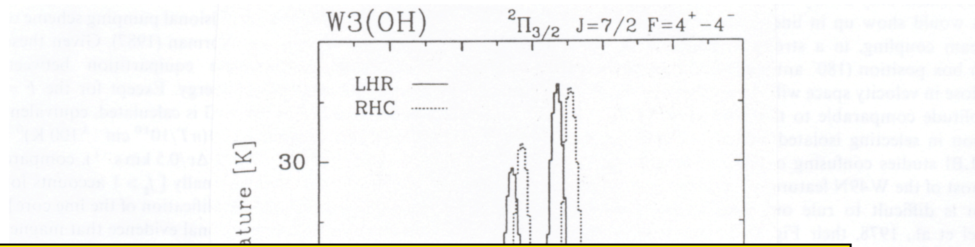

Measured values:

HI 21cm, OH 18cm: few μG (diffuse ISM; $n<100$ cm^{-3})

few μG (dark cloud envelopes; $n\sim10^3$ cm^{-3})

few μG (OH masing layers; $n\sim10^{7\text{-}8}$ cm^{-3})

H_2O 22GHz: 50mG (maser spots; $n\sim10^{10}$ cm^{-3})

$$\frac{\Delta\nu_{\text{mag}}}{\Delta\nu_{\text{therm}}} \approx 10^{-3}\left(\frac{B}{\mu\text{G}}\right)\left(\frac{T_k}{10\text{K}}\right)$$

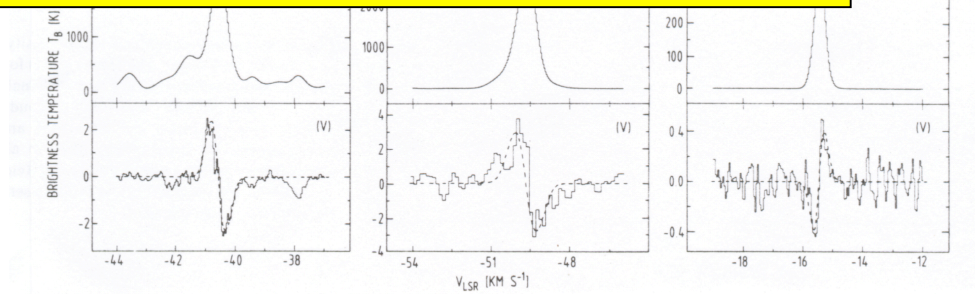

3.27 Hz/μG OH @ 1665 MHz

1.96 Hz/μG OH @ 1665 MHz

7.2 10^{-4} Hz/μG NH_3 @ 22 GHz

2.3 10^{-3} Hz/μG H_2O @ 22 GHz

Güsten et al. 1994

Results for Field Strength

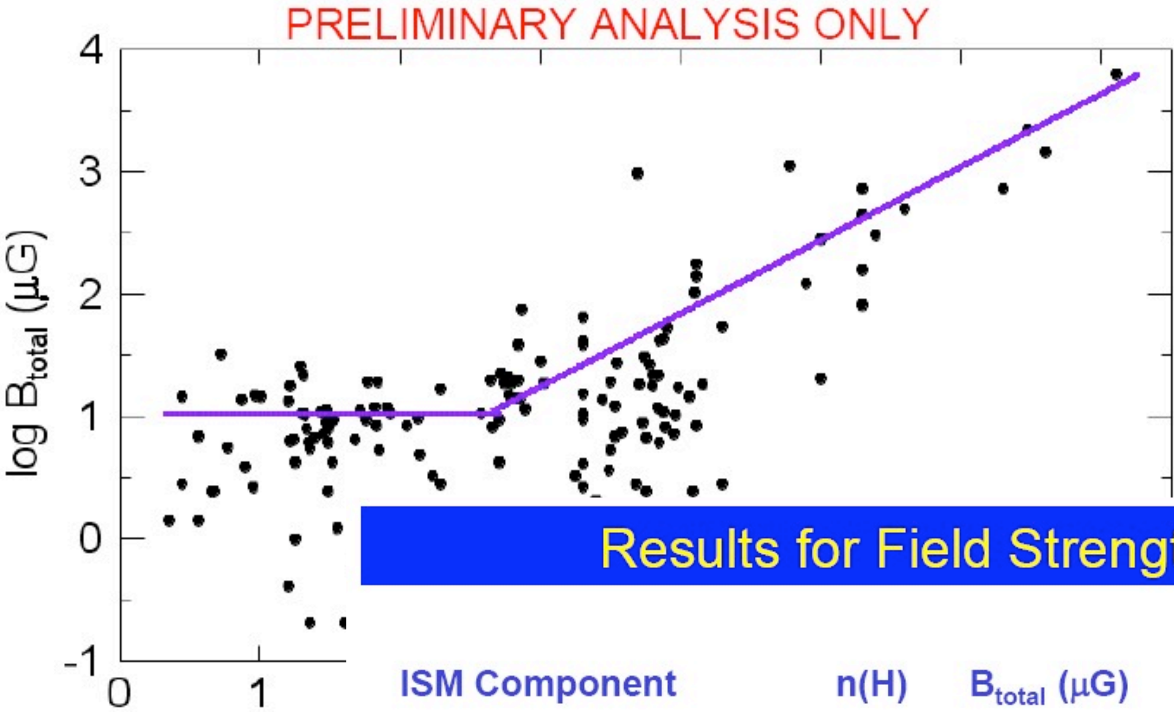

Results for Field Strength

ISM Component	n(H)	B_{total} (μG)	λ_C	κ ($B \propto n^{\kappa}$)
diffuse ionized medium (synchrotron equipartition, RMs)	~0.1	7 ± 3	-	~0
H I clouds (H I Zeeman)	~50	6 ± 2	~0.1	~0
molecular clouds (OH, CN Zeeman)	10^3–10^7	10–3,000+	~1	~0.5

(Crutcher – IAU242, 2007)

Clump stability

Forces working on clumps:

- Clump (self-) gravity
- Clump turbulence (and thermal pressure)
- Interclump pressure
- Magnetic fields

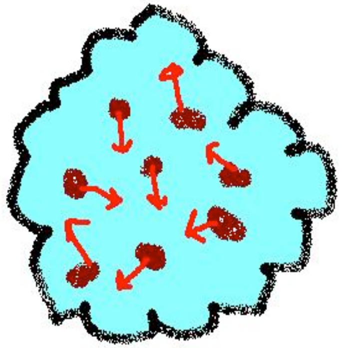

Clump virial theorem (e.g. Fleck 1988):

$4\pi r^3 P = 3M_{CO}\sigma^2 - GM_{CO}^2/r + B^2/8\pi$

Expressed in pressures:

$P/k = \rho\sigma^2/k - GM_{CO}\rho/3rk + B^2/8\pi k$

$\mathbf{P_{ext}/k = P_{turb}/k + P_{grav}/k + P_{magn}/k}$

$P_{turb}/P_{grav} = \alpha = 126\ r[pc]\ \Delta v[kms^{-1}]^2/M_{CO} = M_{vir}/M_{CO}$: virial parameter

$P_{magn}/k = 2.9 \times 10^4\ Kcm^{-3}$ for $10\mu G$

Interclump pressure (self-gravity GMC): $P_{ext}/k = 1.7 \times 10^4 - 5.9 \times 10^4\ Kcm^{-3}$

Clump pressure ratios

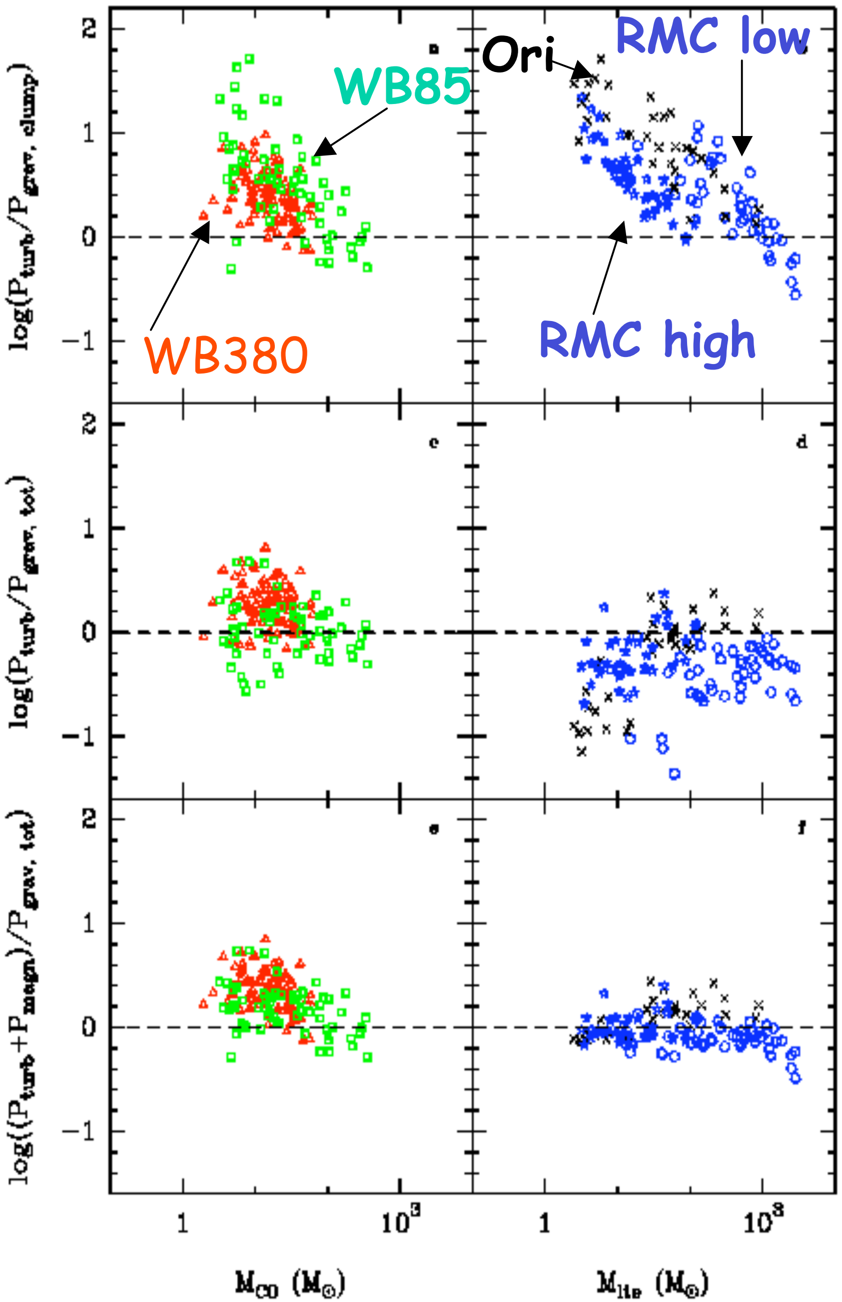

Turbulence
&
gravity

Turbulence
&
total gravity

Turbulence,
total gravity
&
magnetic field
pressure

Brand et al. 2001

Herzsprung-Russel diagram

Palla & Stahler (1990)

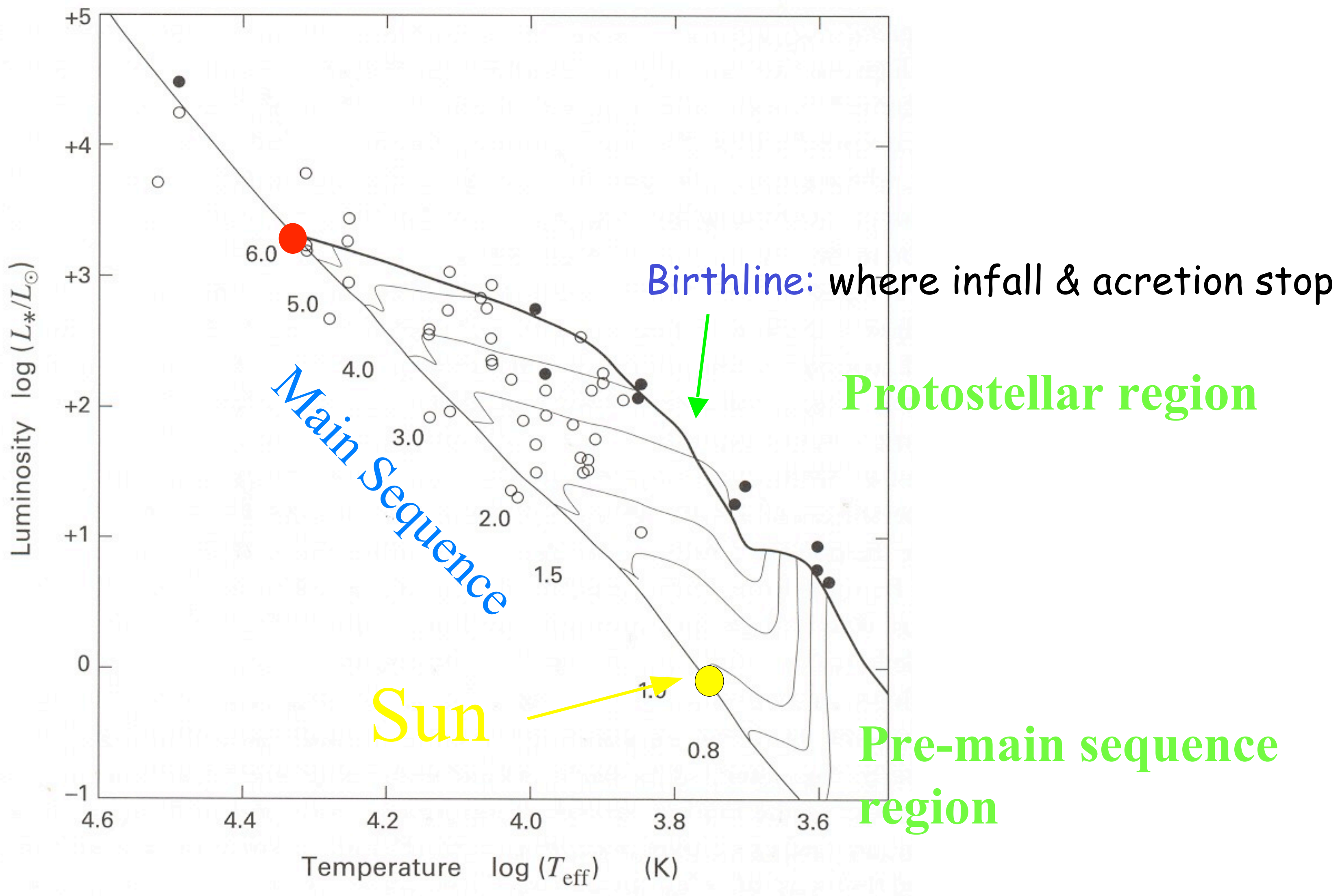

Normal star: evolutionary status determined by location HRD:
L, T_{eff}

Embedded YSOs: associated with natal gas & dust
Cannot be placed in HRD

Protostellar stage: circumstellar gas & dust:
absorbs and reprocesses radiation embedded object
Has extent >> stellar photosphere → dust has wide range of T
SED wider than single-T BB;
shape SED depends on nature & distribution of circumstellar material

More evolved object (pre-ms, ms): envelope, disk almost gone
Shape of SED is f(evolutionary state)

Observationally:
YSOs fall into 4 classes, based on shape of SED

Stars < $8M_{\odot}$

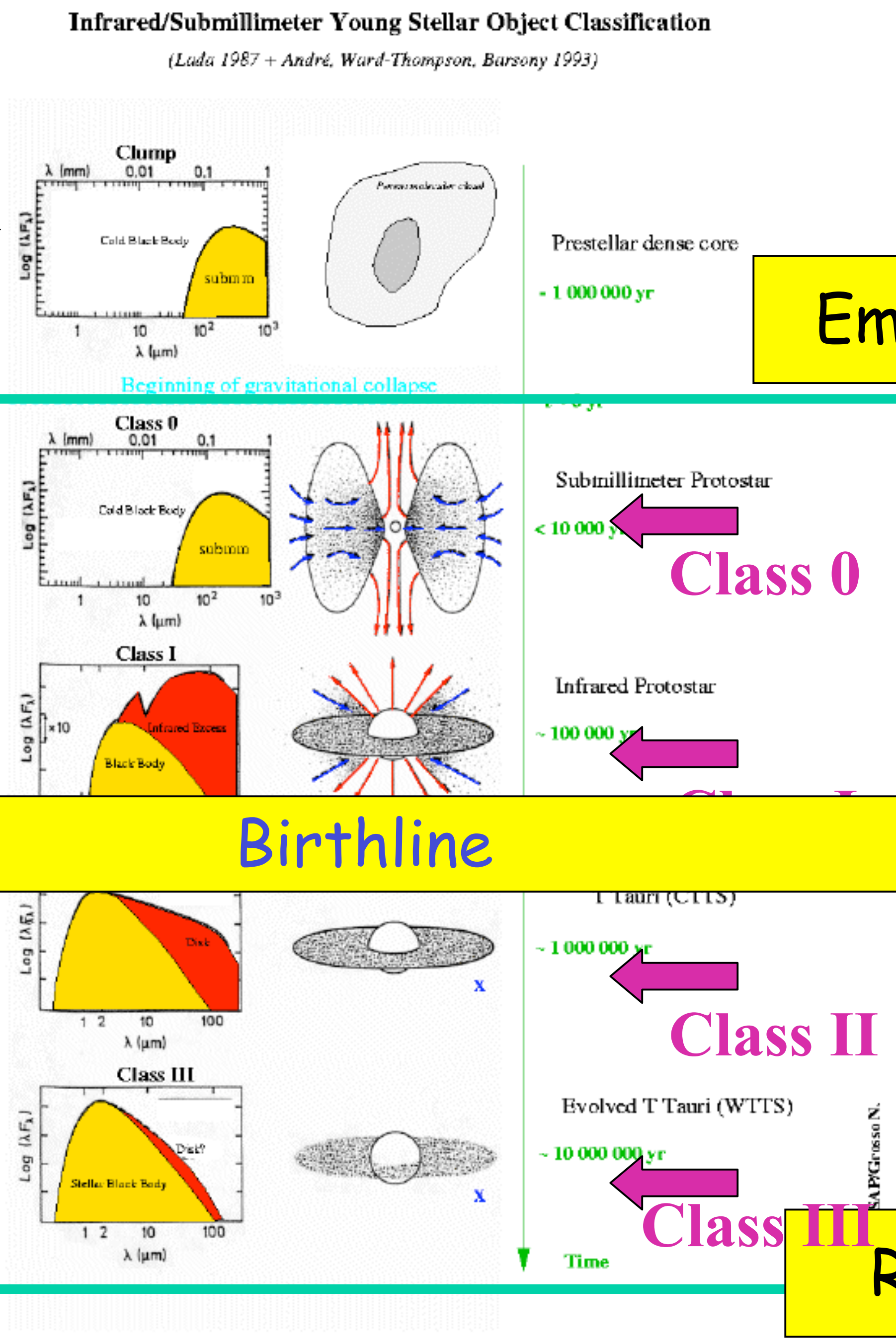

sub-mm — unstable isothermal clump

Embedded phase

Birthline

far-IR — Class 0 — accretion onto protostar

near-IR — Class I — formation of disk & outflow

optical +NIR — Class II — disk without accretion

optical — Class III — protoplanetary disk

Revealed phase

Embedded phase: protostars

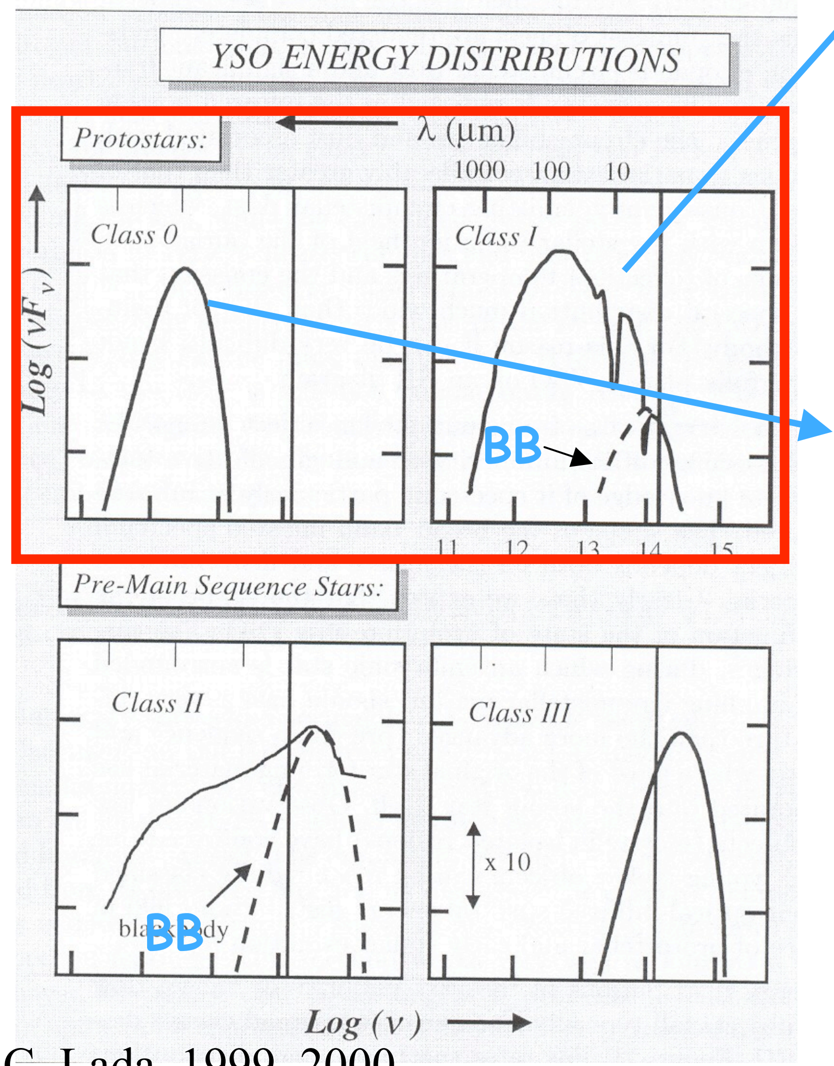

C. Lada, 1999, 2000

Class I:

- SED broader than single-T BB
- At λ>2μm SED rises with λ: huge IR-excess
- Deeply embedded; detected in NIR (freq. assoc'd with RNe)
- Often associated with outflows
- $M_{circumst}$(r<1000AU) << M_*
- Age ca. 1-5 x 10^5 yrs

Class 0:

- Much more extincted & embedded;
- SED peak in submm; not detected at λ<20μm
- SED similar to BB at T=20-30K
- All have energetic, v. highly collimated outflows.
- $M_{circumst}$(r<1000AU) $\approx$ M_*
- Constitute 10% of embedded sources
- Age ca. 10^4 yrs

Protostellar nature embedded YSOs: evidence

Protostar: objects in process of accumulating into star-like configuration the bulk of the material they will contain as ms stars

1) SED can be modeled as embryonic stellar core + circumstellar disk + massive gas & dust envelope with density structure as predicted by theory for ellar cloud cores.

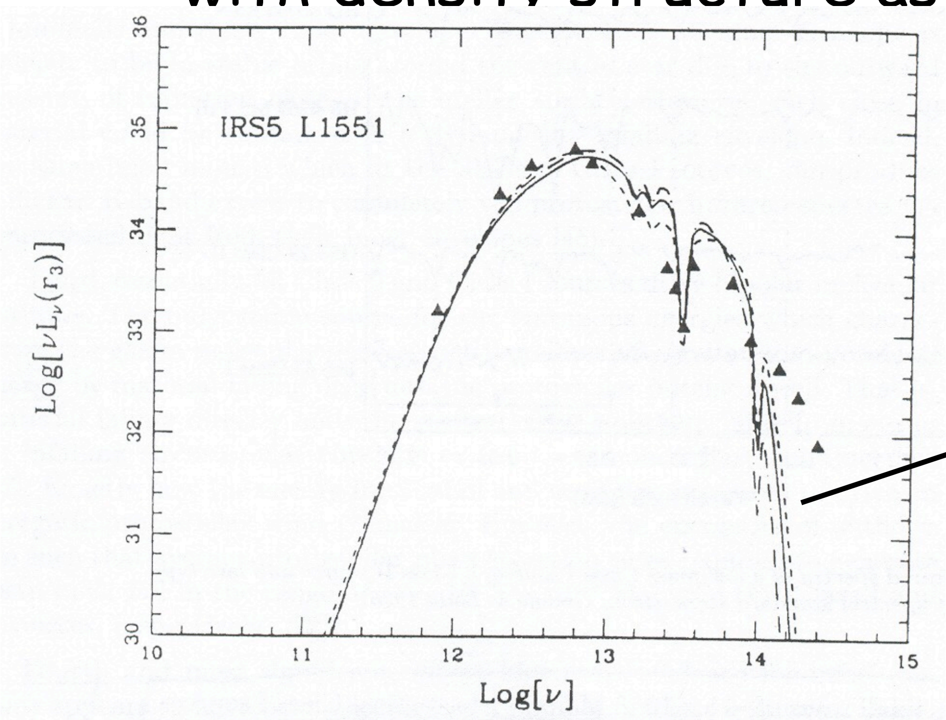

fits: rotating-collapsing isothermal protostellar models

Mass infall rate ~ 5 x 10^{-6} $M_{\odot}$ /yr

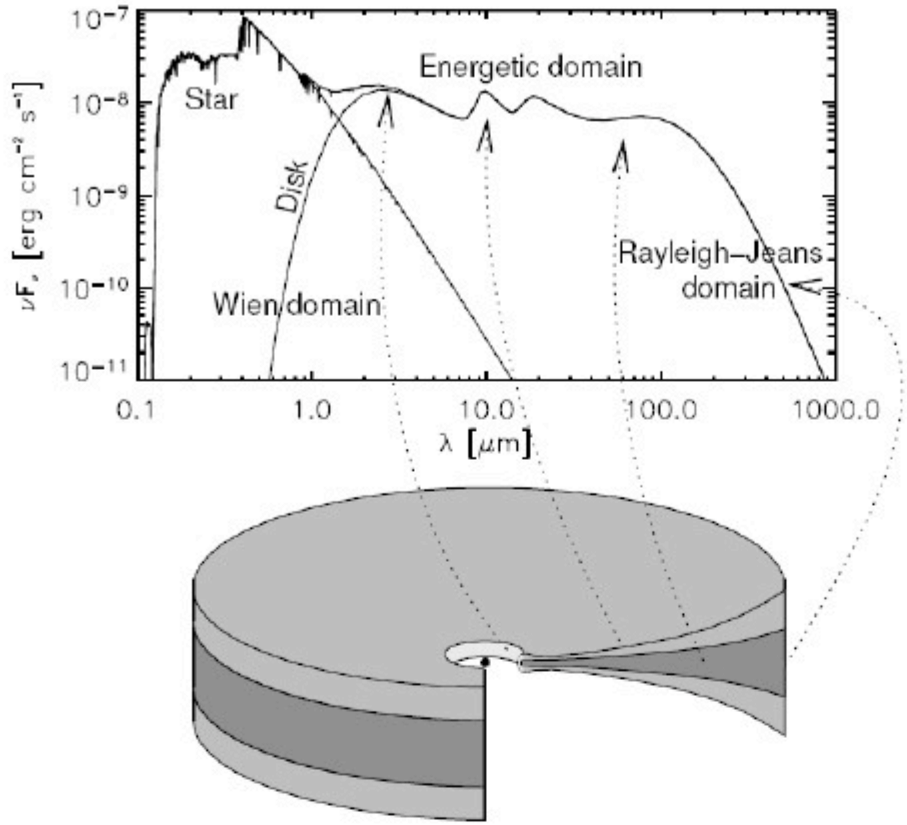

Figure 1.2: From Dullemond et al. (2006). Build-up of the SED of a flaring circumstellar disk and the origin of various components: the near infrared bump is supposed to originate in the puffed-up inner rim, the infrared dust features (as the silicate ones between 10μm and 20μm) from the warm surface layer, and the underlying continuum from the deeper and cooler disk regions. Typically the near and mid-infrared emission comes from small radii, while the far-infrared and the millimeter emission come from the outer disk regions.

Isella 2006: Dullemond et al. 2006

Protostellar nature embedded YSOs: evidence

1) SED can be modeled as embryonic stellar core + circumstellar disk + massive gas & dust envelope with density structure as predicted by theory for rotating, infalling protostellar cloud cores.

2) … es hot dust at << 1AU … ux to 'veil' absorption … that.

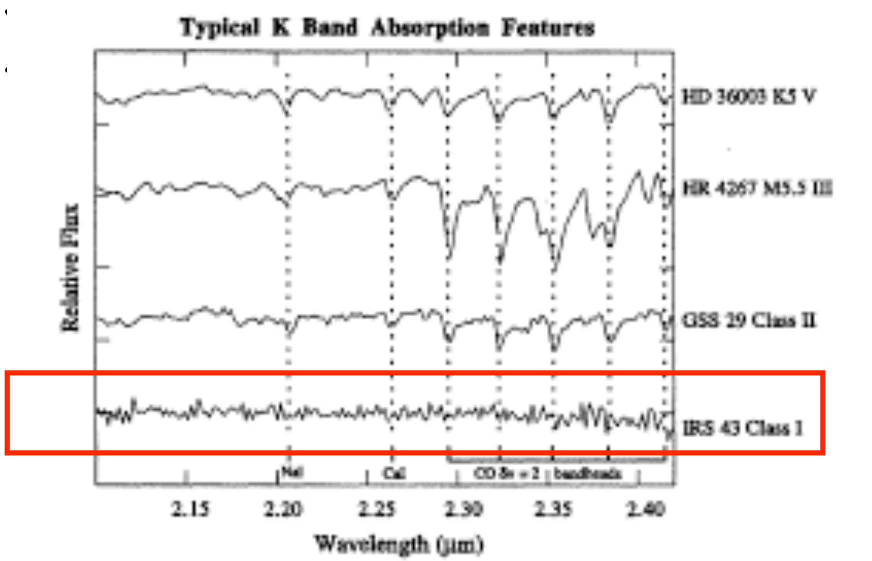

FIG. 1. *K*-band absorption features. The indicated Na I, Ca I, and CO features are commonly seen in the spectra of late-type stars such as the typical MK standards HD 36003 and HR 4267. Class II (and III) YSOs (such as GSS 29 shown) usually show similar features, but Class I YSOs (such as IRS 43 shown) usually do not show any early- or late-type features. The data shown are enlarged subregions of spectra presented in Appendix, but baseline continuum slopes have been removed.

Greene & Lada, AJ 1996

Protostellar nature embedded YSOs: evidence

1) SED can be modeled as embryonic stellar core + circumstellar disk + massive gas & dust envelope with density structure as predicted by theory for rotating, infalling protostellar cloud cores.

2) Featureless spectrum, requires hot dust at << 1AU to provide additional cont. flux to 'veil' absorption lines. Infall models acount for that.

3) Only viable source for outflow energy is gravity (from infall).

4) Direct kinematic evidence for infall motions found in Class 0 sources!

Protostellar infall

Detecting infall from
opt. thick line

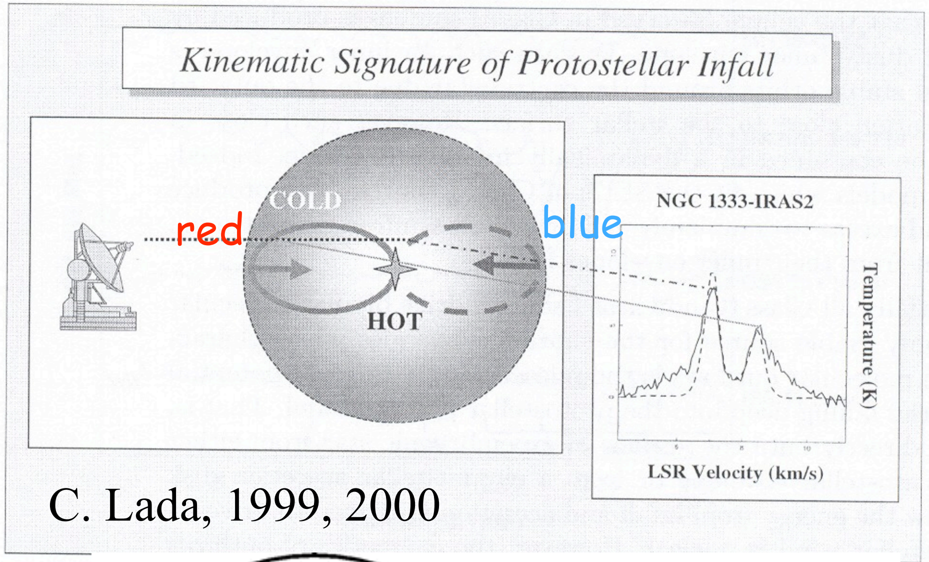

C. Lada, 1999, 2000

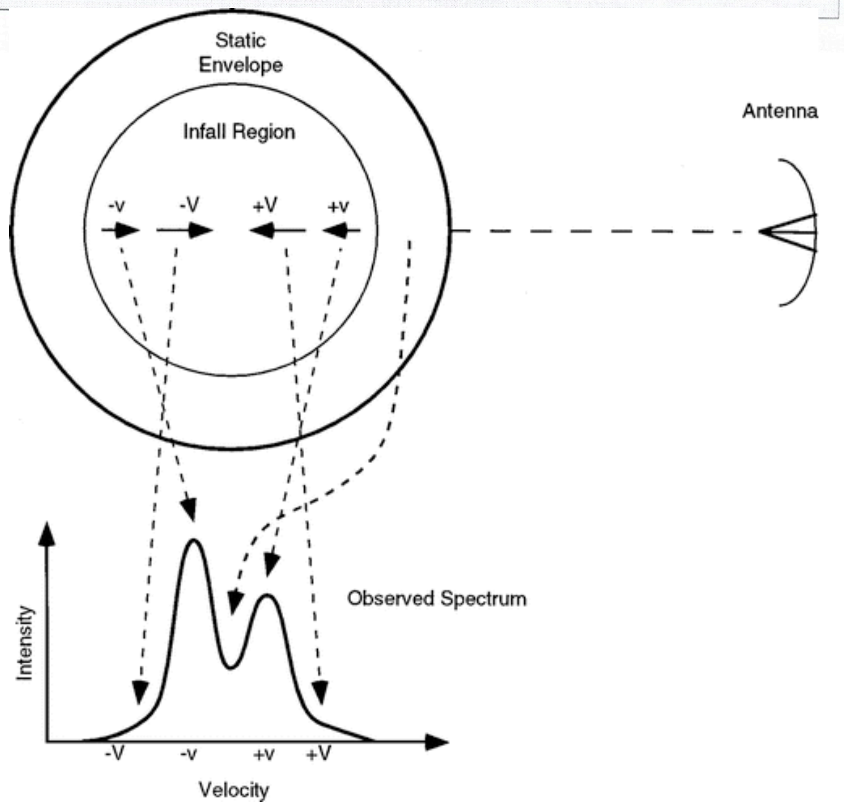

B335; Zhou et al. 1993

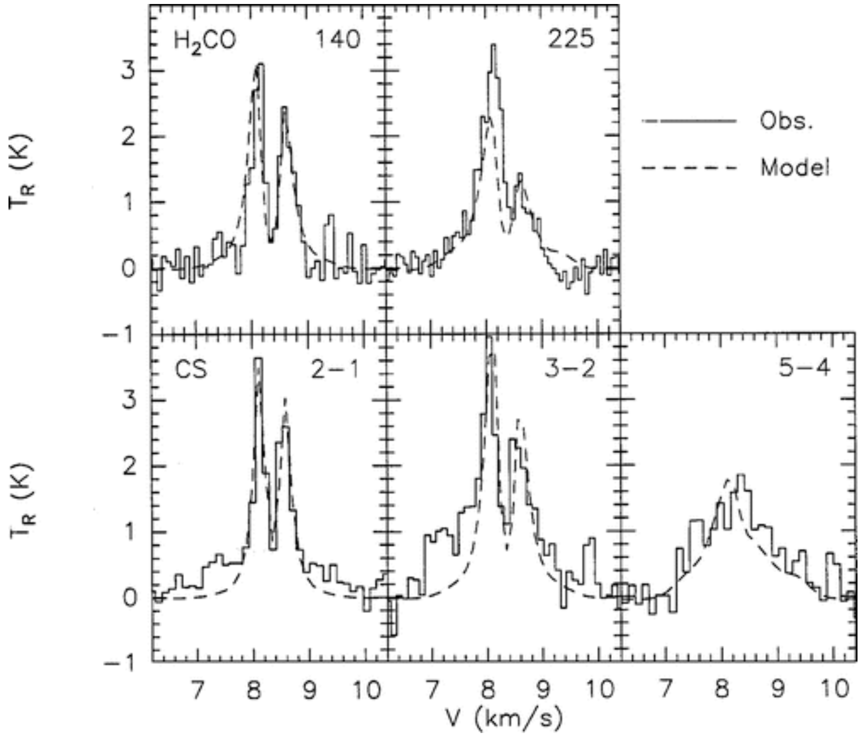

Revealed phase:
Pre-ms stars

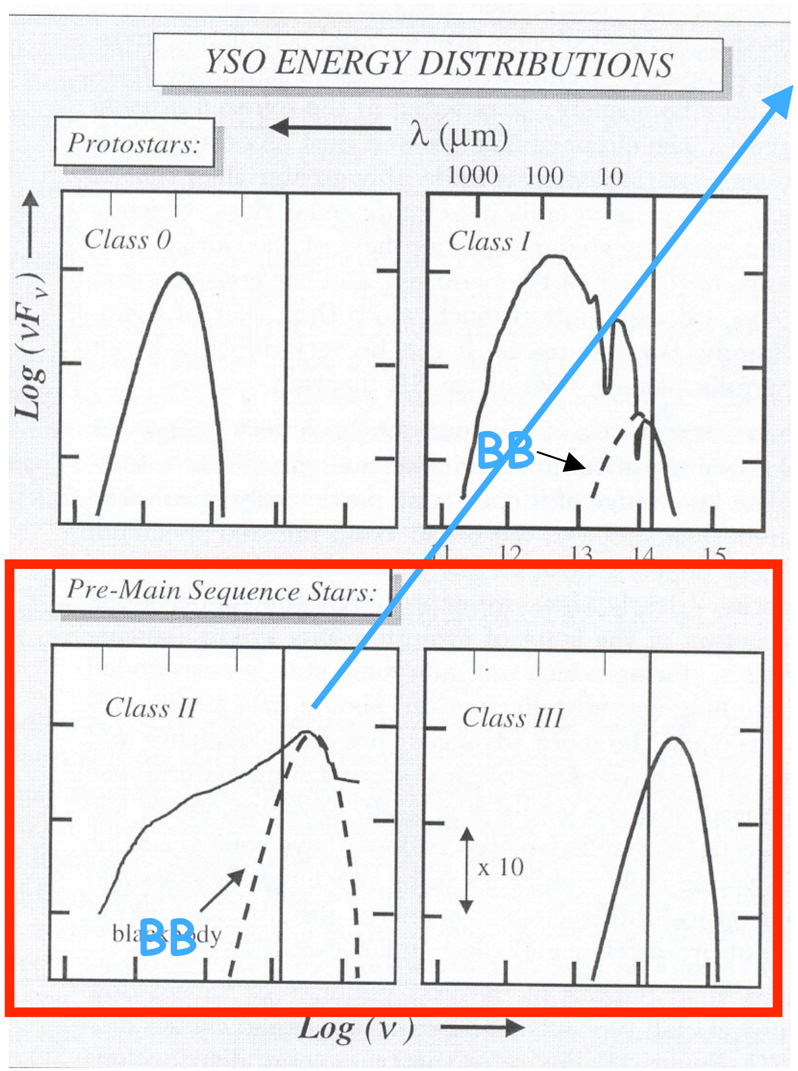

Class II:

- -SED peaks in visible or NIR
- -SED broader than single-T BB
- -At λ>2μm SED falls with λ (power-law): IR-excess, but smaller than Class I
- -Disk, but no massive envelope
- -$M_{disk} \approx$ 0.01-0.1 $M_{\odot}$
- -Accretion rate ~ 10^{-8} $M_{\odot}$/yr
- -in SFRs: 10x more than ClassI
- -in optical, ClassII are CTTS

SED can be fitted with model of disk with T-gradient, reprocessing and reradiating light from central star

C. Lada, 1999, 2000

ClassII model fit

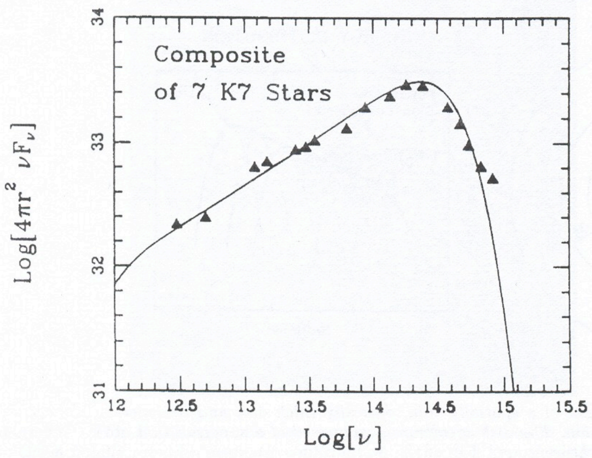

Figure 15. The composite SED of seven Class II stars along with that (solid line) of a model circumstellar disk. (From Adams, Lada and Shu 1988).

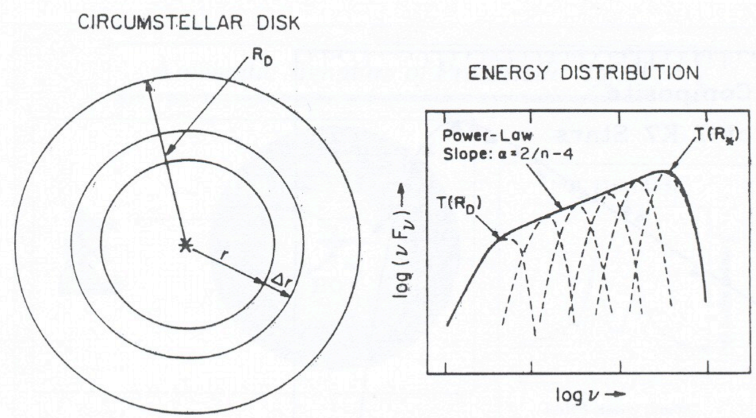

Figure 16. Schematic diagram of a spatially thin, optically thick disk and its emergent spectral energy distribution. The disk spectrum is composed of a superposition of blackbodies of varying temperature.

Disk: each annulus has area $2\pi R\Delta R$ and radiates as BB with $T(R)$

SED is superposition of series of BB-curves

If $T(R) \sim R^{-n}$, then (Wien's law) max. emission at $\nu \sim T(R) \sim R^{-n}$.

Luminosity each annulus: $L_\nu d\nu = 2\pi R\Delta R \sigma T(R)^4 \sim R^{2-3n} d\nu \sim \nu^{3-2/n}$.

For a SED, $\nu L_\nu \sim \nu^{4-2/n}$.

C. Lada, 1999, 2000

Revealed phase: Pre-ms stars

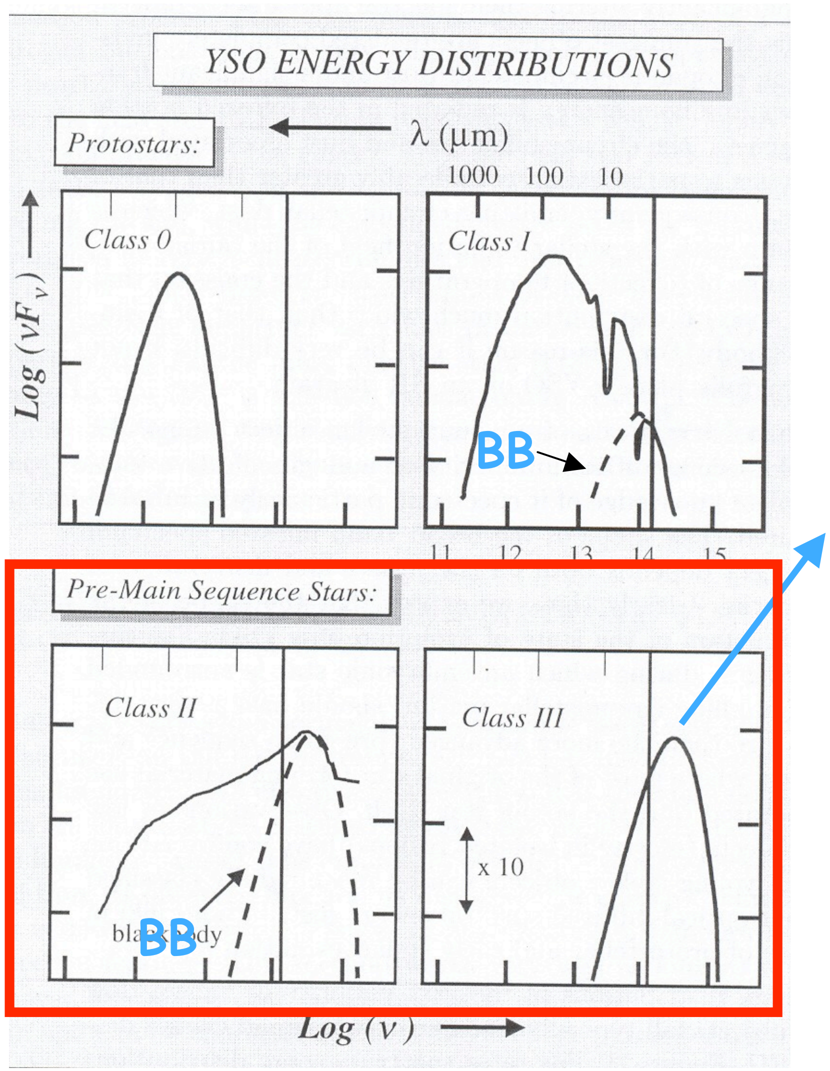

Class III:

-SED peak in visible/NIR
-SED similar to single-T BB; interpreted as photospheres of young stars with extinction.
-No significant amounts circumstellar gas, dust
-ClassIII are WTTS
-Age ca. 10^6 - 10^7 yrs

No IR excess, confused with fore- & background stars in SFRs. But are X-ray sources.

C. Lada, 1999, 2000

Evolutionary sequence low-mass YSOs

Evolution Class 0 $\Rightarrow$ I $\Rightarrow$ II:
requires removal circumstellar material in infalling envelope

Evolution Class II $\Rightarrow$ III:
Requires clearing of circumstellar disk

Total accretion: NO - because SFE is very low ($M_* \ll M_{core}$)

Therefore: very early on cloudy material physically removed
Most likely by bipolar outflows, originating from stellar wind
(virtually all Class 0,I drive molecular outflows).

A protostar can only gain mass if it loses mass at same time

Disk lifetimes

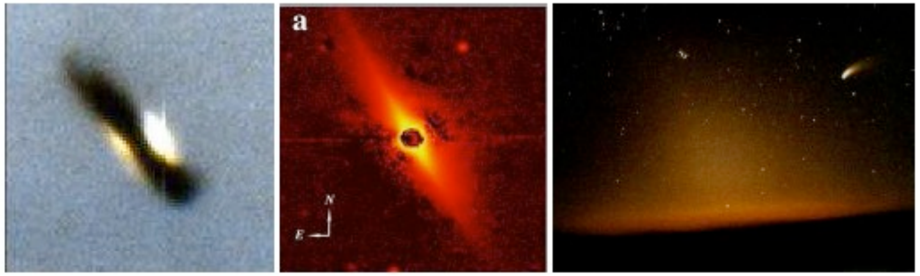

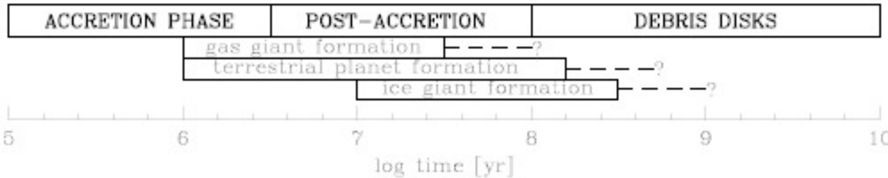

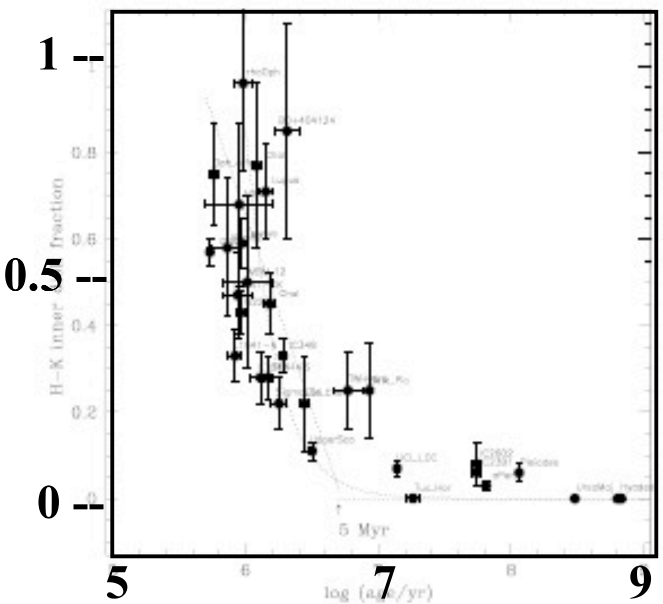

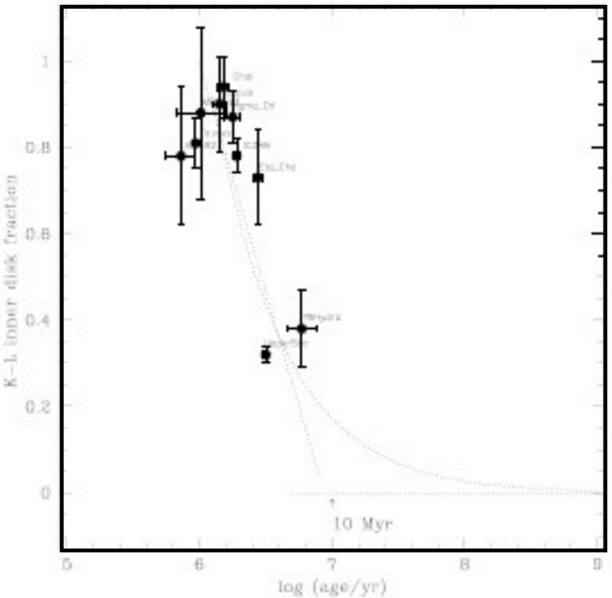

Hillenbrand 2006

Disk fraction vs. log(cluster age) for ca. 3500 stars, 0.3-1 $M_\odot$

YSOs: IR colour-colour diagram

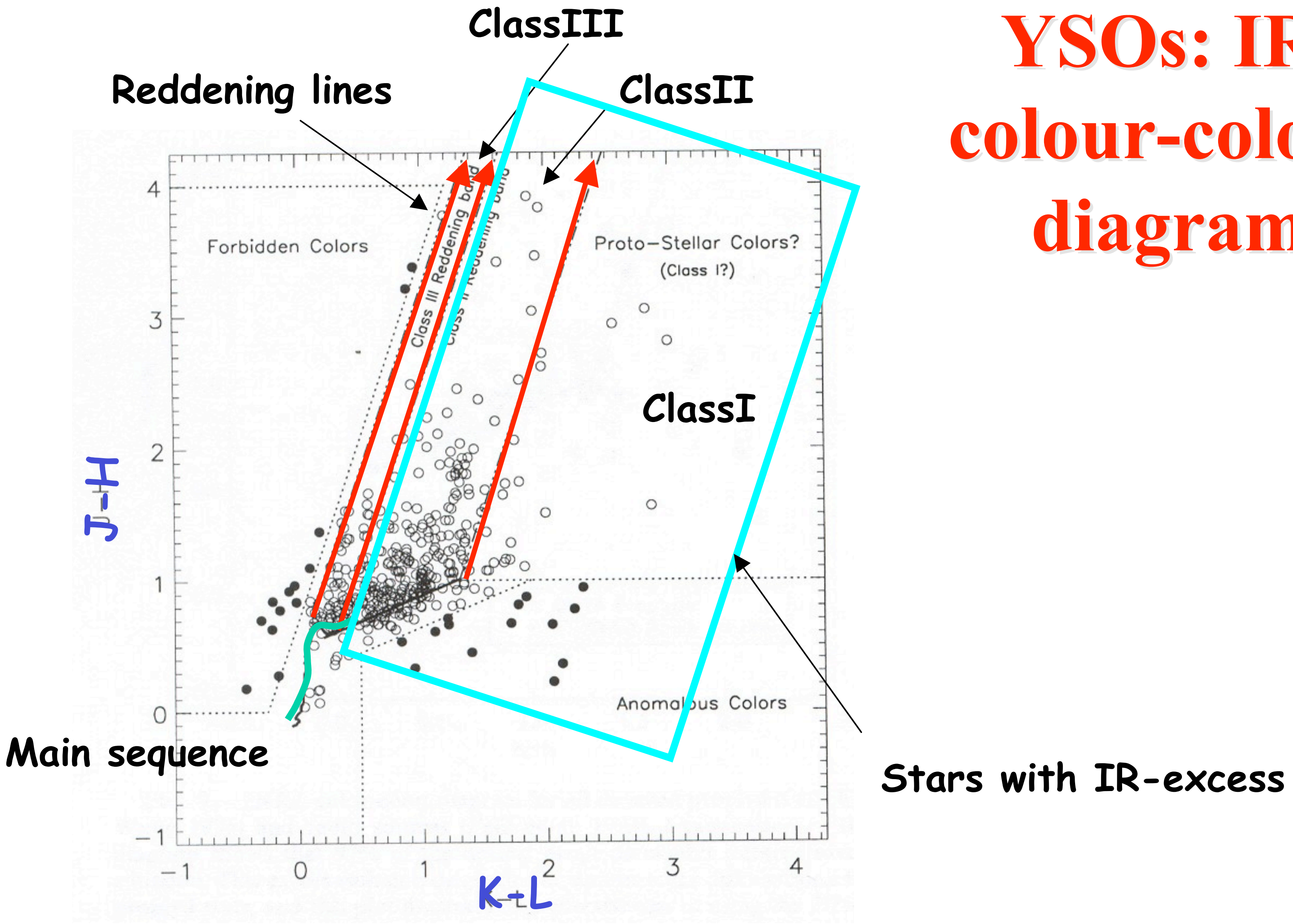

Disks… with HST (IR)

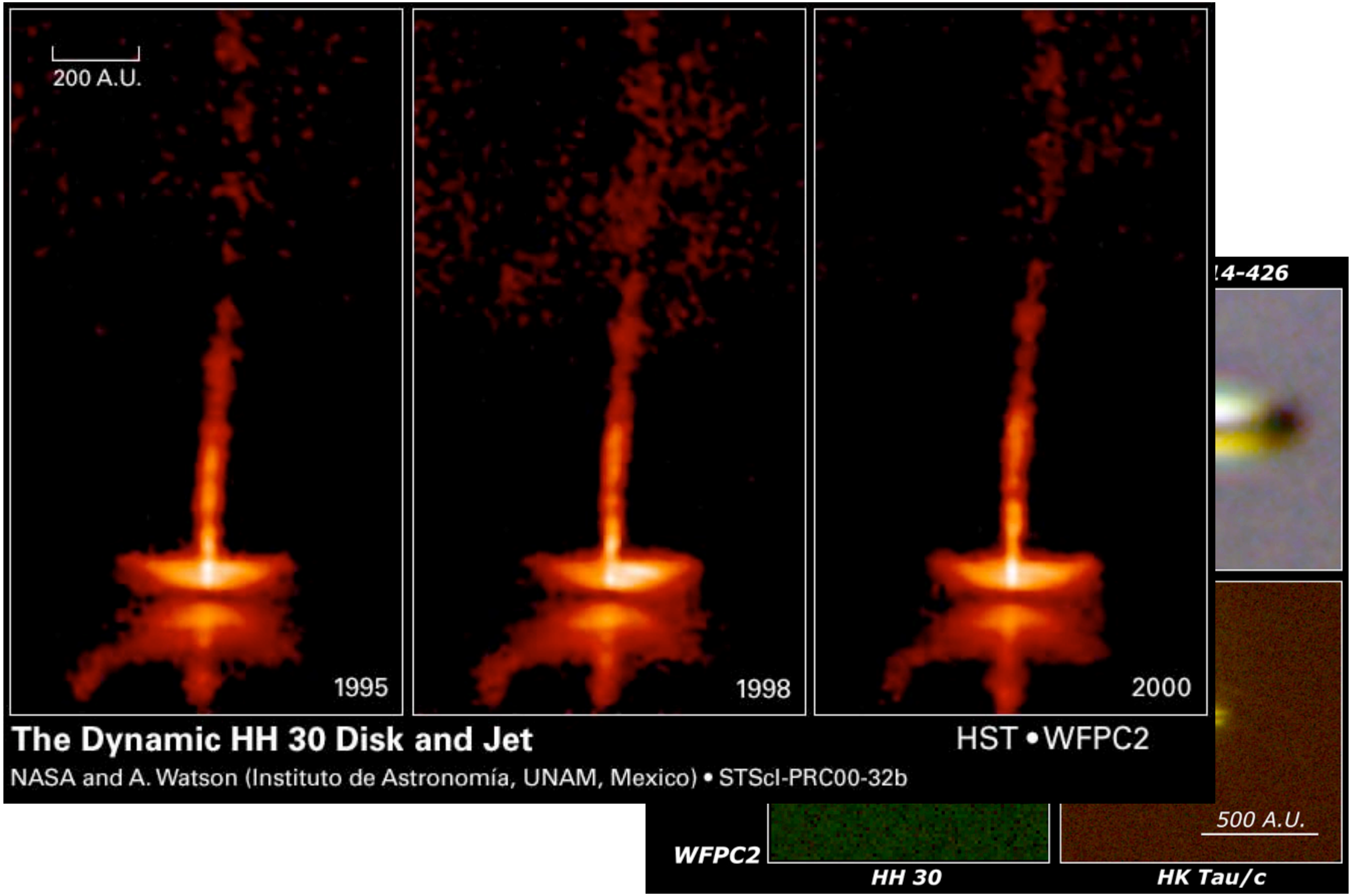

Disks and jets... with HST (IR)

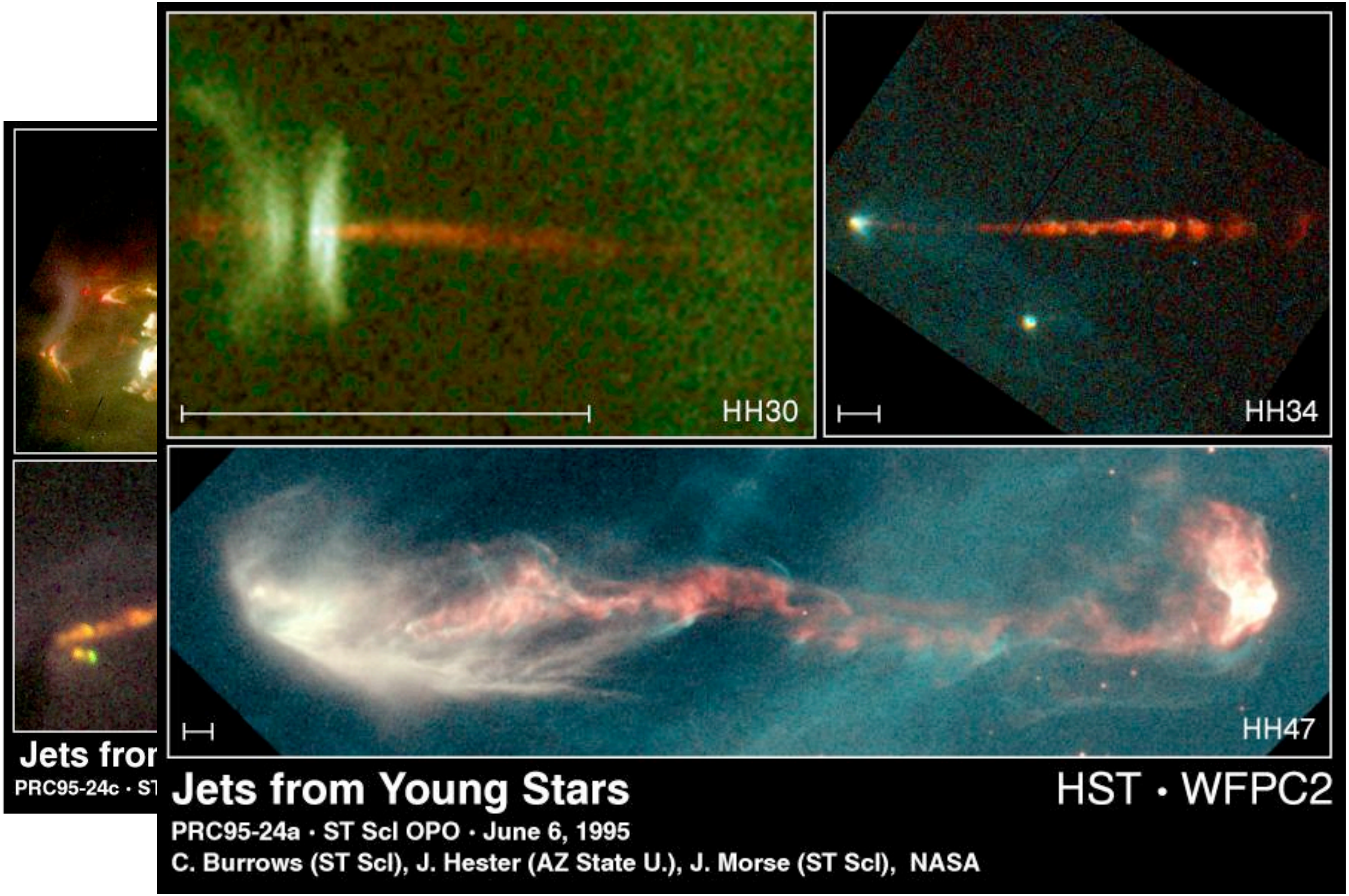

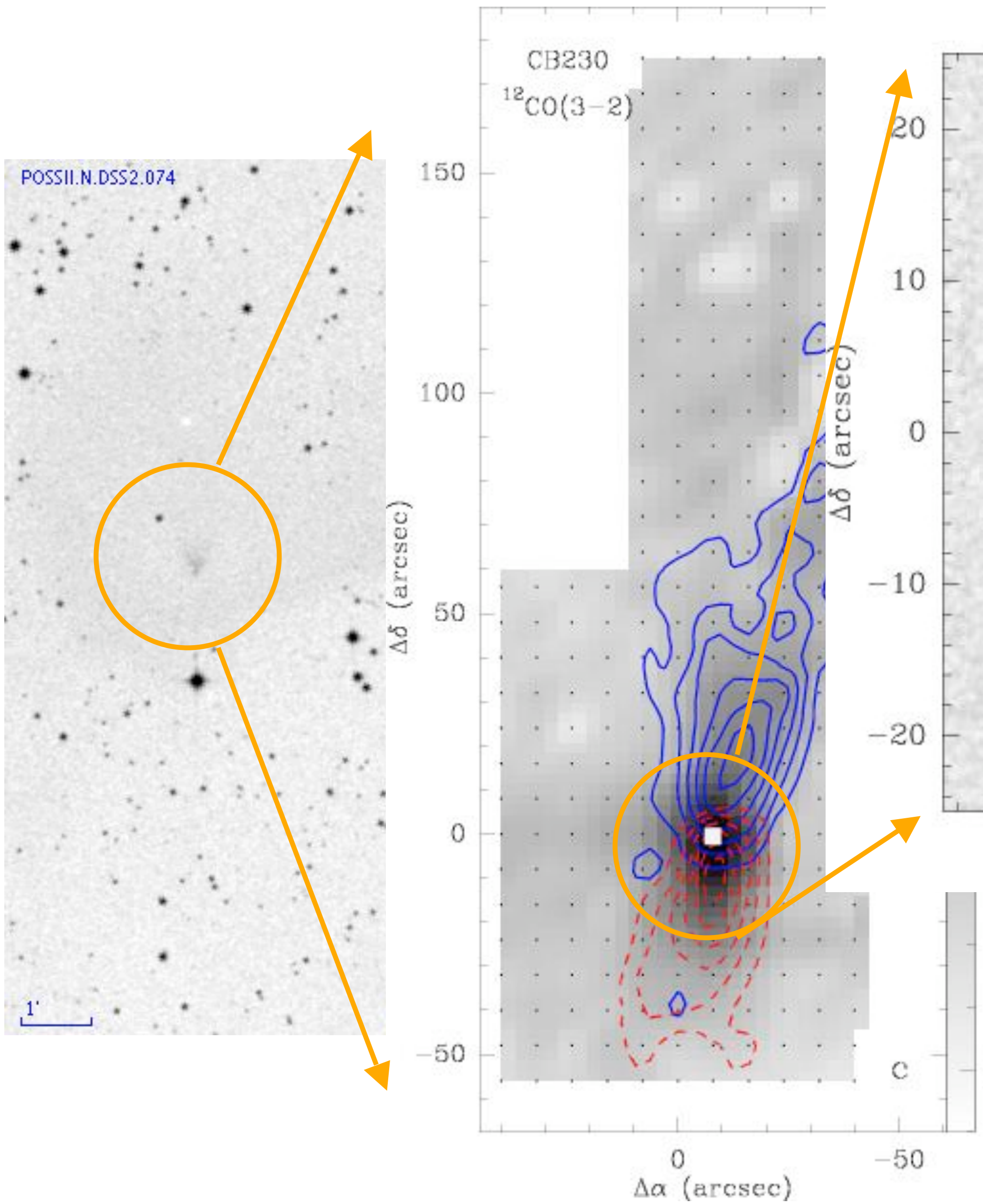

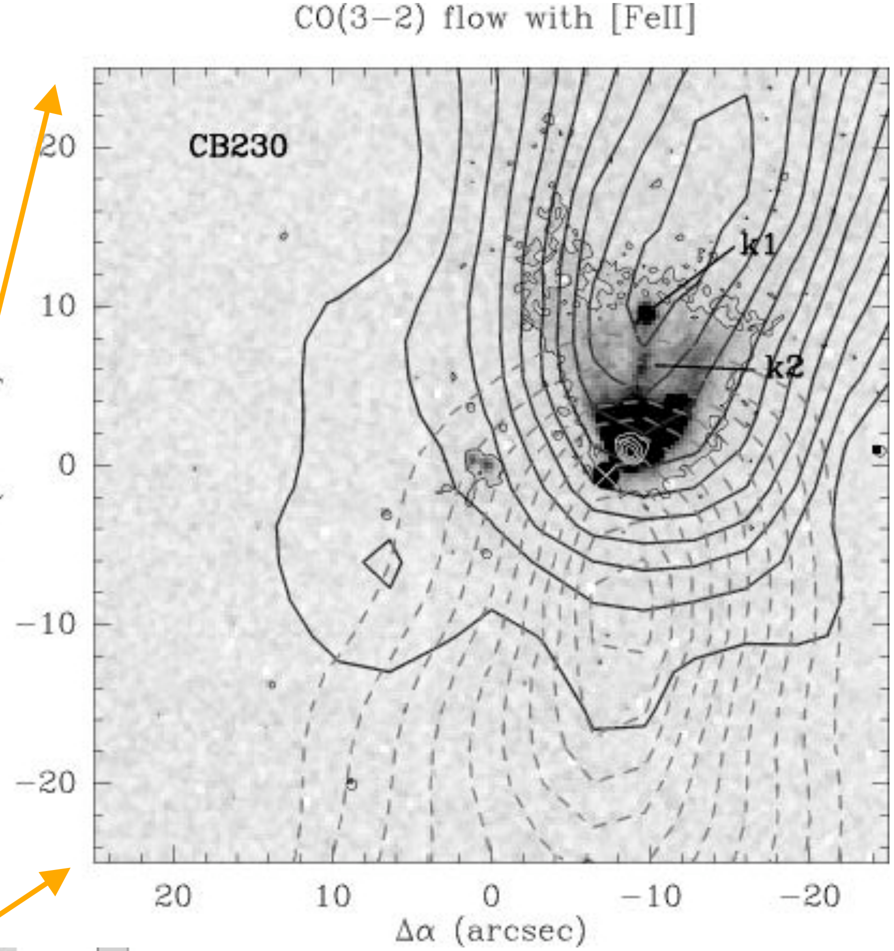

A jet at the base of the outflow

Brand et al., ApSpSci 313, 2008

Massi et al.,A&A 2004, 2008

MASSIVE STAR FORMATION
in the Galaxy

Literature:

Protostars & Planets I-V: conference proceedings. Reviews.
Tetons Conferences 1-4 (Astron. Soc. Pacific. Conf. Series)
(e.g. Tetons 4 (2001), Galactic Structure, Stars, and the Interstellar Medium)
Crete conf. (Kylafis, Lada, Eds.) "The physics of star form. and early stellar evolution"
http://www.cfa.harvard.edu/events/1999/crete/
Ferrière - 2001, Rev. Mod. Phys. 73, 1031 "The interstellar environment of our Galaxy"

Annual Reviews of Astronomy and Astrophysics. A search for 'molecular clouds' results in 376 reviews (!) covering all topics, and more, covered here. E.g.:
Evans - 1999, ARAA 37, 311 "Physical conditions in regions of star formation"
Bergin & Tafalla - 2007, ARAA 45, 339 "Cold dark clouds: the initial conditions for SF"
Lada & Lada - 2003, ARAA 51, 57 "Embedded clusters in molecular clouds"
Cox - 2005, ARAA 43, 337 "The three-phase interstellar medium revisited"
Kalberla & Kerp - 2009, ARAA 47, 37 "The HI distribution of the Milky Way"
Herbst & van Dishoeck - 2009, ARAA 47, 437 "Complex organic interstellar molecules"

Next lecture:
MASSIVE STAR FORMATION
Riccardo Cesaroni